THESIS FOR DEGREE OF DOCTOR OF PHILOSOPHY

Synthesis of Nitrogen Heterocycles and Ruthenium Complexes

JOHAN R. JOHANSSON

CHALMERS

Department of Chemical and Biological Engineering
CHALMERS UNIVERSITY OF TECHNOLOGY
Gothenburg, Sweden 2013

Synthesis of Nitrogen Heterocycles and Ruthenium Complexes

Johan R. Johansson
ISBN 978-91-7385-897-7
© Johan R. Johansson 2013

Cover picture: Top left: Formation of a 1,5-substituted-1,2,3-triazole from sodium azide, benzylbromide and 3-ethynylpyridine. *Top right*: The new luminescent Ru-complex [μ-bidppze$(phen)_4Ru_2]^{4+}$ exhibits faster association and slower dissociation kinetics for DNA threading intercalation, compared to parent compound [μ-bidppz$(phen)_4Ru_2]^{4+}$. *Center Left*: Calculated turn structure **T1**, of the 5Tzl-trimer, stabilized by one H10-bond and one H20-bond. *Bottom left*: Picture of CNT "forests" on a silicon-metal chip. *Bottom middle*: SEM micrograph of CNT bundles. *Bottom right*: Pyrrolidine functionalized CNT.

Doktorsavhandlingar vid Chalmers tekniska högskola
Ny serie Nr 3578
ISSN 0346-718X
Department of Chemical and Biological Engineering
Chalmers University of Technology
SE-412 96 Gothenburg
Sweden
Telephone +46 (0)31 772 1000

Printed by Chalmers Reproservice
Gothenburg, Sweden 2013

Till Johanna och Ellen

Synthesis of Nitrogen Heterocycles and Ruthenium Complexes

JOHAN R. JOHANSSON

Department of Chemical and Biological Engineering

CHALMERS UNIVERSITY OF TECHNOLOGY

ABSTRACT

Because of the diverse properties displayed by nitrogen heterocycles, they are one of the most commonly used structural elements in drug discovery. Due to this variation in properties, however, the chemistry and synthetic pathway to each heterocycle is unique. This is one of the reasons why heterocyclic chemistry is still an important and interesting research field for organic chemists today. Many ruthenium complexes exhibit versatile properties which make them useful tools as catalysts, and several of them can also be applied in the creation of interesting nitrogen heterocycles.

One of the main parts of this thesis concerns the synthesis of 1,5-substituted-1,2,3-triazoles via the ruthenium catalyst azide-alkyne 1,3-dipolar cycloaddition reaction (RuAAC). Several different ruthenium complexes have been employed, and a convenient and safe sequential one-pot microwave procedure has been developed for the RuAAC reaction. The tolerance of several functional groups present on the substrates has been studied, and the $[RuCl_2Cp^*]_x$ catalyst showed remarkably good results in this context. Moreover, 1,5-substituted-1,2,3-triazoles have been applied towards foldamer peptidomimetics by constructing oligomers such as a dimer, trimer and tetramer of the 5Tzl unit. The secondary structure of the 5Tzl-trimer was studied by 2D NOESY experiments and quantum chemical calculations, which concluded that the 5Tzl-trimer is flexible, and that several conformers are present in DMSO solution at 25 °C, where two helical structures (**H10** and **H16**) together with three turn-like structures (**T1-3**) are the most probable conformers. From our initial study it can be concluded that oligomers of 5Tzl can serve as good adaptable foldamer backbones which can adopt various secondary structures and offer improved properties such as water solubility.

The synthesis of other nitrogen heterocycles such as pyrrolidines, imidazoles and phenazines for various purposes are also demonstrated. Synthesis of a the new luminescent Ru-complex $[\mu\text{-bidppze}(phen)_4Ru_2]^{4+}$ for DNA threading intercalation studies has been carried out, and this complex revealed faster association and slower dissociation kinetics compared to previous analogues. Functionalization of carbon nanotubes (CNTs) with active azide functional groups has been applied on a silicon-metal chip, via a 1,3-dipolar cycloaddition of an azomethine ylide to the CNTs. The functionality of these azide groups was also demonstrated by introduction of fluorine via the copper catalyzed azide-alkyne 1,3-dipolar cycloaddition reaction (CuAAC), and this initial study displays the potential of this methodology for applications such as biosensors in the future.

Keywords: 1,2,3-triazole, ruthenium-complex, 1,3-dipolar cycloaddition, microwave heating, azide, alkyne, RuAAC, CuAAC, foldamers, peptidomimetics, $[RuCl_2Cp^*]_x$, 2D NOESY, DNA threading intercalation, azomethine ylide, functionalized CNT

LIST OF PUBLICATIONS

This Thesis is based on the following publications as well as some unpublished results. Papers I and III are reprinted with permission from the publishers.

I. **Sequential One-Pot Ruthenium-Catalyzed Azide-Alkyne Cycloaddition from Primary Alkyl Halides and Sodium Azide**
Johan R. Johansson,* Per Lincoln, Bengt Nordén and Nina Kann
Journal of Organic Chemistry **2011**, *76*, 2355-2359.

II. **δ-Peptidomimetcs from RuAAC-Derived 1,5-Disubstituted Triazole Units**
Johan R. Johansson, Elin Hermansson, Bengt Nordén, Nina Kann, and Tamás Beke-Somfai*
Submitted to Chemistry – a European Journal

III. **Bridging Ligand Length Controls AT Selectivity and Enantioselectivity of Binuclear Ruthenium Threading Intercalators**
Johan R. Johansson, Yubo Wang, Mattias P. Eng, Nina Kann, Per Lincoln,* and Johanna Andersson
Chemistry – a European Journal **2013**, *19*, 6246-6256.

IV. **Covalent Functionalization of Carbon Nanotube Forests Grown In Situ on a Metal-Silicon Chip**
Johan R. Johansson, Niklas Bosaeus, Nina Kann, Björn Åkerman, Bengt Nordén and Waqas Khalid*
Society of Photographic Instrumentation Engineers (SPIE) conference proceedings, San Diego 11-15 March **2012**, 8344-35.

Publications not included in the Thesis are listed below.

Sniffing out early reaction intermediates
Johan R. Johansson, and Bengt Nordén*
Proceedings of the National Academy of Sciences of the United States of America **2012**, *109*, 2186-2187.

Towards Artificial Photosynthesis of CO_2-Neutral Fuel: Homogenous Catalysis of CO_2-Selective Reduction to Methanol Initiated by Visible-Light-Driven Multi-Electron Collector
Yong Na,* Per Lincoln, Johan R. Johansson, and Bengt Nordén*
ChemCatChem **2012**, *4*, 1746 – 1750.

Covalent Functionalization of Carbon Nanotubes Grown on a Surface
Johan R. Johansson and Waqas Khalid
U.S. Provisional Application, Application No.: 61/609,011, Filed: March 9, **2012**.

Conversion of Carbon Dioxide to Methanol Using Visible Light
Yong Na, Per Lincoln, Johan R. Johansson and Bengt Nordén
U.S. Provisional Application, Application No.: 61/650,787, Filed: May 23, **2012**.

CONTRIBUTION REPORT

Paper I: Major contribution towards the formulation of the research problem. Performed all of the experimental work. Performed a major part of the result analysis. Major contribution towards the writing of the manuscript.

Paper II: Major contribution towards the formulation of the research problem. Performed a major part of the synthesis and all the NMR experiments. Supervised MSc student Elin Hermansson. Performed part of the analysis of results. Contributed towards the writing of the manuscript.

Paper III: Minor contribution towards formulation of the research problem, major contribution in the planning and design of the new compounds, performed major part of the synthesis and minor contribution in supervising MSc student Yubo Wang, major contribution in writing the synthetic part of the manuscript.

Paper IV: Major contribution towards the formulation of the research problem. Performed all of the chemical modifications of the CNTs. Performed minor part of the result analysis. Contributed towards the writing of the manuscript.

Performed all of the experimental work of the previously unpublished results except the attempted synthesis of $[\mu\text{-dppzipe(phen)}_4\text{Ru}_2]^{4+}$ which was performed in collaboration with Johanna Andersson.

ABBREVIATIONS

2-MeTHF	2-methyltetrahydrofuran
5Tzl	2-(5-(aminomethyl)-1*H*-1,2,3-triazol-1-yl)acetic acid
ACBC	2-aminocyclobutanecarboxylic acid
ACHC	2-aminocyclohexylcarboxylic acid
ACN	acetonitrile
ACPC	2-aminocyclopentanecarboxylic acid
Aib	2-aminoisobutyric acid
AP	*trans*-3-aminoproline
APC	*trans*-3-aminopyrrolidine-4-carboxylic acid
bidppz	11,11'-bidipyrido[3,2-*a*:2',3'-*c*]phenazine
bidppze	1,2-bis(dipyrido[3,2-*a*:2',3'-*c*]phenazin-11-yl)ethyne
Boc	*tert*-butoxycarbonyl
bpy	2,2'-bipyridine
CDI	carbonyldiimidazole
CM	cross metathesis
CNT	carbon nanotube
COD	cycloocta-1,5-diene
Cp	cyclopentadienyl
Cp*	pentamethylcyclopentadienyl
ct-DNA	calf thymus DNA
CuAAC	Cu(I)-catalyzed azide-alkyne 1,3-dipolar cycloaddition
Cyp	cyclopentyl
DCM	dichloromethane
DIPA	diisopropylamine
DIPEA	diisopropylethylamine
DMA	N,N-dimethylacetamide
DMF	N,N-dimethylformamide
DMP	Dess-Martin periodinane
DMSO	dimethyl sulfoxide
dppz	dipyrido[3,2-*a*:2',3'-*c*]phenazine
dppzI	11-iododipyrido[3,2-*a*:2',3'-*c*]phenazine
dppzip	2-(dipyrido[3,2-*a*:2′,3′-*c*]phenazin-11-yl)imidazo[4,5-f]-1,10-phenanthroline)
dppzipe	11-((1*H*-imidazo[4,5-*f*][1,10]phenanthrolin-2-yl)ethynyl)dipyrido[3,2-*a*:2',3'-*c*]phenazine
dppzp	3-(dipyrido[3,2-*a*:2',3'-*c*]phenazin-11-yl)prop-2-yn-1-ol
dppzpa	3-(dipyrido[3,2-*a*:2',3'-*c*]phenazin-11-yl)propiolaldehyde
EDS (or EDX)	energy-dispersive X-ray spectroscopy
f-CNT	functionalized carbon nanotube
FMO	frontier molecular orbitals
Fmoc	fluorenylmethyloxycarbonyl
HDD	hard disk drive
HPLC-MS	high performance liquid chromatography equipped with mass spectrometer
m-CPBA	3-chloroperoxybenzoic acid
MW	microwave heating
NHC	N-heterocyclic carbene
ni	number of increments
NMR	nuclear magnetic resonance spectroscopy
NOE	nuclear Overhauser effect

NOESY	nuclear Overhauser enhancement spectroscopy
np	number of data points
nt	number of scans
PEPPSI	Pyridine, Enhanced, Precatalyst, Preparation, Stabilization and Initiation
PGMs	platinum group metals
Ph	phenyl
phen	phenanthroline
pq	1,10-phenanthroline-5,6-dione
PyBOP	benzotriazol-1-yl-oxytripyrrolidinophosphonium hexafluorophosphate
RCM	ring closing metathesis
r.t.	room temperature
RuAAC	ruthenium catalyzed azide-alkyne 1,3-dipolar cycloaddition
SEM	scanning electron microscope
SET	single electron transfer
SWCNT	single-walled carbon nanotube
T3P	2,4,6-tripropyl-1,3,5,2,4,6-trioxatriphosphorinane-2,4,6-trioxide
TBTA	tris((1-benzyl-1*H*-1,2,3-triazol-4-yl)methyl)amine
TFA	trifluoroacetic acid
THF	tetrahydrofuran
TMS	trimethylsilyl
TMSA	trimethylsilyl azide
Tr	triphenylmethyl

TABLE OF CONTENTS

Preface

Nitrogen heterocycles in natural products and pharmaceuticals

Nitrogen heterocycles exhibit an exceptional diversity of properties, and it is no surprise that they are so popular in nature where Darwinian combinatorics has successfully exploited their many qualities. Evolution has efficiently utilized nitrogen heterocycles as key substances in many species, in both plants and animals, in the form of venoms, vitamins, DNA/RNA, co-factors, proteins, pheromones etc. Nitrogen heterocycles are a common attribute in natures alkaloids, which are popular and challenging targets in total synthesis for the synthetic chemist. Tubocurarine, morphine, batrachotoxin, epibatidine, quinine, caffeine, sparteine, and nicotine are just a few examples of the endless number of alkaloids containing nitrogen heterocycles produced by Mother Nature.

Nature is an obvious source for inspiration when it comes to molecular architecture and due to the diversity of properties displayed by nitrogen heterocycles, they are also probably one of the most commonly used structural elements in drug discovery and pharmaceutical development. Of the top 200 pharmaceutical products (by sales) in 2009, compiled by the Hjardarson group,[1] 79% are small molecules and 73% of them contain at least one heterocycle. One of these is Tazocin, a combination drug of piperacillin and tazobactam, which has activity against many gram-positive and gram negative pathogens and anaerobes. Tazobactam contains three heterocyclic rings and one of these is the 1*H*-1,2,3-triazole, shown in Figure 1. Another triazole-containing drug is Ticagrelor (Figure 1), the first reversible platelet aggregation inhibitor (P_2Y_{12} antagonist) on the market for the prevention of thrombotic events in patients with acute coronary syndrome or myocardial infarction with ST elevation.[2]

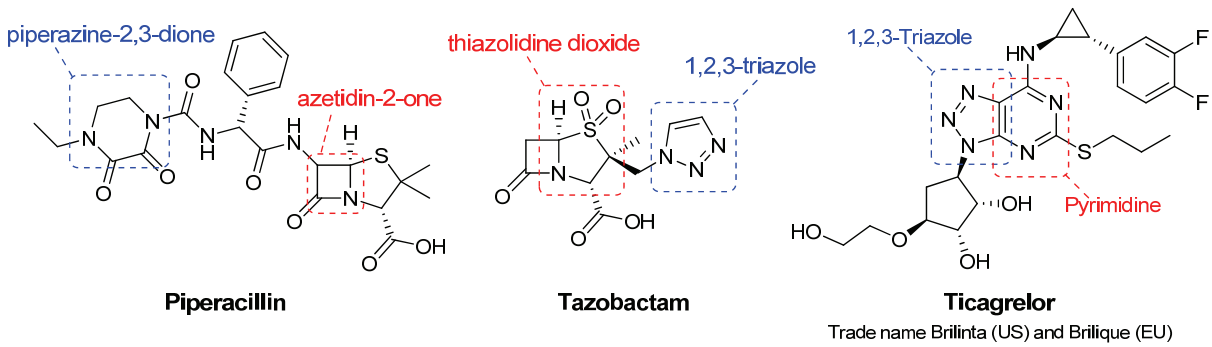

Figure 1. Structure of Piperacillin, Tazobactam and Ticagrelor, which contain several interesting heterocycles.

The chemistry and synthetic pathway to each heterocycle is unique. This is one of the reasons why heterocyclic chemistry is still an important and interesting research field for organic chemists today. Many ruthenium complexes exhibit versatile properties which make them useful tools as catalysts as well as probes, and several of them can also be applied in the creation of interesting nitrogen heterocycles. These are some of the reasons leading up to the focus of this thesis, namely the synthesis and applications of nitrogen heterocycles and ruthenium complexes in different contexts.

1 Introduction to Nitrogen Heterocycles

1.1 Definition and properties

So what is a nitrogen heterocycle? A heterocycle is by definition a cyclic compound consisting of at least two different elements. The ring size can vary from three and upwards, however the most common ring sizes are 3-7. Usually the term macrocycle is used when the ring size exceeds nine. The ring system can be saturated or unsaturated. If it is fully unsaturated, the heterocycle is in most cases also aromatic. Consequently, a nitrogen heterocycle is a cyclic ring system containing one or more nitrogen atoms.[3] The structures of saturated 3-7-membered heterocycles containing one nitrogen atom are shown in Figure 4.

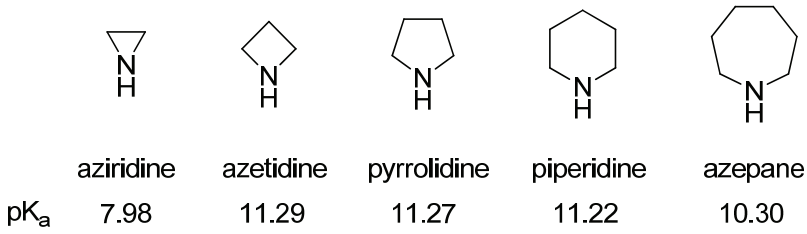

Figure 2. pK_a of saturated 3-7-membered nitrogen heterocycles.

Aziridines are less basic than acyclic amines due to the increased s character of the nitrogen lone pair. The conjugate acid of aziridine has a pK_a value of 7.98 compared to a typical pK_a value of approimately 11 for the conjugate acid of an acyclic secondary amine.[4] Azetidine (11.29), pyrrolidine (11.27)[5] and piperidine (11.22)[6] on the other hand are slightly more basic compared to the acyclic diethylamine (10.73). However, when the ring size is further increased to the 7-membered ring, azepane (10.30),[7] the pK_a drops below the pK_a of the acyclic diethylamine. Heterocycles may have different degree of unsaturation, and examples for 5- and 6-membered nitrogen heterocycles are shown in Figure 3.

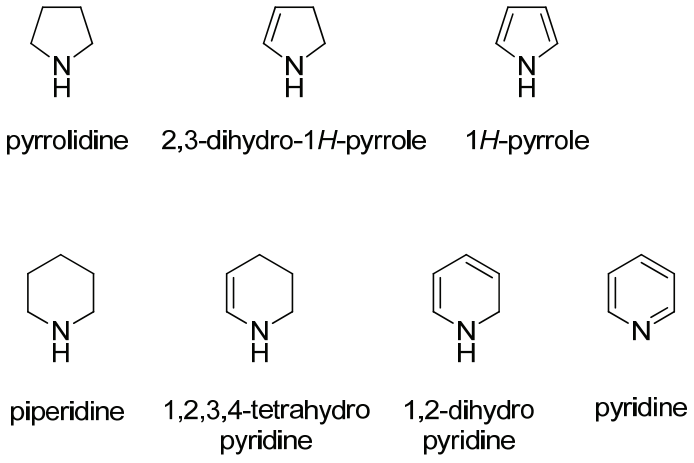

Figure 3. Examples of unsaturation in nitrogen heterocycles.

The fully unsaturated 6-membered nitrogen heterocycle, pyridine, is aromatic and is a weak base. Pyridine has a much lower pK_a value (5.25) of the conjugate acid compared to piperidine.[8] Pyrrole on the other hand is not basic at all ($pK_a \sim -4$), since the nitrogen lone pair is part of the aromatic system and delocalised in the ring. A protonation of pyrrole results in loss of the aromaticity and is highly unfavourable. On the other hand, the pyrrole ring is electron rich in itself, and its charge separated tautomers can act as nucleophiles and react with electrophiles to form 2-substituted pyrroles as the major product (Figure 4), although mixtures of the 2- and 3- regioisomer can be formed. Direct N-substitution is generally not possible, but the hydrogen on the pyrrole nitrogen is a weak acid, with a pK_a value of 15.8, and can be deprotonated with a strong base. The formed anion is resonance-stabilised over the whole ring, and a reaction of the pyrrole anion with an electrophile will usually result in the N-substituted pyrrole as major product. If one wants to obtain the 3-substituted pyrrole, one way to prepare it is to use a sterically hindered protecting group on the pyrrole nitrogen, such as triphenylmethyl (Tr) which favours the formation of the less sterically hindered 3-substituted pyrrole.

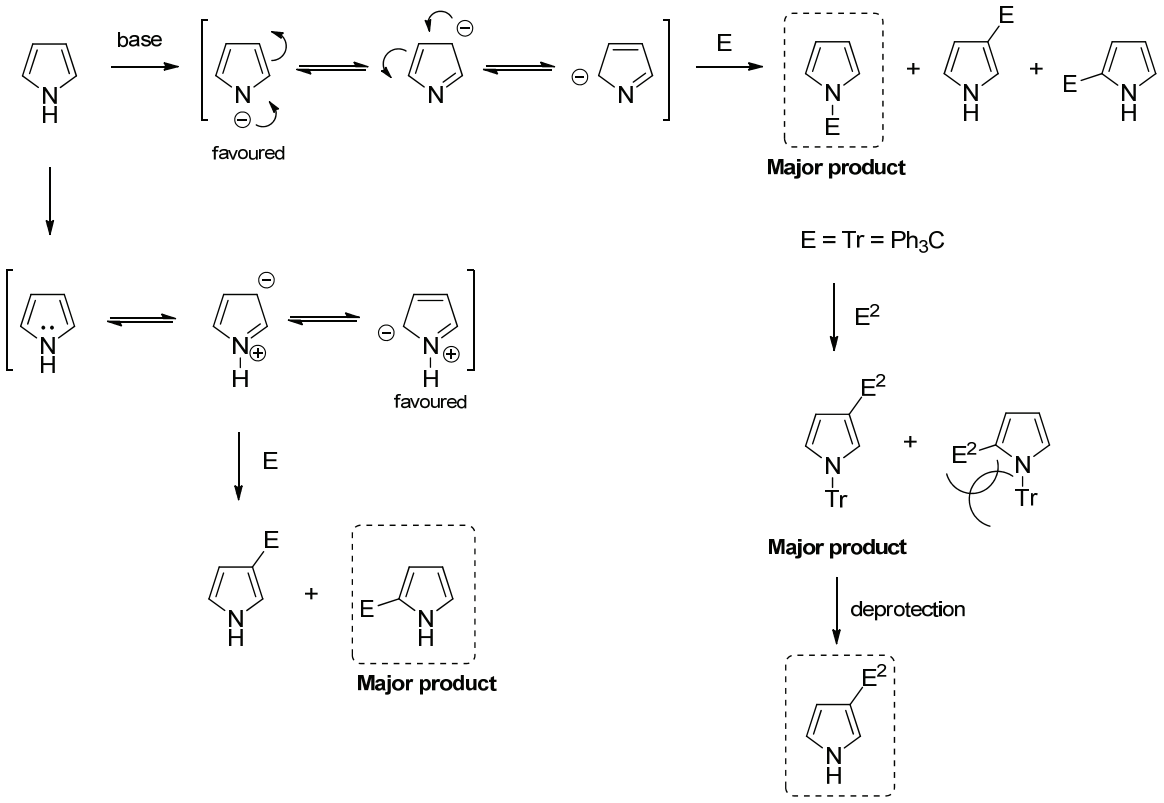

Figure 4. Possible strategy to control the regioselectivity in pyrrole chemistry.

Another example of problems with the formation of regioisomers concerns the alkylation of 1,2,4-triazoles. The anion is resonance stabilized over the ring and all three nitrogen atoms can react. If one of the carbons is substituted, alkylation can lead to the formation of three different regioisomers, as shown in Figure 5. The properties of the substituent on the ring will affect the ratio between the product isomers. Also, reaction conditions such as solvent and/or base may favour the formation of one isomer over the others. There are thus ways to control the regioselectivity. However, the reactivity and selectivity are not the same when going from

one heterocycle to another. Each heterocycle has its own unique properties and this is probably why heterocycles are so popular in drug discovery.

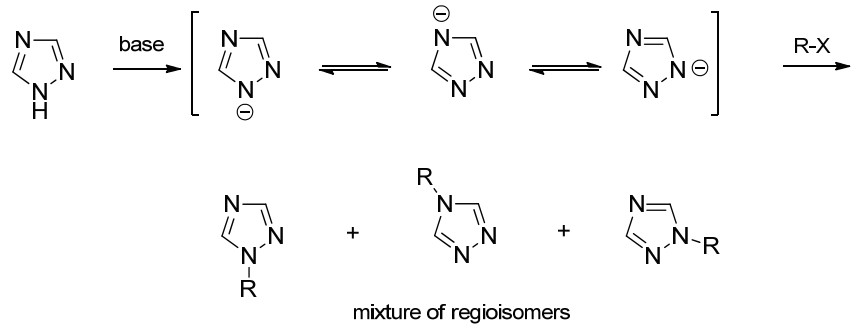

Figure 5. Alkylation of 1,2,4-triazole results in a mixture of regioisomers.

There is a wide range of nitrogen heterocycles known in the literature and some of the most common 5-membered nitrogen heterocycles are shown in Figure 6. Note that all aromatic 5-membered nitrogen heterocycles except pyrrole are named –azoles. The suffix in the name of the nitrogen heterocycle denotes the degree of saturation, i.e. -le, -line, -lidine. As can be divined from the name, diazoles contain two nitrogens, and there are many different diazoles known in the literature.

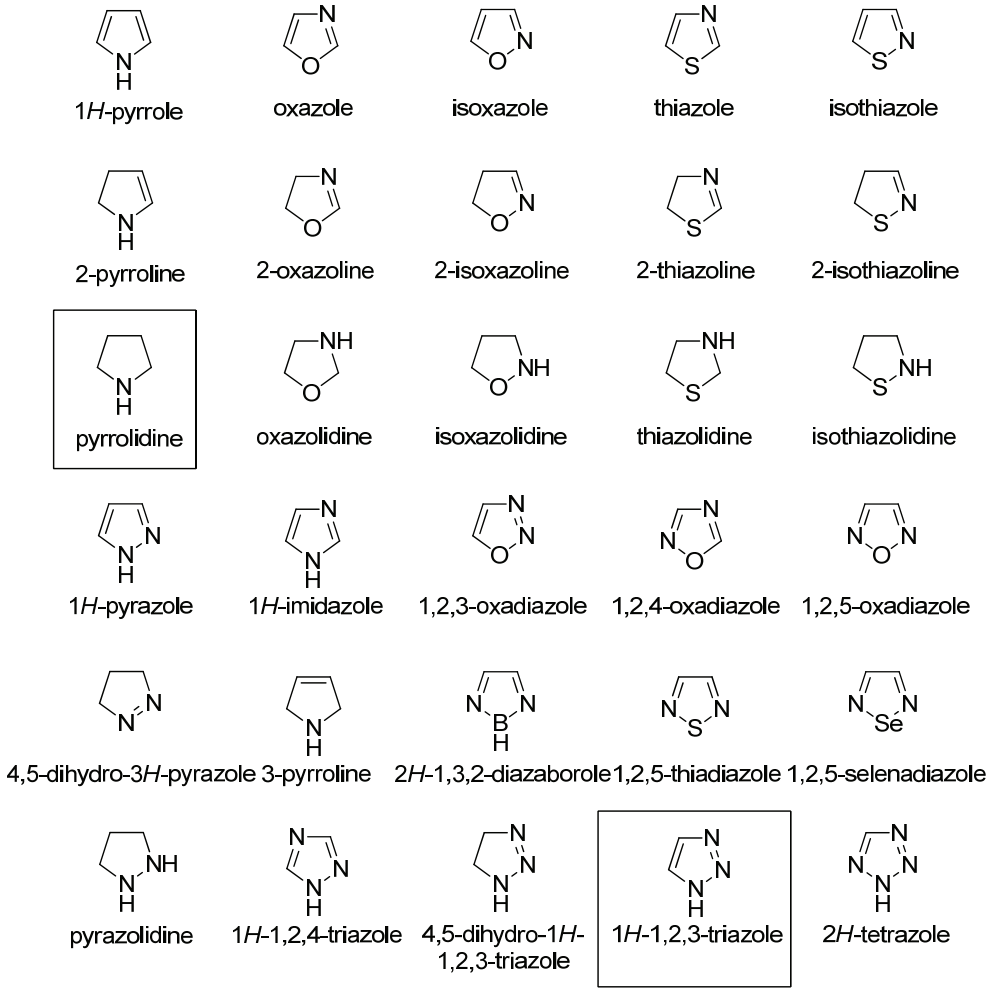

Figure 6. The most common 5-membered nitrogen heterocycles.

1.2 Imidazoles

One the many possible structures of diazoles is the imidazole (1,3-diazole), which is a weak base (pK_a ~7.0) which is taken advantage of in the useful synthetic amide coupling reagent, carbonyldiimidazole (CDI),[9] as well as in Nature, since histidine residues are frequently important in the mechanisms of enzyme catalysis. The saturated version of imidazole, imidazolidine is usually not so stable and will be easily hydrolysed into the corresponding diamine and aldehyde. However there are many examples of stable imidazolines and imidazolidines, in the form of N-heterocyclic carbenes (NHC) coordinated to a transition metal (Pd and Ru most commonly).[10,11] One example is in the palladium catalyst PEPPSI, shown in Figure 7, which is a popular catalyst in Buchwald–Hartwig aryl aminations.[12]

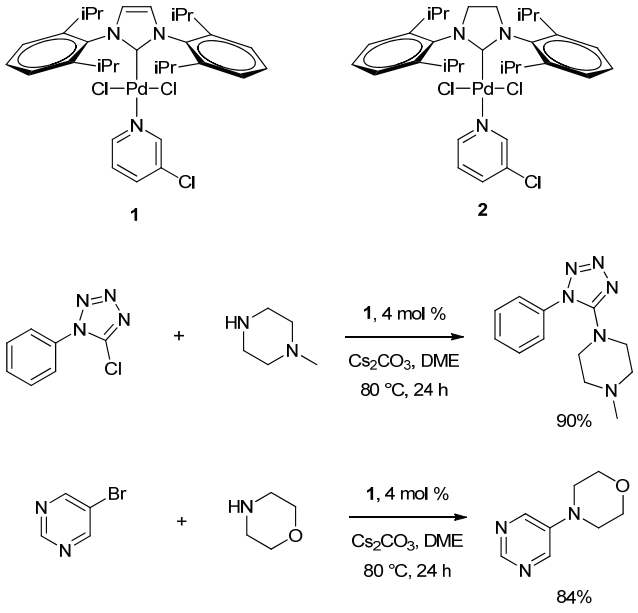

Figure 7. Pd-PEPPSI (Pyridine, Enhanced, Precatalyst, Preparation, Stabilization and Initiation) precatalyst complexes **1** and **2**, and use of **1** in Buchwald – Hartwig aryl aminations of heterocycles.[12]

1.3 Triazoles

The number of different triazole heterocycles is more limited as compared to diazoles. The 1,2,4-triazole, described earlier, and the 1,2,3-triazole are the two most common forms of triazoles. The synthetic route to Ticagrelor (Figure 2) described in the introduction, involves 28 synthetic steps and in one of these the 1,2,3-triazole is formed.[13] By employing diazotization conditions on the diaminopyrimidine and subsequent *in situ* cyclization of the formed diazonium-intermediate, the 3*H*-[1,2,3]triazolo[4,5-*d*]pyrimidine was obtained in 88% yield, as shown in Figure 8.

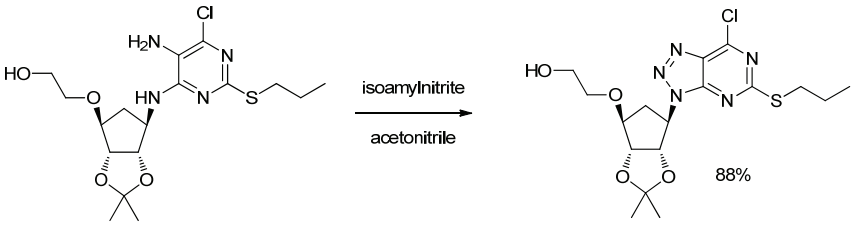

Figure 8. Synthesis of the 1,2,3-triazole unit in the synthesis route to Ticagrelor.[13]

Other synthetic routes to 1,2,3-triazoles will be discussed in more detail in later chapters of the thesis.

1.4 Tetrazoles

There are only a few possibilities for different tetrazole structures since there is only one atom which is not nitrogen. The most common tetrazole is the 5-substituted 1*H*-tetrazole, which is a bioisostere to carboxylic acids, and utilized as the active structure of the sartans. Sartans are a class of compounds, AT_1-receptor antagonists, used for the treatment of hypertension, chronic heart insufficiency condition after a heart attack, and diabetic nephropathy. Examples of bioisosteric replacements in the sartan family are shown in Figure 9, together with an example of how the tetrazoles can be synthesized from arylnitriles and NaN_3.[14]

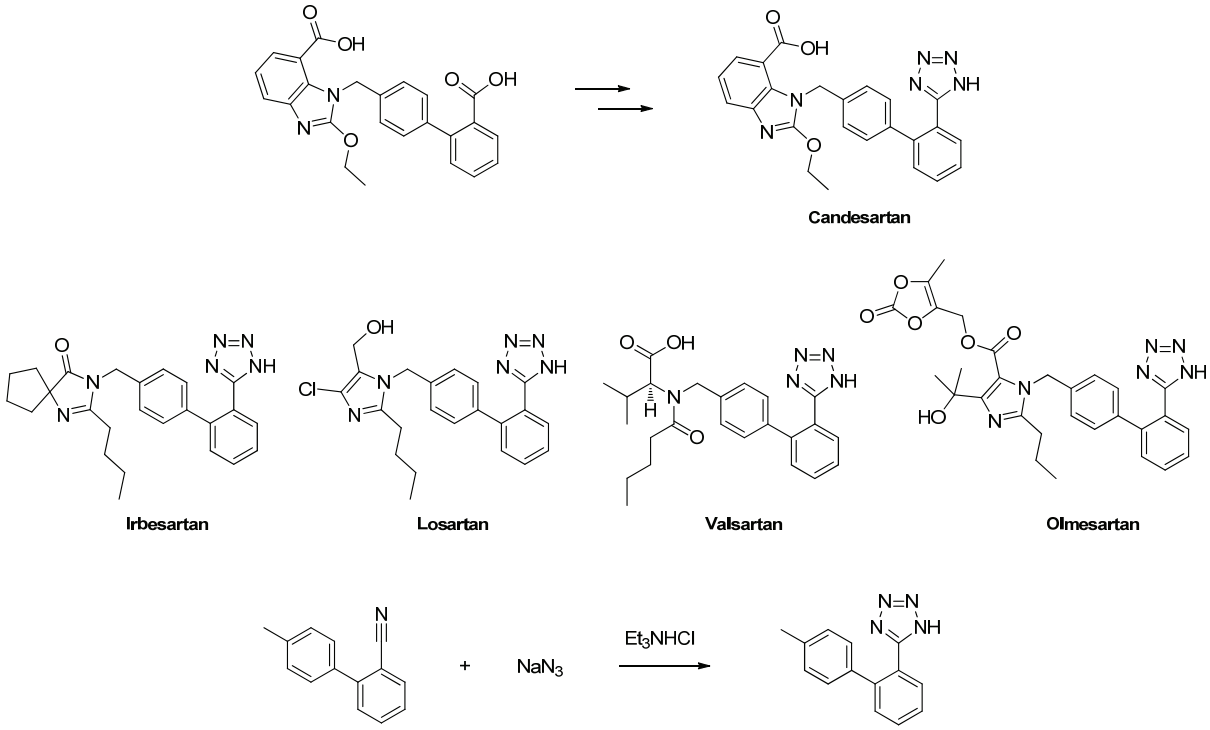

Figure 9. Bioisosteric replacement of a carboxylic acid functionality into a 1*H*-tetrazole, commonly used in the sartan family. An example of how the crucial tetrazole can be synthesized is also shown.[14]

Another tetrazole structure is the tetrazolinone, which can be synthesized via the reaction of an isocyanate with an azide (NaN_3 or TMSA), as shown in Figure 10. Phenyl tetrazolinone derivatives are used as herbicides in rice fields for example.[15-17] Pentazole is an extremely rare heterocycle, probably due to its high energy and instability. It can, however, be synthesised from aryldiazonium chlorides and azide ion at – 80 °C.[18]

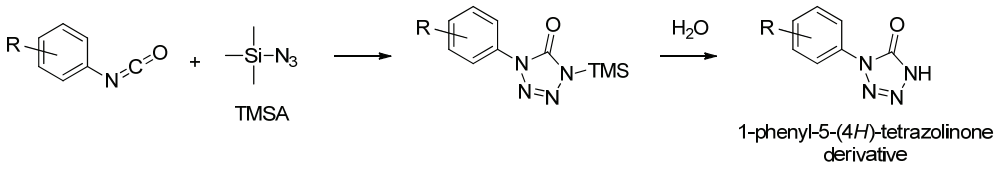

Figure 10. Synthesis of phenyl tetrazolinone derivatives used as herbicides in rice fields.[18]

2 Ruthenium complexes

2.1 Ruthenium history, mining and isolation

Ruthenium is a white silvery metal and is one of the six elements that together with Os, Rh, Ir, Pd and Pt forms the platinum group metals (PGMs), located in Group 8-10 (period 5 and 6) of Mendeleev's periodic table. Ruthenium was first isolated by Klaus[19-20] in 1844, in residues left after crude platinum ore from the Urals had been dissolved in aqua regia. It is named after *Ruthenia*, the Latin name for Rus' which is the medieval name for today's west Russia. The natural abundance of ruthenium in the earth's crustal rock is estimated to be only 0.0001 ppm, making it a rare element. Ruthenium is generally found in the metallic state along with the other PGMs and the coinage metals (Cu, Ag and Au). The major source of ruthenium is the nickel-copper sulfide ore found in South Africa and Sudbury in Canada and also in the river sands of the Urals in Russia.[21] Despite the rarity of ruthenium, it is much less expensive (~75$/oz or ~16 kr/g, aug 2013) than Rh, Ir, Pd and Pt, and a price comparison can be seen in Figure 11. The reason for the lower price of ruthenium is mainly because the demand is much lower, and also the fact that ruthenium is produced as a by-product from copper and nickel mining and processing, and from the processing of platinum group metal ores. About 20 tonnes of ruthenium is produced every year.

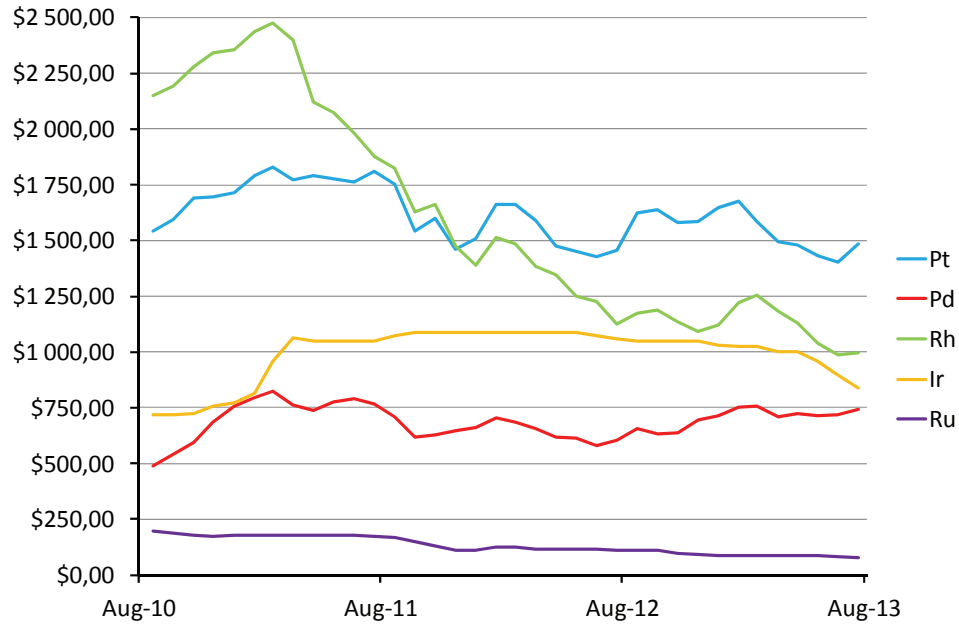

Figure 11. Price comparison of Ru with other Platinum metals. Monthly average price in $/oz over the last three years. (1 troy ounce, oz = 31.103 g)

All the platinum group metals (PGMs) are isolated from platinum concentrates which are commonly obtained either from electrolytic refining of nickel, copper, silver and gold (where PGMs settle to the bottom of the anode solution) or from melting of sulfide ores.[22] The platinum concentrates are initially treated with hydrochloric acid and chlorine, yielding the

volatile tetraoxides of Ru (RuO_4) and Os (OsO_4), which can be distilled off. The ruthenium is separated from osmium by further distillation or by precipitation as ammonium hexachlororuthenates (mixtures of isomers), $(NH_4)_3RuCl_6$, by treatment with ammonium chloride. Reduction of the isomeric mixture of $(NH_4)_3RuCl_6$ with hydrogen leads to a Ru-metal powder that can be treated using powder metallurgy techniques or argon-arc welding.

The major use of ruthenium today can be divided into three different areas.[23] 1. *Electronics*: The main application of Ru is in the hard disk drive (HDD) industry. By adding a thin layer of the metal to the magnetic coating of a hard disk, the data storage density is increased substantially. 2. *Alloys*: Ru is commonly alloyed with other PGMs like Pd and Pt in jewellery, but it also works exceptionally well with titanium. By adding 0.1% of ruthenium to titanium, the corrosion resistance is enhanced a hundredfold, and this property is for example utilized in electrodes for the electrolytic production of chlorine gas. 3. *Chemicals*: Ruthenium has become a useful metal in catalysis, and can for example be used to remove hydrogen sulfide from oil refineries to make sulfur-free fuels, as well as to remove ammonia from natural gas and acetic acid from methanol.

2.2 Stability and reactivity of ruthenium complexes

Ruthenium is the 44th element in the periodic table, has seven naturally occurring isotopes and exhibits the electron configuration $[Kr]4d^75s^1$. This electron configuration enables the formation of many different ruthenium complexes in a broad range of oxidation states, ranging from -II ($[Ru(CO)_4]^{2-}$) to +VIII (RuO_4), where +II and +III are the most commonly observed. Ruthenium is one of the few elements together with Os, Xe, and Ir that can form complexes in its +VIII oxidation state.[24] Almost all ruthenium complexes are in some way derived from $RuCl_3$,[25-27] which in itself can be prepared in two different ways. Evaporation of a solution of RuO_4 in aqueous hydrochloric acid under a stream of HCl gas produces red $RuCl_3 \cdot 3H_2O$. Anhydrous $RuCl_3$ is prepared by heating powdered ruthenium metal at 330 °C in carbon monoxide and chlorine, yielding the dark-brown β-form, which if heated above 450 °C in $Cl_2(g)$ is converted to the black α-form.[21]

By coordination of ligands, ruthenium can form many different and useful complexes. Two systems have been developed for the classification of ligands in transition metal organometallic chemistry, and the choice of system is a matter of preference. In the first system, ligands are assigned to be neutral or charged. In the second system, all ligands are considered to be neutral. In the latter case, some ligands donate two electrons and have been termed “L-type” ligands, and other ligands donate one electron to the metal center and are called “X-type” ligands. Ligands that donate more than two electrons have been named LX ligands (three electrons), L_2 ligands (four electrons), L_2X (five electrons), etc.[28]

When it comes to stability or reactivity of various ruthenium complexes, there are several key factors affecting the metal-ligand bond strength. The spectrochemical series used in ligand field theory is more or less a measure of the σ-donor strength plus the π-donor and acceptor strength (back bonding), and can give an estimated bond strength. However, other factors

such as the *chelate effect*, the *trans effect* (kinetic) and *trans influence* (thermodynamic), will have a large influence of the metal-ligand bond strength and will also effect the rate of ligand substitution.[28]

2.3 Reactive ruthenium complexes in organic synthesis

Many ruthenium complexes possess a number of properties that make them suitable as catalysts in organic synthesis. Ruthenium complexes containing ligands such as carbonyls, halides, phosphines, pyridinyl, aminoalcohols, cyclopentadienyl, dienes and carbenes, have proven to serve effectively as the activating factors for generation of coordinatively unsaturated species by the dissociation of ligands, and/or stabilization of reactive intermediates. Moreover, ruthenium complexes also exhibit a variety of useful properties, such as low redox potential, high electron transfer ability, high ability to coordinate heteroatoms, Lewis acid acidity, unique reactivity of metallic species and intermediates including oxo-metals, metallacycles, and metal carbene complexes.[29] Therefore, scientists around the world have been able to develop a broad range of useful reactions by applying catalytic amounts of various ruthenium complexes.[29-51] The field of ruthenium catalysis is too large to cover completely or to discuss in detail, but in order to illustrate the broad scope of complexes and applications in catalytic reactions, some selected examples of catalytically active ruthenium complexes are shown in Figure 12.

Examples of ruthenium catalyzed reactions include hydrogenation, transfer hydrogenation, oxidation of alcohols, alkenes and amines, water oxidation, and hydrogen autotransfer reactions. Moreover, C-C bond formation via ruthenacycle intermediates and via π-allylruthenium intermediates, as well as reductive amination of allylic alcohols, ring closing metathesis (RCM) and cross metathesis (CM) have become very popular tools in organic synthesis. Development of cyclopropanation, nucleophilic addition to alkynes, and hydrosilylation also utilizes various Ru-complexes as catalysts. Even further, C-H activation (sp, sp^2, sp^3), C-halogen bond activation, cycloaddition reactions, reduction of CO_2, isomerization, and racemisation of secondary alcohols are also popular transformations using Ru-complexes. Some selected examples from the literature are shown in Figure 13, employing the Ru-complexes shown in Figure 12. The use of various [RuCp*Cl]-complexes as catalysts in alkyne-azide 1,3-cycloaddition, i.e. the RuAAC reaction, will be discussed in more detail in Chapters 3, 5 and 6.

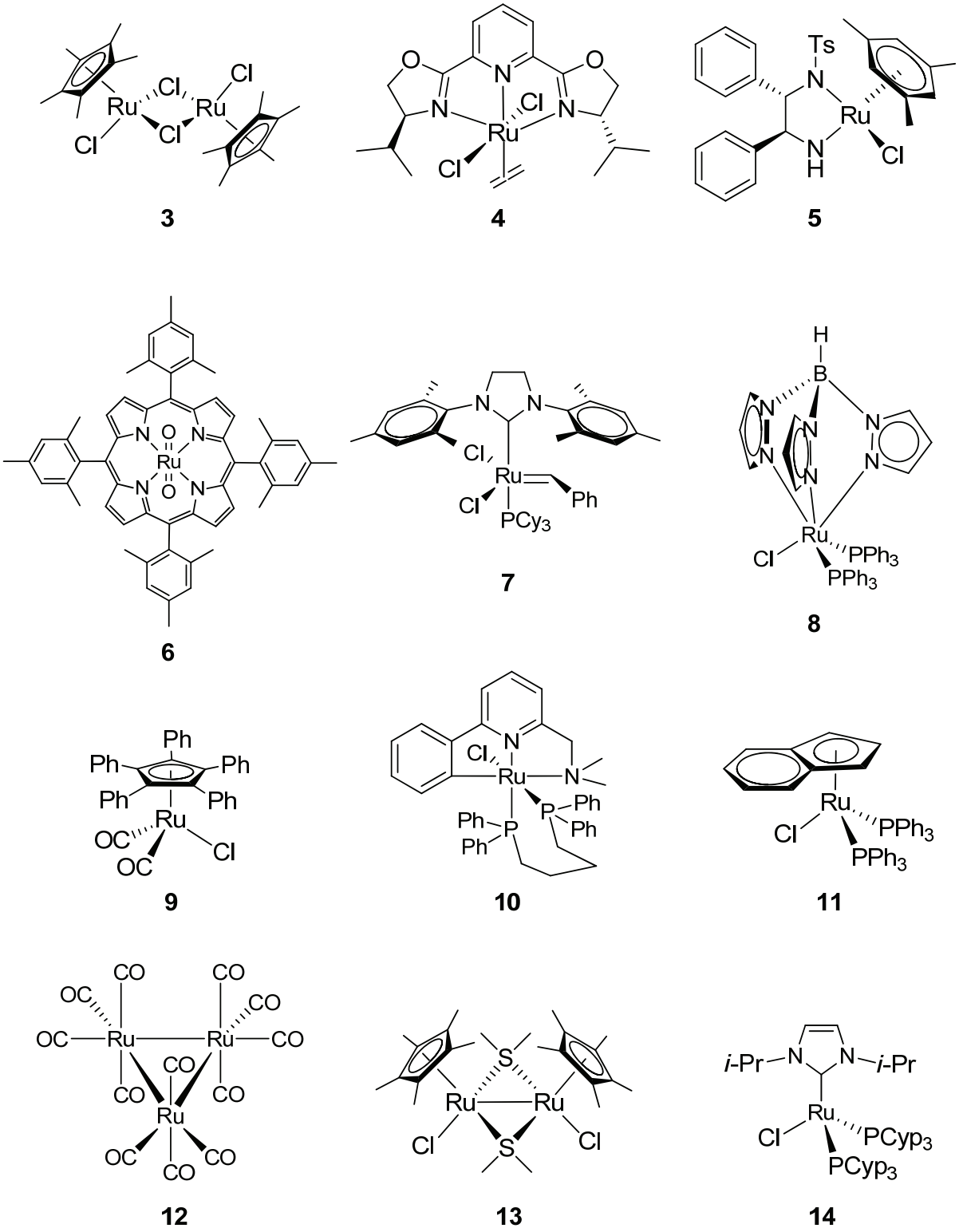

Figure 12. Various examples of catalytically active Ru-complexes used in organic synthesis (Cyp = cyclopentyl).

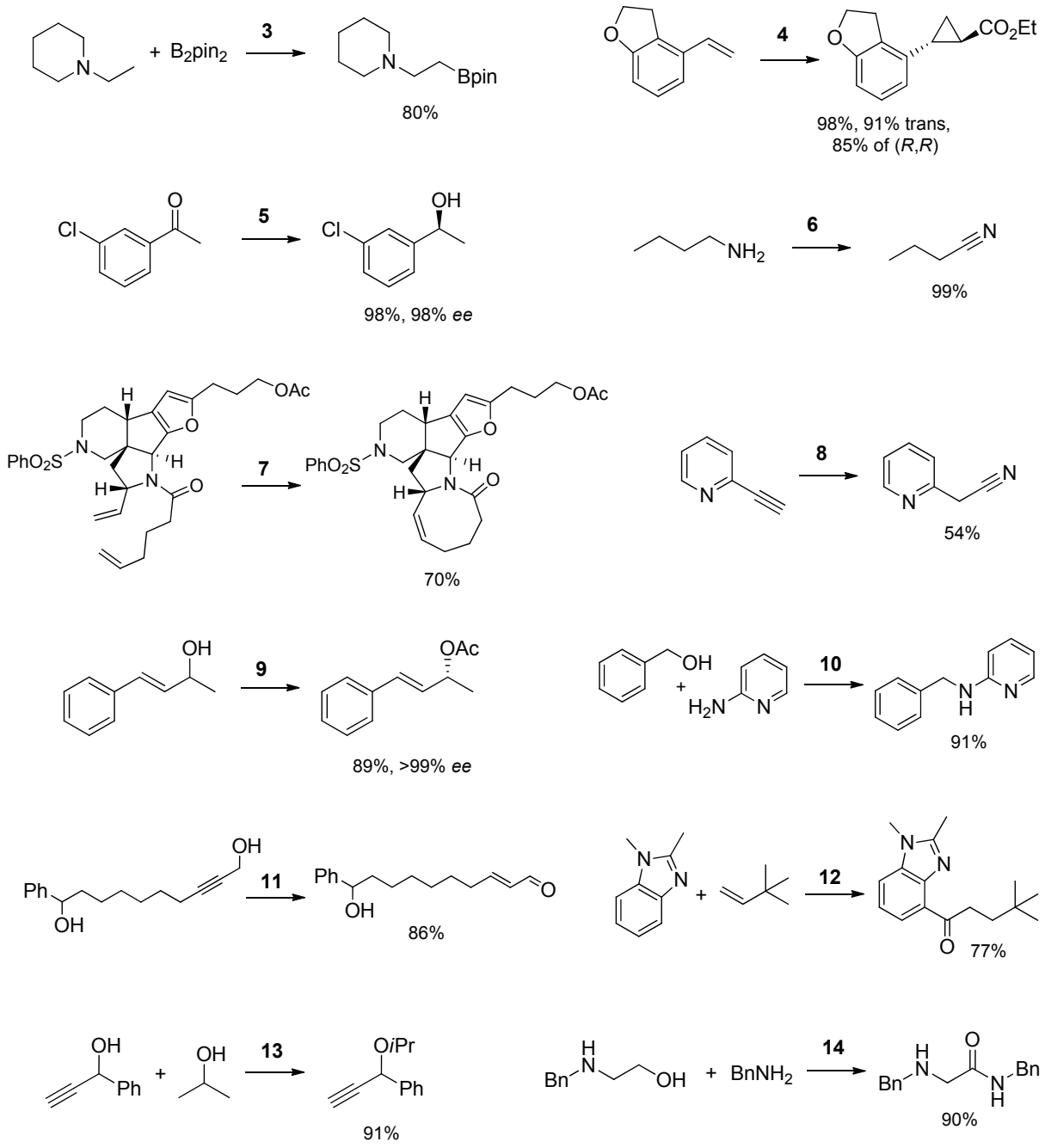

Figure 13. Some diverse examples of chemical transformations achieved by Ru-catalysis. Regiospecific borylation of methyl C-H bond by Ru-complex **3**.[39] Asymmetric cyclopropanation by Ru-complex **4**.[52] Asymmetric transfer hydrogenation by Ru-complex **5**.[53] Aerobic dehydrogenation of amines by Ru-complex **6**.[54] Ring-closing metathesis by Ru-complex **7**.[55] Addition of hydrazines to terminal alkynes catalyzed by Ru-complex **8**.[56] Metal- and enzyme-catalyzed dynamic kinetic resolution by Ru-complex **9**.[57-58] Selective alkylation of amines with alcohols catalyzed by Ru-complex **10**.[59] Redox isomerisation of propargyl alcohols by Ru-complex **11**.[60] sp^2-C-H activated carbonylation catalyzed by Ru-complex **12**.[61-62] Propargylic substitution catalyzed by Ru-complex **13**.[63-71] Amide formation catalyzed by Ru-complex **14**.[72]

2.4 Stable ruthenium complexes as probes and single electron transfer catalysts

Ruthenium complexes containing stable bidentate ligands such as 2,2'-bipyridine (bpy) can form very stable octahedral complexes like $[Ru(bpy)_3]^{2+}$ (Figure 14), which exhibit interesting and useful photochemical properties, and are not suitable as catalysts in chemical transformations in the same sense as the ones shown in Figure 12. Nevertheless, $[Ru(bpy)_3]^{2+}$ has become very popular as a sensitizers in photoredox catalysis.[73] $[Ru(bpy)_3]^{2+}$ absorbs light in the visible region (452 nm) of the electromagnetic spectrum to give stable, long-lived photoexcited states (τ = 1100 ns).[74] The lifetime of the excited species is sufficiently long that it may participate in bimolecular electron-transfer reactions in competition with deactivation pathways,[75] as well as a being an efficient single electron transfer (SET) catalyst.[76]

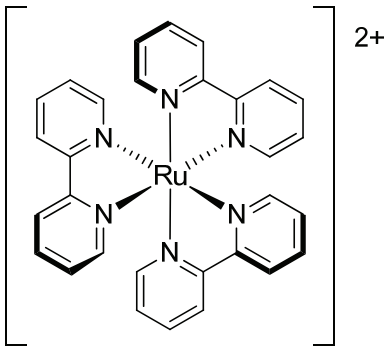

Figure 14. The structure of $[Ru(bpy)_3]^{2+}$.

These properties of Ru-complexes such as $[Ru(bpy)_3]^{2+}$ have made them an interesting and useful tool as fluorescent probes in physical chemistry, in many different contexts. By varying the ligands on ruthenium, the emission properties of a Ru-complex can be fine-tuned.[77-80] The complexes becomes even more useful as probes when one of the ligands is replaced by a dipyrido[3,2-*a*:2',3'-*c*]phenazine (dppz) ligand, which makes their luminescent properties very sensitive towards the environment. The complexes $[Ru(phen)_2dppz]^{2+}$ and $[Ru(bpy)_2dppz]^{2+}$, shown in Figure 15, are called light-switching complexes due to the fact that they are brightly luminescent upon intercalation into DNA, while in water the excited states are almost completely quenched by water H-bonding to the dppz's phenazine nitrogens.[81-83]

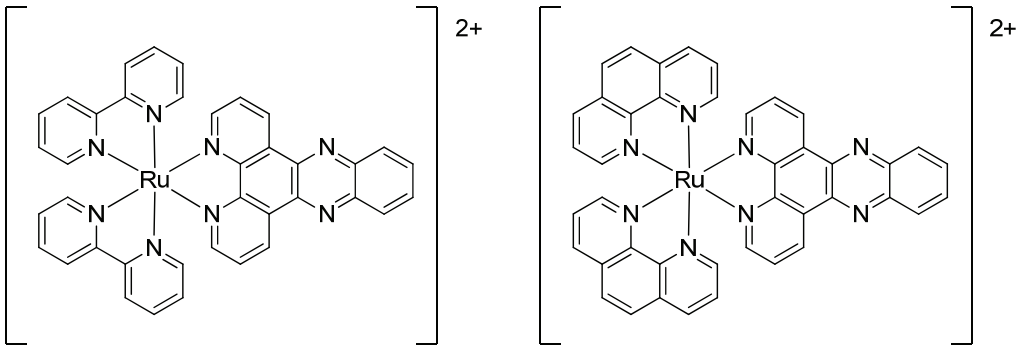

Figure 15. The light-switch complexes $[Ru(phen)_2dppz]^{2+}$ and $[Ru(bpy)_2dppz]^{2+}$.

The long-lived excited states of these Ru-probes also makes them vital tools for studying dynamics and rotational motions of biological molecules.[84] In 1984, Barton et al. reported a

DNA-binding study of $[Ru(phen)_3]^{2+}$, which was an important milestone for the field of ruthenium-based DNA-probes. [85] Since then, several examples of ruthenium complexes that selectively bind to different DNA and RNA bulge structures,[86] compact DNA,[87-88] display cytotoxic activity,[89-90] or stain various cellular components, [91-93] have been studied with the hope for potential applications as diagnostic probes, anti-cancer drugs, imaging agents or gene delivery vectors. The use of binuclear ruthenium complexes as DNA threading intercalators will be discussed later in this thesis in Chapter 7, together with synthesis of new binuclear ruthenium complexes.

3 1,3-Dipolar Cycloadditions as a Route to Nitrogen Heterocycles

3.1 1,3-Dipoles

There are many ways to synthesize nitrogen heterocycles, including ring closure, ring expansion, condensation, and cycloaddition reactions. From now on we will focus on 1,3-dipolar cycloadditions as a route to form 5-membered nitrogen heterocycles.

The work done by Curtius in 1883, when he reported the first synthesis of diazoacetic esters,[94] enabled the first 1,3-dipolar cycloadditions between diazoacetic esters with α,β-unsaturated esters, to be carried out by Buchner *et al*. a few years later. [95] In 1963 Huisgen *et al.* published a systematic study on concerted 1,3-dipolar cycloadditions,[96] based on previous work by Smith and co-workers,[97] including also kinetic studies on the mechanism.[98] The reaction between a highly polarized 1,3-dipole (a-b-c) and a dipolarophile (d-e), i.e. a double or triple bond, is often called a 1,3-dipolar cycloaddition, shown in Figure 16.

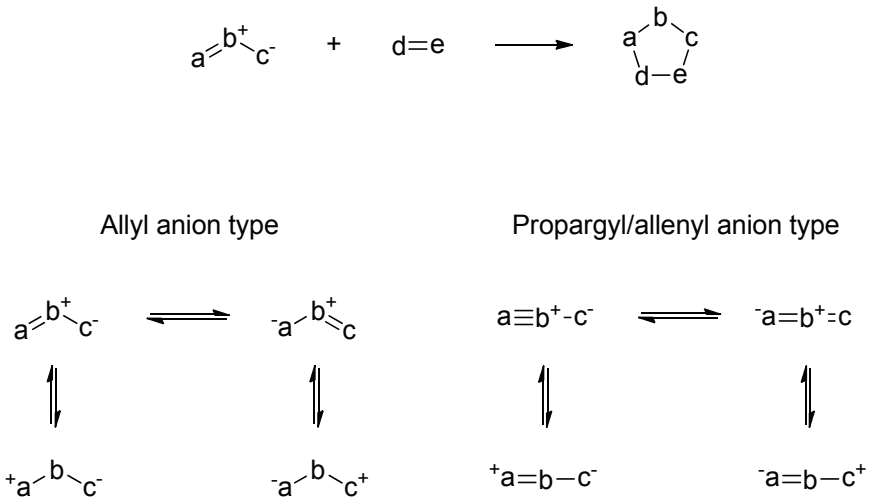

Figure 16. Two types of dipoles, allyl- and propargyl anion type, are used in 1,3-dipolar cycloadditions.

However, the formal name is a [3+2] cycloaddition, and this reaction leads to a remarkably wide variety of 5-membered heterocyclic compounds. The classification of the most common 1,3-dipoles are outlined in Figure 17.[99-100]

Besides the concerted mechanism of 1,3-dipolar cycloadditions reported by Husigen, a stepwise mechanism via a singlet diradical intermediate has been proposed.[101] In a computational study of the 1,3-cycloaddition between nitrones and alkenes, Di Valentin et al. found that the concerted mechanism should be much more favourable than the stepwise diradical mechanism.[102-103] To date, the Husigen 1,3-dipolar cycloaddition is described as nonconcerted when catalysts, proceeding via metallacycle intermediates, are used, leading to substituted heterocycles in excellent selectivity.[104]

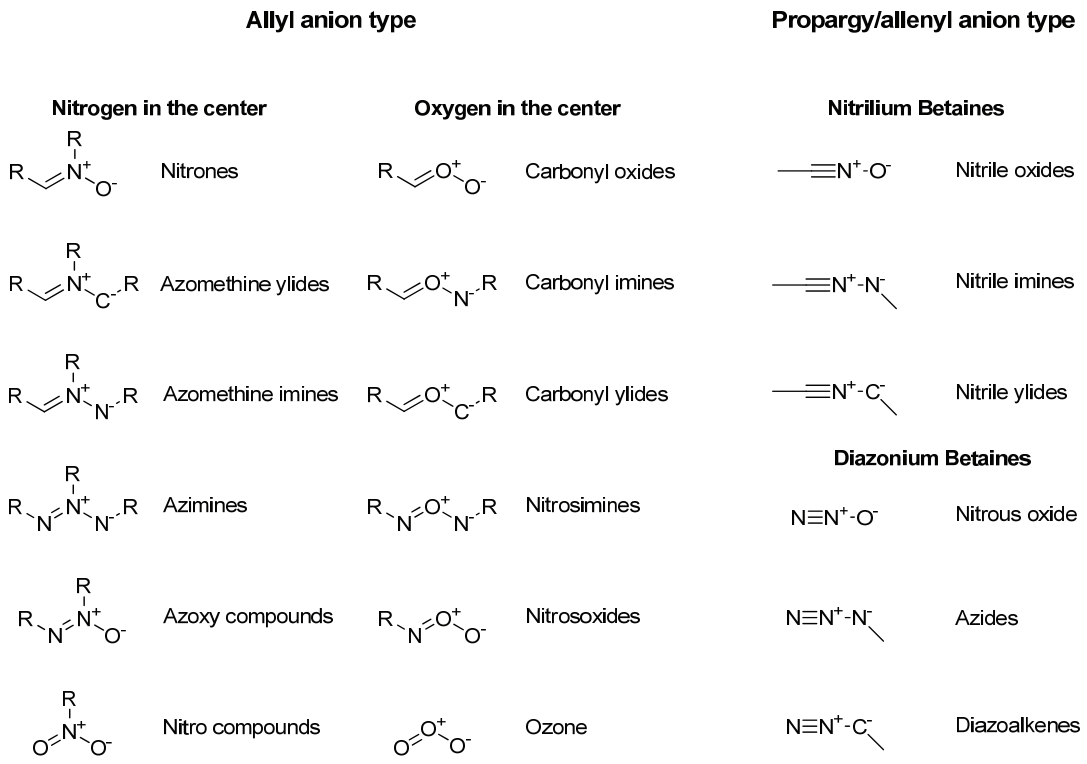

Figure 17. The classification of the most common 1,3-dipoles.

The understanding of the reactivity and regioselectivity of 1,3-dipolar cycloadditions is not always straightforward. However, frontier molecular orbitals (FMO) theory has shown to be a first approximation to a perturbation treatment of chemical reactivity and has been used to predict/explain the regioselectivity of several 1,3-dipolar cycloadditions[105-110] As an example, the thermal 1,3-dipolar azide-alkyne cycloaddition will result in a mixture of the two regioisomers (1,4- and 1,5-). By choosing the appropriate catalyst, the regiochemistry can be controlled and this will be described in more detail in the following chapters.

This thesis will focus on the 1,3-dipolar cycloaddition as a route to form 5-membered nitrogen heterocycles, more specifically, pyrrolidines and 1,2,3-triazoles (highlighted in Figure 6). Azides were used as dipoles in paper I and an azomethine ylide was used in paper IV.

3.2 CuAAC

The Huisgen reaction between azides and alkynes is very slow in the formation of triazoles at room temperature, and at higher temperatures the triazoles are formed as mixtures of the 1,4- and 1,5-regioisomer. Due to the superb independent discovery of the Cu(I)-catalyzed azide-alkyne 1,3-dipolar cycloaddition, also known as CuAAC,[111-112] in 2002 by both Meldal[113] and Sharpless,[114] 1,4-disubstituted 1,2,3-triazoles can now be obtained in excellent yield and regioselectivity (Figure 18). Not only does the Cu(I) catalyst control the selectivity, yielding only the 1,4-isomer of the product, but it also increases the reaction rate by approximately 10^7 times, and enables performance in aqueous media. The CuAAC reation offers several supplementary advantages that are characteristic of “Click Chemistry”, an expression coined

by Sharpless *et al.*[115] The definition of the term "Click Chemistry" is as follows: *"The reaction must be modular, wide in scope, give very high yields, generate only inoffensive byproducts that can be removed by nonchromatographic methods, and be stereospecific (but not necessarily enantioselective). The required process characteristics include simple reaction conditions (ideally, the process should be insensitive to oxygen and water), readily available starting materials and reagents, the use of no solvent or a solvent that is benign (such as water) or easily removed, and simple product isolation. Purification - if required - must be by nonchromatographic methods, such as crystallization or distillation, and the product must be stable under physiological conditions."* Today the CuAAC reaction is the most commonly used 1,3-dipolar cycloaddition reaction in organic synthesis.[116]

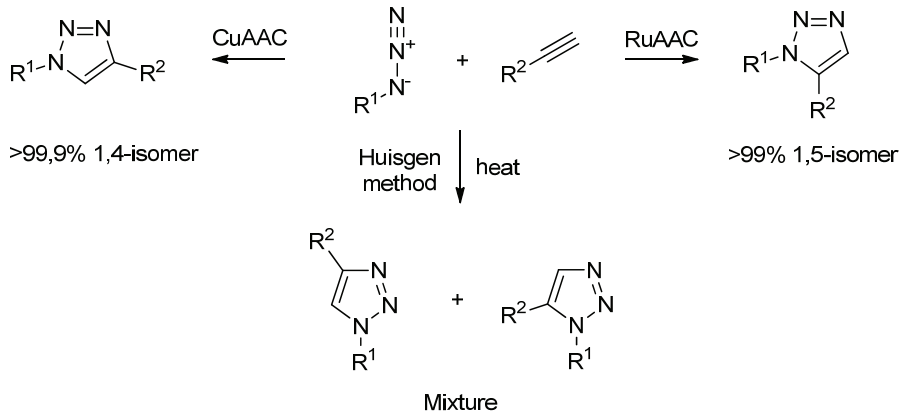

Figure 18. Control of the regiochemistry in azide-alkyne 1,3-dipolar cycloaddition.

The active copper species in the CuAAC reaction is Cu(I), but both Cu(0) and Cu(II) may be used as well. Most frequently, Cu(II)-salts are selected as an appropriate copper source, since they can easily be reduced *in situ* to Cu(I) in the presence of a reducing agent. Sodium ascorbate is the most commonly used reducing agent for Cu(II)-salts when the CuAAC reaction is performed in an aqueous media.[114,118-120] In order to ensure that all Cu(II) has been reduced to Cu(I) and remains as Cu(I) during the reaction, an excess of the reducing agent is required. The direct use of Cu(I)-salts is less frequent, due to the instability of the Cu(I)-species under aerobic conditions. To prevent oxidation of the active catalyst, the CuAAC reaction needs to be performed under anaerobic conditions or a stabilizing ligand can be added. A number of ligands that have been used to stabilize the Cu(I)-species are shown in Figure 15. Several of these ligands are known to increase the life time of the Cu(I)-species, thereby allowing reactions to be performed under air. The most well-known stabilizing ligand is the tris((1-benzyl-1*H*-1,2,3-triazol-4-yl)methyl)amine (TBTA) ligand **15** investigated by Fokin *et al.* [121] Not only do the ligands **15** – **26** (shown in Figure 19) protect the active Cu(I)-species under aerobic reaction conditions, they also accelerate the rate of triazole formation. Beside the rather complex amine ligands in Figure 19, the use of more common bases like, pyridine[124] and lutidine[125] and also amino acids like proline[126-128] and histidine[129-130] have been studied as rate accelerating additives.

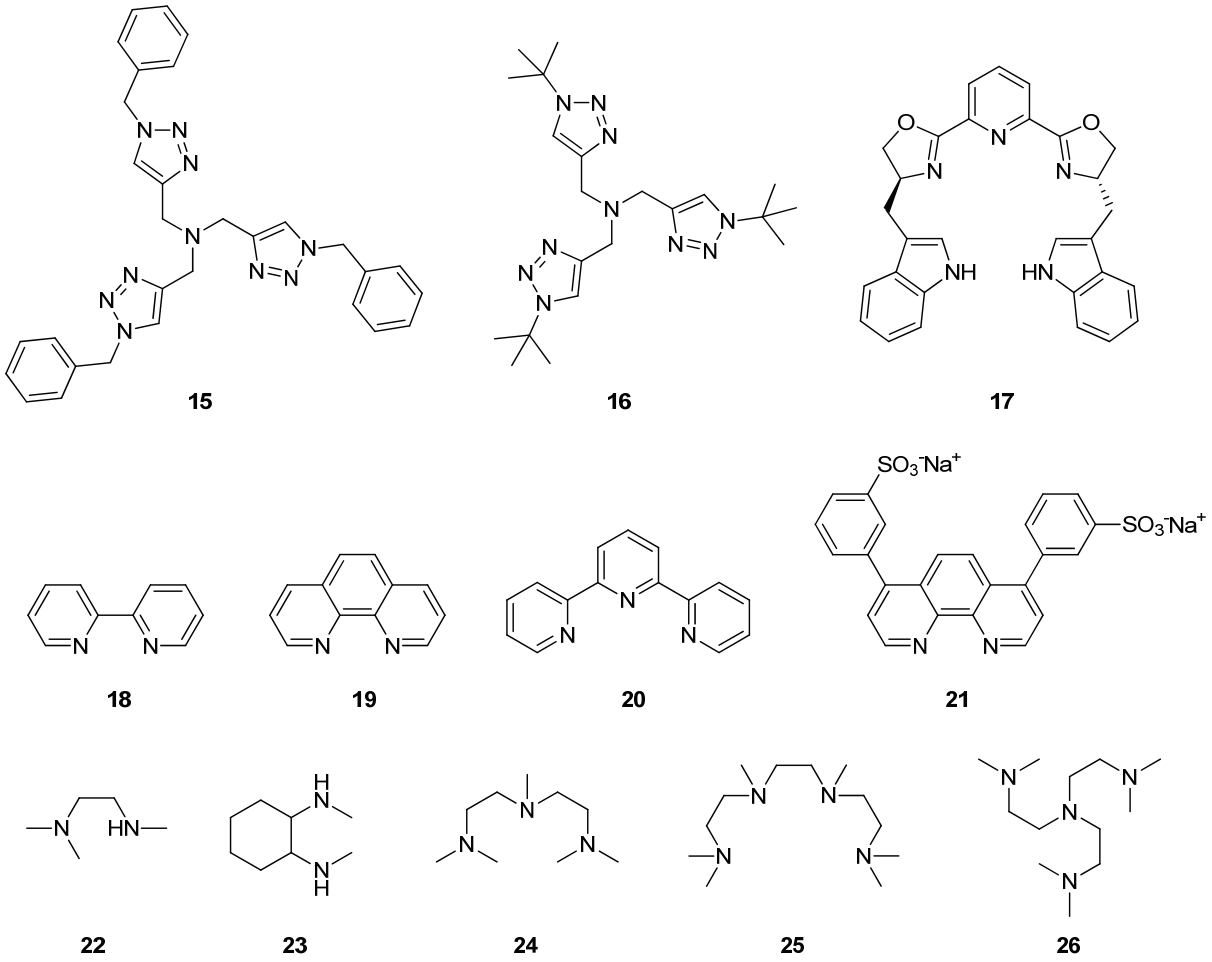

Figure 19. Structure of several ligands which have been used to stabilize Cu(I)-species.

Today the two most active catalysts for the CuAAC reaction are the Cu(I)-TBTA complex[118,131-133] and the Cu(I)-bathophenanthrolinedisulfonic acid complex.[129,134-137] The use of $[Cu(CH_3CN)_4]PF_6$,[114] $[Cu(CH_3CN)_4]BF_4$[117] and $[Cu(PPh_3)_3]Br$[122-123] have been shown to enhance solubility in non-aqueous systems as compared to the normal CuBr and CuI salts. Moreover, Cu(I)-species have been loaded onto solid supports,[138,139] zeolites[140,141] and Al_2O_3 nanoparticles.[142] Cu(0) can also catalyze the CuAAC reaction indirectly *via* the formation of Cu(I) by comproportionation of Cu(II) and Cu(0). The essential Cu(II)-species can be added, but is not mandatory due to the presence of traces of copper oxides and carbonates on the metal surface. However the disadvantage of this procedure is that it suffers from long reaction times.

Despite several mechanistic investigations and computational studies, the proposed mechanism of the CuAAC reaction outlined in Figure 20 has not yet been completely proven.[114, 116, 118, 143-146] Some details, especially those concerning the complexation of the Cu(I)-species and the origin of selectivity of the cycloaddition, are still unknown.

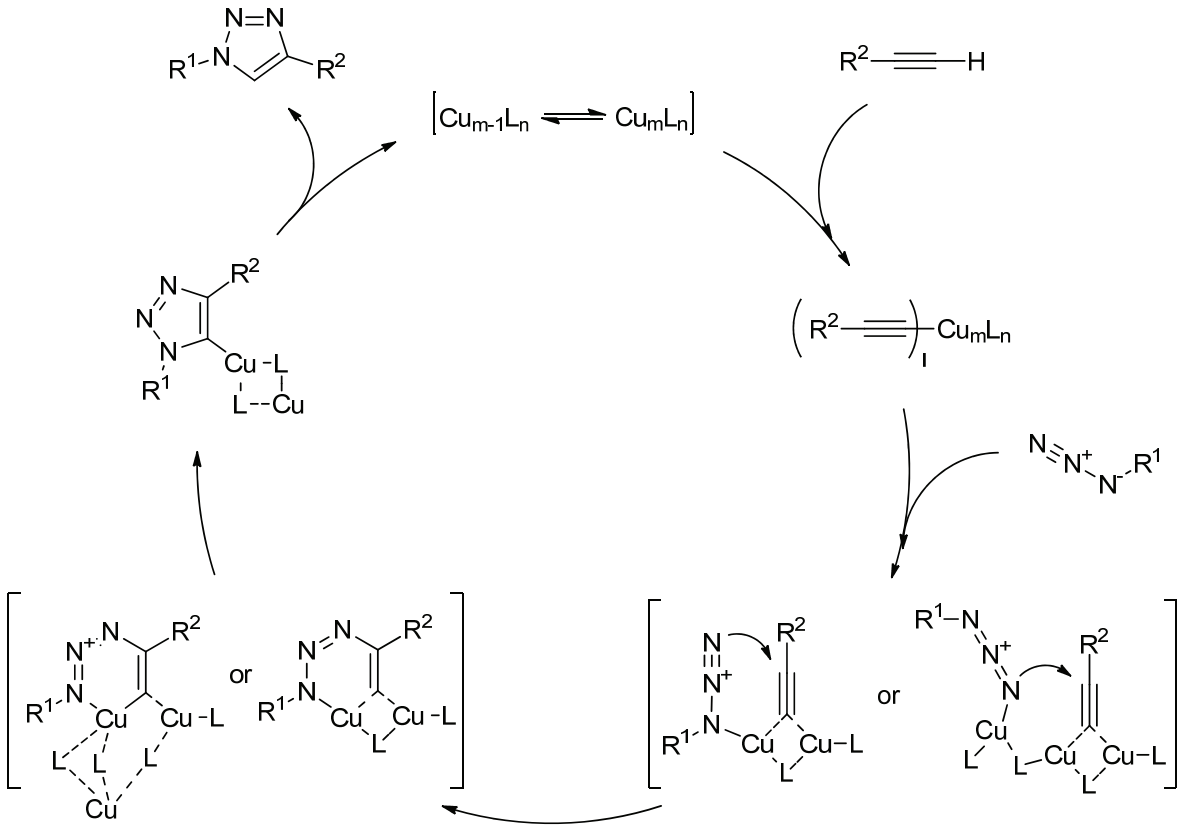

Figure 20. Proposed mechanism for CuAAC reaction.[116]

3.3 RuAAC

Selective formation of 1,5-disubstituted 1,2,3-triazoles can today also be achieved by the use of a ruthenium catalyst in the so called RuAAC reaction (Figure 18), first reported in 2005 by Fokin in collaboration with Jia.[147] In contrast to the CuAAC reaction, the RuAAC reaction also works well on internal alkynes, giving rise to trisubstituted 1,2,3-triazoles. The selectivity of unsymmetrical internal alkynes has been studied by Majireck and Weinreb.[148] Since the first report on the RuAAC reaction, a few studies on the scope and reaction mechanism have been carried out,[149-151] and the RuAAC reaction has been used in various applications,[152-155] but to a far lesser extent compared to the popular CuAAC reaction. The reason is probably due to lower tolerance towards functional groups on any of the substrates and sterical hindrance on the azide, as well as limitations in terms of the solvents that can be used.

The active species of the ruthenium catalyst seems to be [RuCp*Cl] and a number of complexes with different ligands have shown good activity and selectivity. Many results point toward the Cp* ligand (pentamethylcyclpentadiene anion) as the key element in the catalyst responsible for the high 1,5-selectivity. The mechanism for the RuAAC reaction has been studied by theoretical calculations, and the proposal by Fokin and Jia is outlined in Figure 21,[150] and a recent proposal from the Nolan group is shown in Figure 22.[151] The electronic effects on internal alkynes have been studied by Hou et al.[156] and recently an interesting

method to assign the regiochemistry of 1,2,3-triazoles by ^{13}C NMR has also been reported by Creary et al.[157]

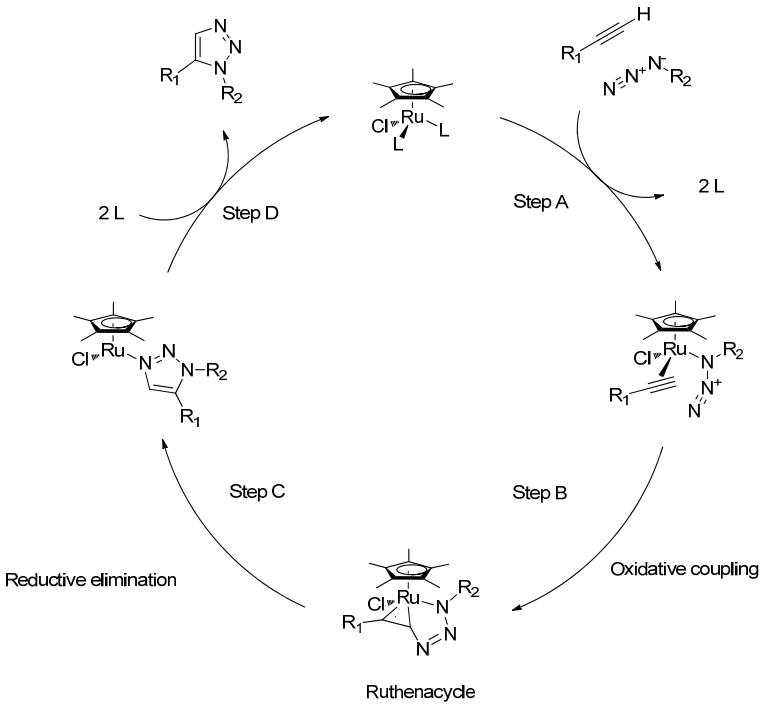

Figure 21. Mechanism for the RuAAC reaction proposed by Fokin. L = PPh_3 or 2 L = COD.[150]

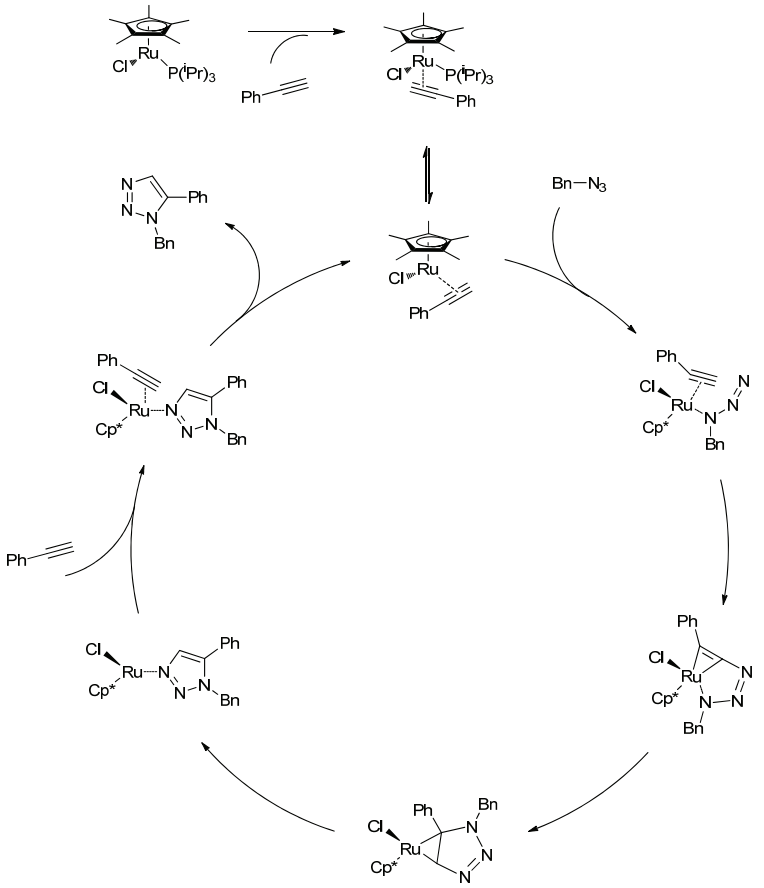

Figure 22. Mechanism for the RuAAC reaction proposed by Nolan.[151]

3.4 Azomethine ylide cyclizations

Another 1,3-dipolar cycloaddition is the one between azomethine ylides and activated double bonds, forming pyrrolidines. One example is the solvent free microwave-assisted [3+2] cycloaddition of stabilized azomethine ylides **27** with nitrostyrenes **28**, leading to the sterioisomeric 4-nitropyrrolidines **29** in 79-87% yield, reported by Arrieta et al. and shown in Figure 23.[158] The azomethine ylide in this reaction is a resonance form of the imine, stabilized by the ester group.

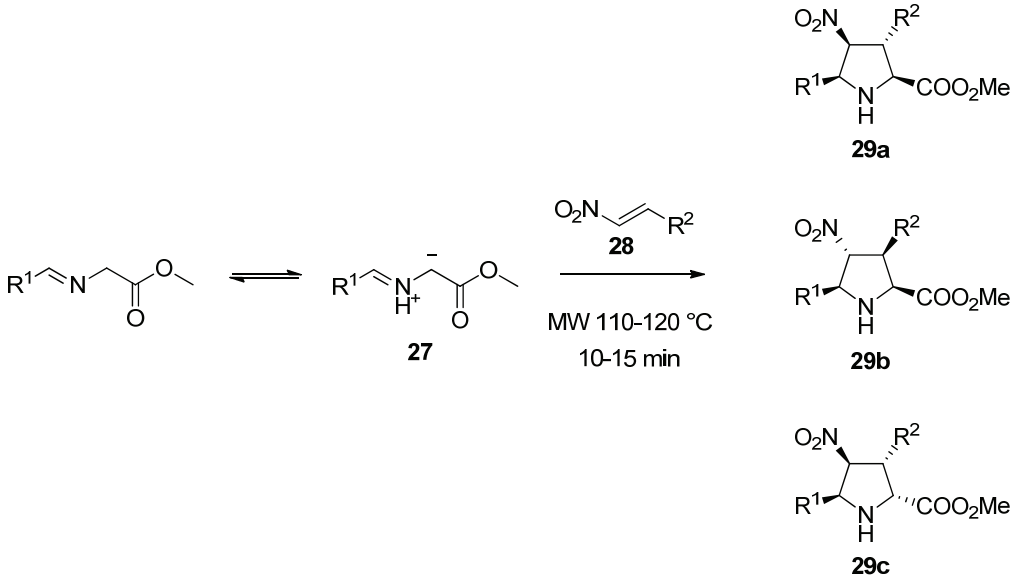

Figure 23. 1,3-Dipolar cycloaddition of azomethine ylides with nitro styrenes.

Azomethine ylides have also been used in the synthesis of *C*(2)-unsubstituted penems, in the form of β-lactam-based azomethine ylide **31**. Thermolysis of β-lactam **30** by microwave heating in toluene led to azomethine ylide **31** and *in situ* cycloaddition with *S*-methyl dithioformate yielded the thiazolidine **32** in 76%.[159,160] Subsequent mild oxidation and base treatment affords the *C*(2)-unsubstituted penem **33**, as shown in Figure 24.

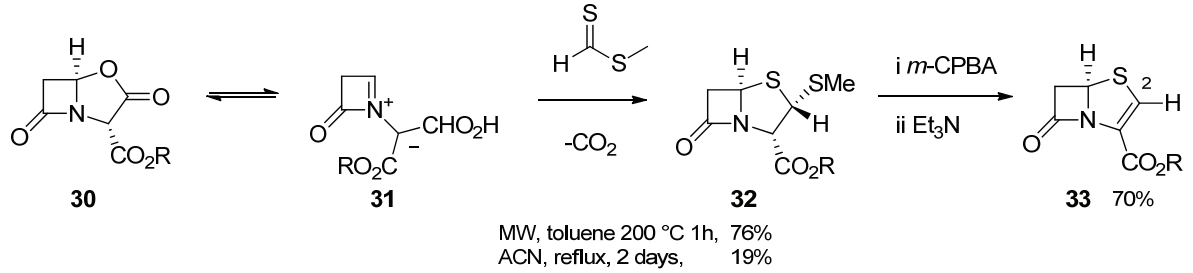

Figure 24. Azomethine ylide formation by thermolysis of β-lactam **30**.

More importantly from our point of view is the broad number of reports on the 1,3-dipolar cycloaddition of azomethine ylides to C_{60}, first described by Prato,[161] and also to carbon nanotubes (CNTs) in solution.[162-172] An example where the azomethine ylides are generated by decarboxylation of iminium ions derived from the condensation of amino acids with aldehydes affording fulleropyrrolidines **34**, is shown in Figure 25.

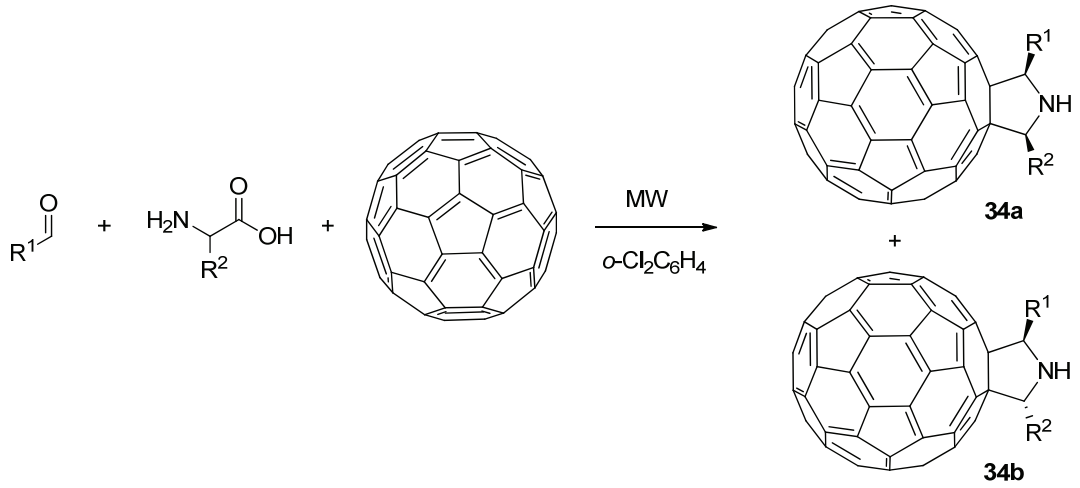

Figure 25. 1,3-Dipolar cycloaddition of azomethine ylides to C_{60}.

Worth to mention is that the functionalized CNTs can also be converted back to unmodified CNT upon heating to above 350 °C, as reported by Prato and Ballerini.[173,174] This technique is often used to purify CNTs.

4 Peptidomimetic Foldamers

4.1 Foldamers

A foldamer is a non-natural folded peptidomimetic oligomer.

Over the last two decades, non-natural biocompounds, with structure and function mimicking the natural biocompunds, have attained exceptionally increased scientific attention due to their potential applicability in diverse areas such as chemical biology, pharmacology, or bionanotechnology. The most successful advances in the future are anticipated in areas where the synthetic compounds are capable of retaining the beneficial characteristics of natural molecules, while showing significant enhancement in other properties where the latter have limitations. As such an example, the study of foldamers has become a separate field.[175-178]

The term *foldamer* as defined by DeGrado:

"*Foldamers are sequence-specific oligomers akin to peptides, proteins and oligonucleotides that fold into well-defined three-dimensional structures"*

Because of the diversity of sizes, shapes and properties available to non-natural monomers, this field offers a myriad of opportunities for the design of molecular interaction modules supported by foldamer scaffolds. The creation of these scaffolds has already resulted in many useful and functionally interesting foldamers, capable of mediating cell penetration,[179-180] and showing advantageous qualities such as enzyme resistance,[181] antitumor,[182] antiviral, antifungal and antibacterial activity.[183-193] Moreover, designed foldamers with specific binding to various targets, including proteins,[194-201] RNA,[202] DNA,[182, 203-204] membranes,[205-214] and carbohydrates[215] have also been reported. Often these foldamers show affinities matching or even outperforming those of natural α-peptides.

4.2 Foldamer classes and structures of monomers

Foldamers can generally be divided into two classes, aliphatic foldamers and aromatic foldamers, depending on if the amine and acid functional group of the monomer is interrupted by an aromatic unit or not. Aliphatic foldamers can for example consist of α-,[195, 216] β-,[217-219] γ-[220-222] or δ-amino acids,[223-224] oligoureas,[225] or azapeptides.[226-227] Some examples of a few common frameworks are shown in Figure 26.

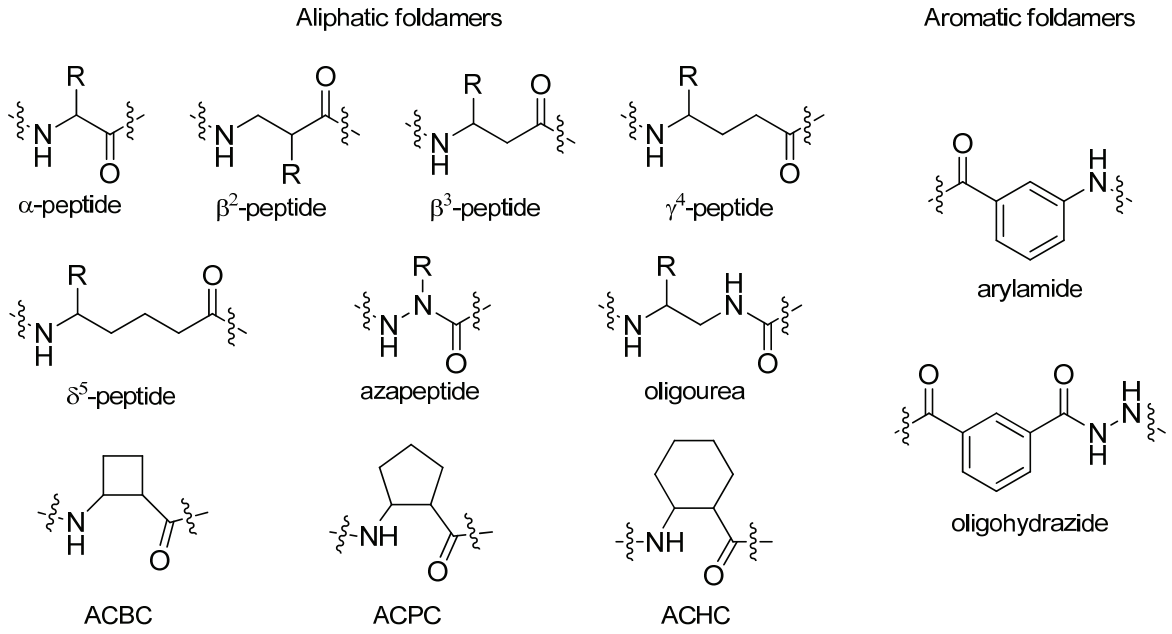

Figure 26. Examples of foldamer frameworks

4.3 Secondary structures of foldamers

When foldamer monomers are combined into homo-oligomers or hetero-oligomers, they exhibit an affinity to fold into different secondary structures depending on the type of residue, sequence, chirality, and substituents. These secondary structures are stabilized by non-covalent intramolecular interactions, most often hydrogen bonds (H-bonds), and give rise to different conformers. Their nomenclature is commonly based on the size of the pseudo-ring formed by the intramolecular interaction and on the type of the resulting secondary structure. In Figure 27 some of the simplest conformers of *β*-peptides are shown. Here *C* stands for conformer, *H* for helix and the number denotes the number of atoms in the intramolecular H-bond pseudo-ring. Predictions by *ab initio* MO theory[177] of short sequences of unsubstituted *β*-alanine have shown that C_6 and C_8 oligomers are favoured by the backbone, and also as the sequence is increased, structures such as H_{10} and H_{12} are favoured internally by cooperative effects. In contrast, these calculations also suggest that for non-cyclic peptide backbones the H_{14} is disadvantaged, however polar solvents and appropriate sequences will greatly stabilize it, making it one of the most commonly observed helices experimentally. This shows the important influence of the chemical environment (the solvent) on the stability of the different conformers.

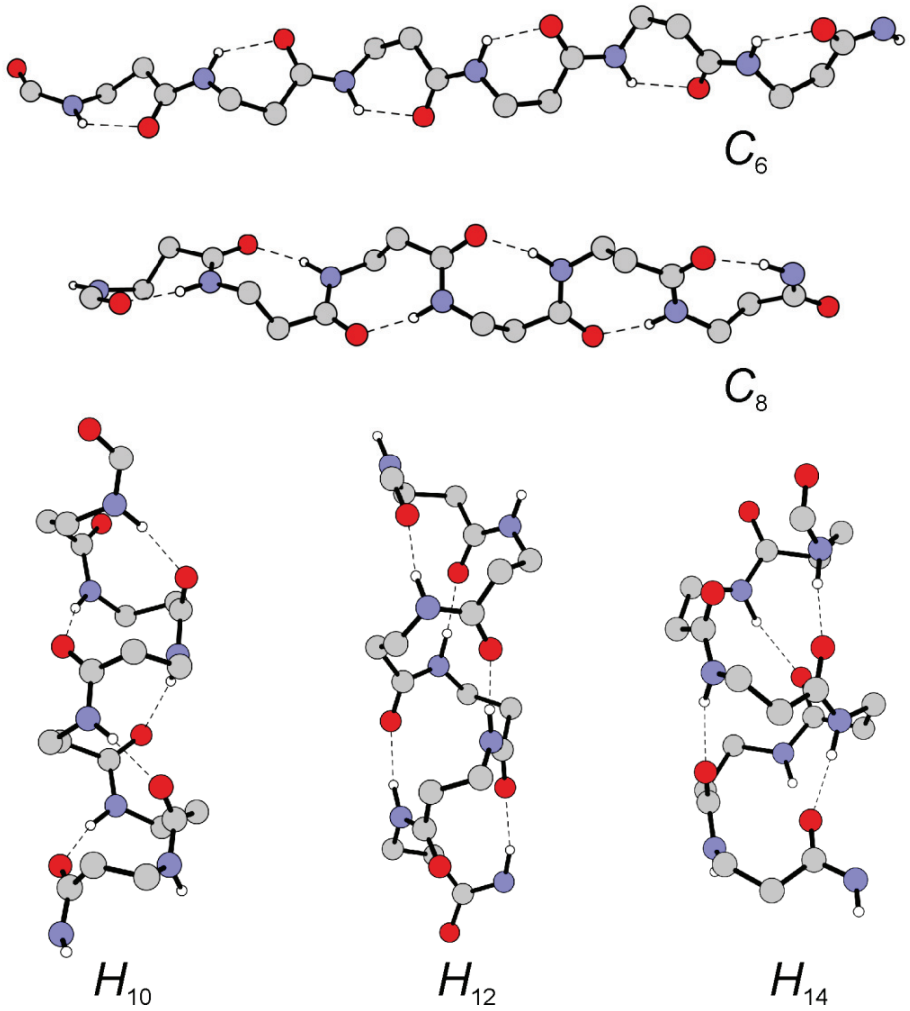

Figure 27. Oligomers of β-peptides can adopt several conformational structures, such as C_6-ribbon, C_8, H_{10}, H_{12} and H_{14}.

In order to stabilize a preferred secondary structure from all the possible conformers, suitable substituents can be introduced at specific positions with the appropriate chirality on the monomer.[218, 219, 229-231] Recent work has further extended the concept of stabilizing secondary structures with cyclic side-chain topology. De Pol et al. have reported helix-like foldamers built up from β-amino cyclopropanecarboxylic acids.[231] Likewise, Izquierdo et al. observed a 14-membered H-bonded ring for a tetramer containing two *cis*-aminocyclobutanecarboxylic acid (*cis*-ACBC) residues and two β-alanines in alteration, indicating the tendency of the ACBC unit to fold.[232] If the *cis*-ACBC is elongated into homo-oligomers, they exhibit strand-like structures that are stabilized by 6-membered intramolecular H-bonds, which facilitate supramolecular interactions and self-assembly, producing nanosized fibres or gels.[233-235] However, by switching to the *trans*-ACBC residue, hexamers and octamers demonstrate a preference to fold into well-defined H_{12}-helical conformers, both in solution and in the solid state.[236]

Not only can a foldamer form different helix structures depending on the H-bond ring-sizes, but also chiral left-handed (*M*) and right-handed (*P*) helixes. If a foldamer backbone is achiral, both the *M* and *P* helices will be present and most probably also be in fast equilibrium with each other (Figure 28.). By introducing chiral residues in a foldamer sequence, the equilibrium will shift and the framework will favour either the *M*-helix or the *P*-helix structure.

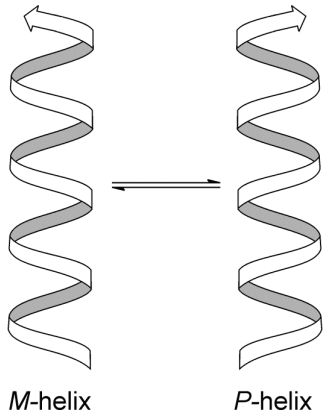

Figure 28. *M*- and *P*-helixes in equilibrium.

The Clayden group have made some very interesting foldamer research where they investigated how far information can be transferred by conformational changes.[237-241] They used amino-*iso*-butyric acid (Aib) as the monomer to synthesize long oligomers. Oligomers of Aib adopt stable H-bonded helical structures, usually H_{10}, with a low barrier to inversion between the enantiomeric *M*- and *P*-forms. By attaching a switchable reporter unit (3-phenyllactate) in one end and a receiver unit (^{13}C-labelled Aib helicity detector) in the other end, they have demonstrated conformational communication through the helices up to 12-residues of Aib by using ^{13}C NMR to read the output signal.[242] Figure 29 shows the schematic structure of Claydens switchable foldamer helix.

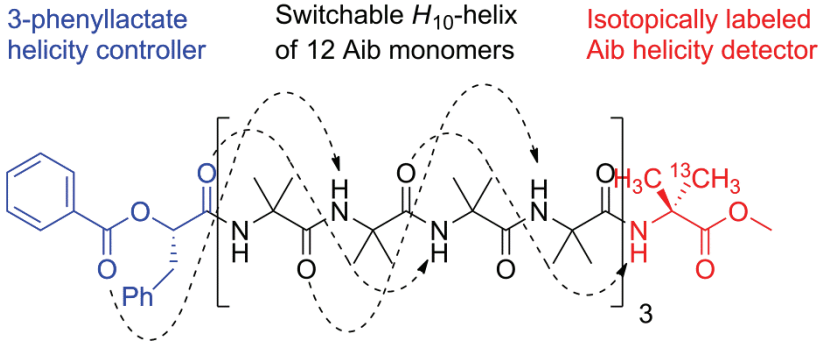

Figure 29. Clayden's switchable Aib foldamer, capped by a 3-phenyllactate controller and a ^{13}C-labelled Aib detector.[242] Dashed arrows shows interresidual H-bonds, responsible for the formation of the H_{10}-helical secondary structure.

By hydrolysis of the benzoate ester and inversion of the stereochemistry of the alcohol via the Mitsunobu reaction,[243-245] the readout in terms of the intensity of the ^{13}C-shifts for the methyl-groups on the end Aib-receiver was inverted. This result proves that the switchable chirality

on the controller unit determines the favoured chirality of the foldamer helix, which is transferred all the way through to the detector unit.

4.4 Triazoles in peptidomimetics and foldamers

The triazole unit, both in the form of the 1,4- and the 1,5-regioisomer, has become a popular building block in peptidomimetics over the last 10 years.[246-247] This is mainly because their structural and electronic characteristics are similar to those of a peptide bond, but also because general synthesic methods are now available via the CuAAC[113-115, 248] and the RuAAC[147-150, 249] reactions, both described in more detail in Chapter 3. 1,4- and 1,5-triazoles are good analogues of peptide bonds because they are planar, while at the same time possessing a strong dipole and H-bond properties that mimic those of a peptide bond. The 1,4-substituted triazole is a fine mimic of a common *trans*-peptide bond, even though it will give rise to slightly longer distances between the side chains, as seen in Figure 30. The 1,5-triazole on the other hand is a good mimic of the usually more unfavoured *cis*-peptide bond, which enables turn- and bent-peptidomimetic structures.

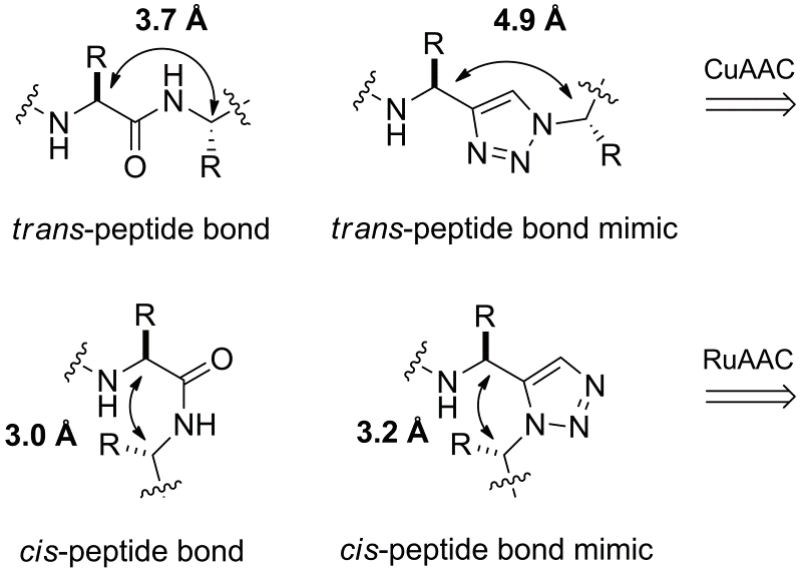

Figure 30. Comparison of 1,4-substituted triazoles with *trans*-peptide bonds and 1,5-substituted triazoles with *cis*-peptide bonds.

One of the greatest advantages with triazoles is that, unlike peptide bonds, they are proteolytically and metabolically stable. In addition, the azide and the alkyne precursors are relatively inert, enabling in vitro CuAAC reactions.[250-251] More recent development of the Huisgen cycloaddition of strained cyclic alkynes with azides,[252-253] has facilitated selective in vivo labelling of biomolecules in live mice.[254]

The 1,4-substituted triazole has been utilized to a great extent, both in linear and cyclic peptidomimetics,[255] as well as, in a few short oligomers, with and without intercepting peptide bonds.[256-260] Improved CuAAC reaction conditions, where the ratio between intramolecular cyclization and linear dimerization was increased, have been reported by Chouhan and

James.[261] The 1,5-substituted triazole, unit on the other hand, has not been exploited as much as the 1,4-isomer in the field of peptidomimetics. However, a few very interesting applications have been reported including their use in constrained histidine mimics,[262] in cyclic Vancomycin-inspired peptidomimetics,[263] as *cis*-peptide bond surrogates in RNase A variants from bovine pancreas and *Escherichia coli*[264] and in the peptoid oligomer **35** to induce turn formation,[265] which is shown in Figure 31.

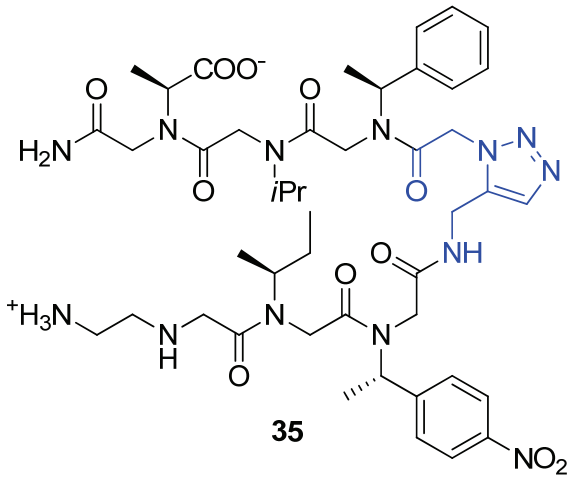

Figure 31. Incorporation of the 1,5-substituted triazole in a peptoid turn.

This leaves the foldamer field open for opportunities to investigate oligomers consisting of 1,5-substituted triazoles. Our initial results in this area will be presented in Chapter 6.

5 Ruthenium Catalyzed Azide-Alkyne 1,3-Dipolar Cycloadditions

5.1 Aim of the project

When we started to work with the RuAAC reaction, our aim was to develop a one-pot procedure where the hazardous organic azide is generated *in situ*. Such a procedure would be more simple and safe to use for the synthetic chemist since no isolation and handling of the neat organic azide would be needed. A convenient one-pot procedure has been reported for the CuAAC reaction[127] and our main goal for this project was to develop a similar method for the RuAAC reaction that would hopefully increase the use of the reaction.

5.2 Results

To begin our study, we started by reproducing the method from the literature, with our model reaction between 3-ethynyl pyridine and benzylazide, catalyzed by [RuClCp*(PPh_3)$_2$]. After heating the reaction mixture to 60 °C for 6 h in dioxane, 3-(1-benzyl-1*H*-1,2,3-triazol-5-yl)pyridine **36** was obtained in 92% yield after purification on silica. We also ran the reaction using microwave heating for 30 min at 100 °C, and this method gave similar results. We continued our study by reinvestigating in which polar solvents the RuAAC reaction can be performed and by varying the ratio between the azide and the alkyne. The results from the solvent investigation are shown in Table 1.

Table 1. RuAAC reaction to form triazole **36** with an alkyne/azide ratio of 1:1 in different solvents (conv. estimated by LCMS).

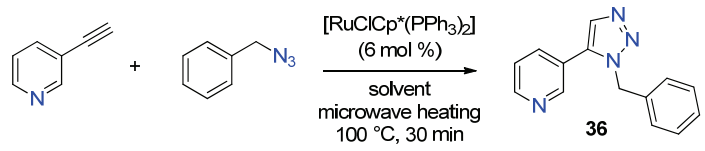

Solvent	Conv.	Solvent	Conv.	Solvent	Conv.
Dioxane	~95%	DMA	~95%	H_2O	~5%
THF	100%	DMSO	<5%	THF/H_2O 3:1	~10%
2-MeTHF	100%	CH_3CN	~5%	CH_3CN/H_2O 3:1	~5%

Apart from the good conversions obtained for the RuAAC reactions in dioxane, toluene and THF, DMA as well as 2-MeTHF also gave satisfying results. In contrast, the use of DMSO or ACN as the solvent gave only traces of product in the reaction. The use of water or other protic solvents such as ethanol, as well as mixtures of polar solvents with water, lead only to very low yields of the desired 1,5-disubstituted 1,2,3-triazole. Dimerization of the alkyne was found as the major by-product of the reaction,[266] albeit in small amounts (only a few %). The formation of the enyne by-product **38** could be suppressed to a minimum by employing two equivalents of the azide, but increased when an excess of the alkyne was used. Fokin *et al*. reported the formation of a stable catalytically inactive "azide dimerization - catalyst complex" **37** inhibiting the RuAAC reaction when an excess of azide was used, or when the azide was added to the catalyst prior to the alkyne.[75] However, in our system we could never detect (by LCMS or ^{1}H NMR on the crude reaction mixture) this complex during our reactions, even though two equivalents of the azide were used. Figure 32 shows the structure of these two possible by-products.

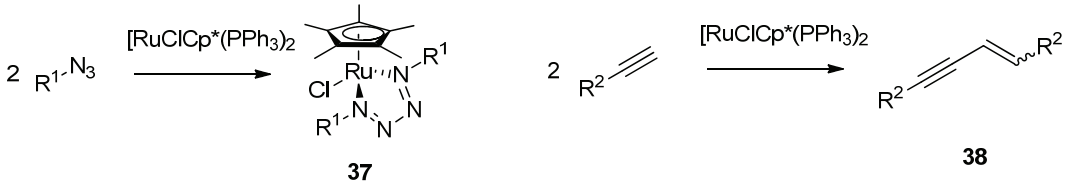

Figure 32. Possible by-products in the RuAAC reaction.

With the reaction conditions tuned, we turned our attention to developing a one-pot procedure. We wanted to investigate the possibility of using sodium azide in combination with an alkyl halide to generate the organic azide *in situ*, and to let this azide react directly in the RuAAC reaction without the need for isolation. Since the synthesis of organic azides from sodium azide and halides is usually performed in a polar solvent like DMSO, water or DMF (or mixtures thereof), the obvious choice for a one-pot procedure is DMF or DMA according to the results of the solvent screening. DMF has a lower boiling point than DMA and is thus easier to evaporate after the reaction, but it is also more toxic and starts to decompose when heated in a microwave above 130-140 °C. These properties lead to our choice of DMA as the solvent for a potential one-pot procedure. However, initial studies of a direct one-pot procedure were unsuccessful. Only traces of the triazole product was seen, and substantial amounts of starting materials remained unreacted. We believe that this procedure fails due to a side reaction of sodium azide with the catalyst. By substitution of the chloride with the nucleophilic azide anion an inactive catalyst complex **39** can be formed as shown in Figure 33.[267]

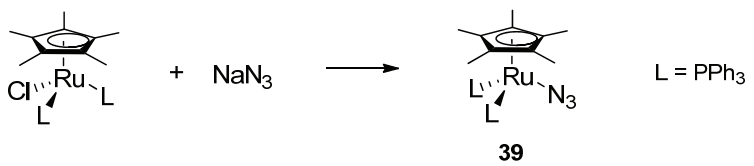

Figure 33. Possible deactivation of the [RuClCp*L_2] catalyst by sodium azide.

By simply changing the procedure into a sequential one-pot reaction, the 1,5-disubstituted 1*H*-1,2,3-triazole **36** (Table 3, entry 4) was successfully obtained, as shown generically in Figure 34. The key message is to avoid an excess of sodium azide in order for the sequential method to be successful.

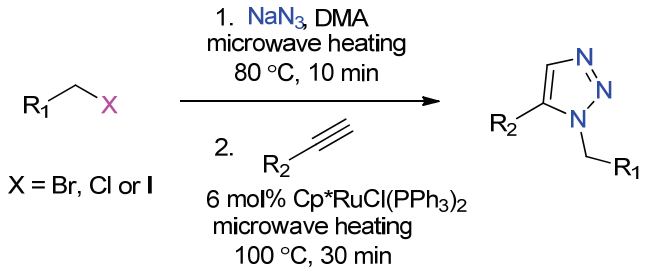

Figure 34. Sequential one-pot RuAAC reaction.

With a practically simple and rather safe sequential one-pot procedure in hand, we wanted to investigate the scope of the reaction and the tolerance to different functional groups in the azide as well as alkyne substrates. A broad range of different substrates were tested and the results are summarized in Tables 2-5. As can be seen in Table 2, small volatile halides such as iodomethane, allyl chloride and 2-bromoethanol gave unsatisfying yields. The question whether they fail to produce the triazoles products due to the low boiling point of the halide and/or azide formed, or due to the instability and possible decomposition of the small labile azides, or because there is a problem with sodium azide poisoning the catalyst due to an uncompleted substitution reaction remains unanswered. Secondary bromides such as bromocyclohexane gave no triazole formation at all in our sequential procedure. However, it has been demonstrated with several examples in the literature that secondary azides do react in the RuAAC reaction, although they require longer reaction times and sometimes also high temperatures. It is thus more likely that there is a problem in the formation of the cyclohexyl azide, also since bromocyclohexane is known to be a poor substrate for S_N2-reactions, and can undergo an elimination reaction to form cyclohexene instead. It would be interesting to test the sequential procedure on a benzylic secondary bromide such as (1-bromoethyl)benzene or similar to see if such substrates reacts.

Primary bromides on the other hand work very well, and a number of examples are shown in Table 3. Among the number of functional groups tolerated in the sequential one-pot procedure are: ester, amide (or imide), Boc protected amine, alchohol, sulphide, chloride and basic heterocycles such as pyridine and imidazole. Activated bromides, both benzylic (Table 3, entries 2-5), and in the form of an α-bromo ester (Table 3, entry 1) react smoothly and afford the triazole product in 82-93% yields.

Table 2. Sequential one-pot RuAAC reaction using small volatile halides and secondary halides. A = $[RuClCp^*(PPh_3)_2]$ and B = $[RuClCp^*]_4$.

Entry	Halide	Alkyne	Product	Isolated Yield	Ru cat
1.			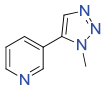	0%	B, r.t
2.		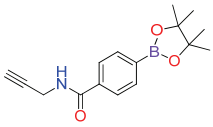	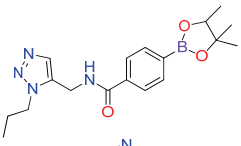	0%	A
3.				0%	A
4.			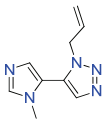	0%	A
5.			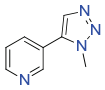	18%	A
6.		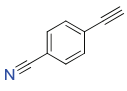	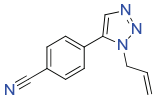	16%	A
7.		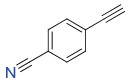	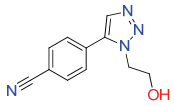	20%	A
8.			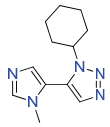	0%	B
9.			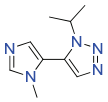	0%	A
10.		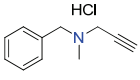	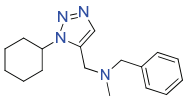	0%	A

Alkyl bromides also work well but seem to react more slowly, leading to a slightly lower yield i.e. ~70% (Table 3, entries 6 and 8). However, by increasing the temperature from 80 °C to 100 °C for the substitution reaction, and from 100 °C to 120 °C for the cycloaddition, an excellent yield was obtained (Table 3, entry 9).

Table 3. Sequential one-pot RuAAC reaction using primary bromides and [RuClCp*(PPh_3)$_2$].

Entry	Halide	Alkyne	Product	Isolated Yield
1.			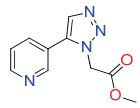	88%
2.		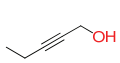	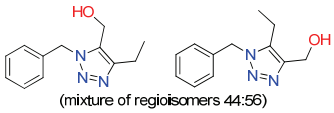 (mixture of regioisomers 44:56)	85%
3.	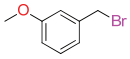		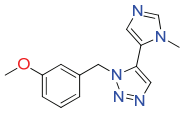	93%
4.			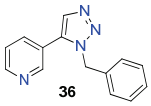 36	82%
5.	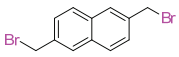	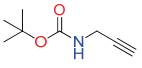	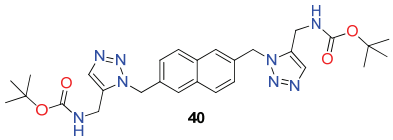 40	52%
6.	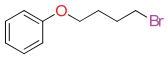		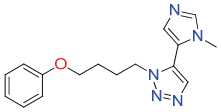	70%
7.	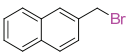	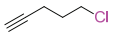	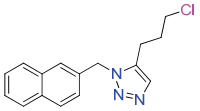	58%
8.		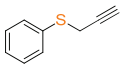	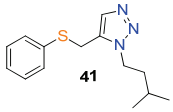 41	73%
9.	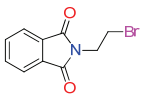		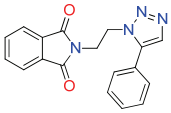	92%
10.		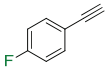	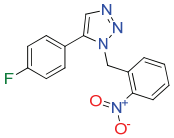	92%

Interestingly we found that any substrate in the form of a HCl- or HBr-salt or containing a carboxylic acid were unsuccessful in the formation of triazole product. Some examples are shown in Table 4. We draw the conclusion that the active [RuClCp*] complex is sensitive towards acidic protons. Moreover, primary chlorides also form the 1,5-disubstituted 1,2,3-triazoles in acceptable to excellent yields, and a few examples are shown in Table 5.

Table 4. Sequential one-pot RuAAC reaction using substrates containing HCl-salts or carboxylic acids. A = $[RuClCp^*(PPh_3)_2]$ and C = $[RuCl_2Cp^*]_x$.

Entry	Halide	Alkyne	Product	Isolated Yield	Ru cat
1.		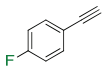	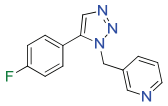	0%	A
2.	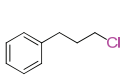	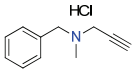	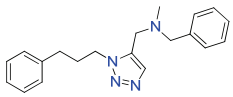	0%	C
3.	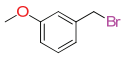	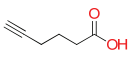	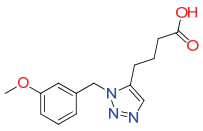	0%	C
4.		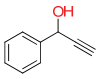	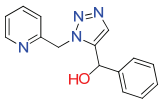	0%	C
5.		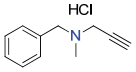	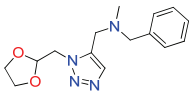	0%	A

Worth to mention is also that alkyl chlorides as well as the aliphatic bromides benefit from higher reaction temperatures. Interestingly, fluoride substituents are also acceptable on both the halide and the alkyne substrates. In addition to the $[RuClCp^*(PPh_3)_2]$ catalyst, we also tested a Ru(III) complex, $[RuCl_2Cp^*]_x$, which surprisingly also showed excellent activity in the sequential one-pot procedure. Preliminary results even point towards higher isolated yields compared to the $[RuClCp^*(PPh_3)_2]$ catalyst, as shown in Table 6.

Table 5. Sequential one-pot RuAAC reaction using primary chlorides.

Entry	Halide	Alkyne	Product	Isolated Yield
1.	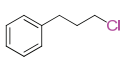		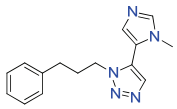	47%
2.		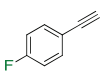	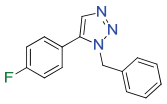	97%
3.	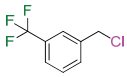		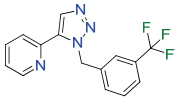	61%

Table 6. Sequential one-pot RuAAC reaction using $[RuCl_2Cp^*]_x$ as catalyst.

Entry	Halide	Alkyne	Product	Isolated Yield	Isolated Yield Using $[RuClCp^*(PPh_3)_2]$
1.	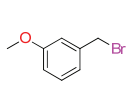		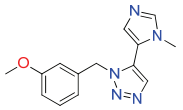	**98%**	93%
2.			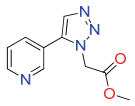	**97%**	88%
3.			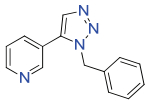	**quant.**	82%
4.	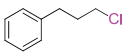		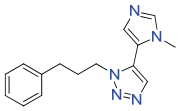	**79%**	47%

However, when looking into the literature in more detail it was found that both Fokin[75] and Qing[268] had already observed good yields with this catalyst as well.

In order to verify the 1,5-regioselectivity of the 1,2,3-triazoles produced, we performed 2D NOESY experiments on triazole **40** and **41** in Table 3. The 1,4-regioisomer of triazoles **40** would not give rise to any NOE-cross peak between H_A and H_B, which is the key NOE for the 1,5-regioisomer, shown in Figure 35. The triazole proton H_C gives a NOE cross-peak to H_B for the 1,5-isomer, but for the 1,4-isomer it should give rise to cross-peaks to both H_A and H_B. As can be seen in the 2D NOESY spectra in Figure 37, a clear NOE cross-peak between H_A and H_B can be seen which proves the 1,5-regioisomer structure. Further, the H_C proton lacks any NOE-cross peak to H_A, which also supports the structure assignment. Figure 36 shows the expected NOE's for proton H_A and H_B in the 1,5-regioisomer. All 4 NOE's for H_A and all 5 NOE's for H_B could be assigned in the 2D NOESY spectra in Figure 37. The 1,5-disubstitution pattern was successfully confirmed by the 2D NOESY experiment.

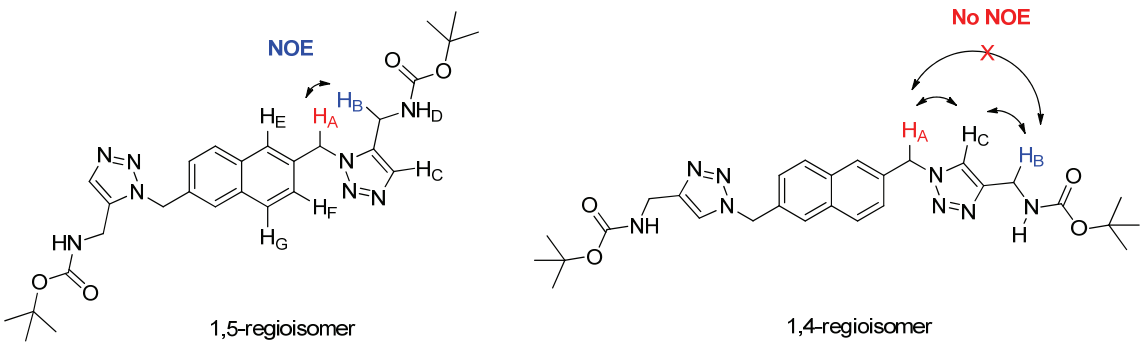

Figure 35. The key NOE for the 1,5-regioisomer of triazole **40** is between H_A and H_B which is absent in the 1,4-regioisomer. Also, a NOE cross-peak for H_A and H_C is present in the 1,4-regioisomer, but absent in the 1,5-regioisomer.

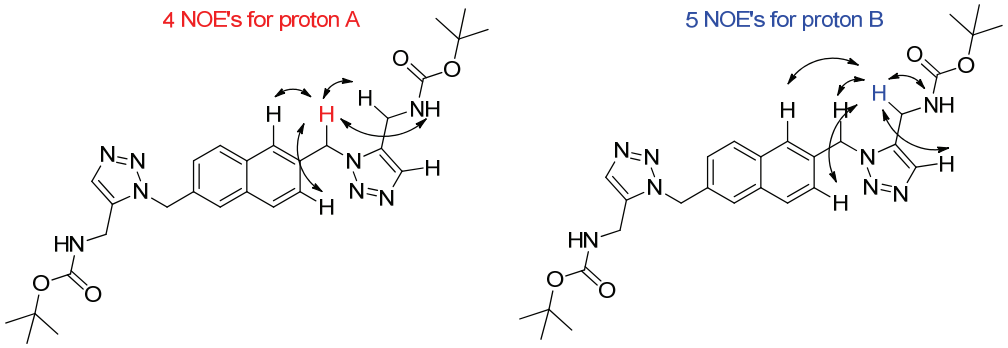

Figure 36. Four expected NOE's for protons H_A and five for H_B in triazole **40**.

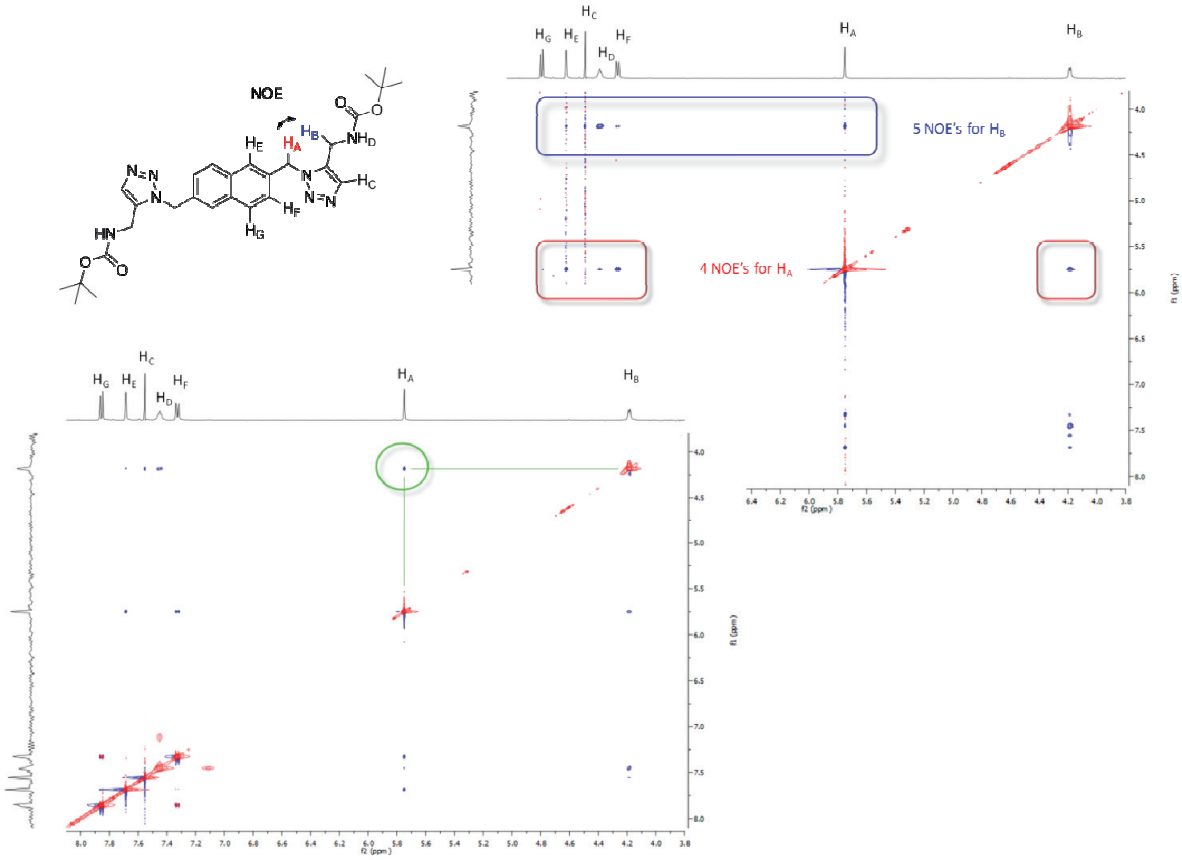

Figure 37. 2D NOESY spectra on 28 mg of triazole **40** (in Table 3) in DMSO-d_6. The spectrum was recorded at 25 °C using a mixing time of 700 ms, delay time of 3 s, np = 4096 (f2), ni = 512 (f1) and nt = 8.

The 2D NOESY experiment of triazole **41** (in Table 3) also confirmed the 1,5-regioisomer structure. Although the quality of the spectra was not as good as for triazole **40** (in Table 3) and all expected NOE's were not assigned, the key NOE between H_A and H_B (α-azide and α-alkyne) was identified.

5.3 Summary

A safe and experimentally simple sequential one-pot procedure for the RuAAC reaction, starting from alkyl halides has been developed. This procedure avoids handling of the hazardous neat alkyl azides and forms the 1,5-regioisomer in good to excellent yields. The scope of the reaction is broad, and functional groups such as alcohol, ester, amide, chloride, carbamate, fluoride, sulfide, nitro and heterocycles such as pyridine and imidazole can be tolerated in the substrates. However, there are some limitations. Functional groups such as carboxylic acids and HCl-salts of mild bases have not been successful in the sequential one-pot procedure. Small volatile halides have also been problematic and only low yields of the triazole have been obtained in a few cases. However, both primary bromides and chlorides, benzylic as well as aliphatic, yield the 1,5-disubstituted-1,2,3-triazoles in good yields and excellent regioselectivity. Moreover the $[RuCl_2Cp^*]_x$ was also found to be an efficient catalyst for the RuAAC reaction.

5.4 Future plans

Development of a solid supported catalyst for the RuAAC reaction would be greatly appreciated by synthetic chemists. We have initiated a project towards synthesis of a polymer-bound RuAAC catalyst using a modified Cp*-ligand. Introduction of a functional group on the Cp*-ligand could potentially facilitate attachment to any type of solid support. However, recent work from the Astruc group has demonstrated the construction of a ruthenium complex supported on magnetic nanoparticles, having the phosphine ligands bound to the nanoparticle.[269] The active catalyst is probably dissociated into the solution under the reaction conditions, keeping the homogeneous catalysis reaction rate. We envision that despite this first solid-supported RuAAC catalyst, there would still be of great interest to create a Cp*-bound catalyst for the RuAAC reation, and also such a Cp*-bound ligand could easily be employed to anchor useful transition metal complexes for other catalytic reactions. Such a catalyst would greatly simplify the purification process and enable recycling and reuse of the catalyst. It would also be of interest to further explore the tolerance of functional groups present on the substrates, as well as to look further into the substrates that did not afford the desired product.

6 Synthesis and NMR-Studies of δ-Peptidomimetics

6.1 Introduction

Non-natural peptidomimetics is currently an exponentially growing field, owing to the great biomedical potential of this class of compounds as well as their self-assembling affinity, and high enzyme resistance.[175-178,181-182,270] The key for the successful application of foldamers, i.e. non-natural folded peptidomimetic oligomers, is basically finding compounds which can reproduce some of the fundamental properties of natural peptides and proteins, such as structural flexibility and water solubility. Moreover, easy access to diverse amino acid units by robust modular synthesis also plays an important role in facilitating the construction of such foldamers.

The structural and constitutional composition of most foldamers can be derived back to natural peptide backbones, where α-amino acids and their homologues, β-, γ-, etc. amino acids, are used. Since these homologues result in increased backbone flexibility, both aliphatic and aromatic cyclic insertions have been applied to facilitate folding into various, mainly helical, secondary structures.[175,246,271-275] By today, many diverse examples can be found; however, in many cases the elongated hydrocarbon chains and the aliphatic cyclic insertions have raised solubility problems.[246, 276-277] Accordingly, despite showing some very interesting potential in the field,[177,276] peptide derivatives built from longer homologues, such as δ-peptides are still rare among foldamers. Further exploration of δ-amino acid substituents is expected to have significant importance, as the backbone constitution of δ-amino acid derivatives easily fits into sequences of natural α-peptides.[278]

With recent gain in knowledge of the RuAAC reaction from our previous work (paper I), we identified the possibility to apply this reaction towards the *cis*-peptide bond mimic, 2-(5-(aminomethyl)-1*H*-1,2,3-triazol-1-yl)acetic acid (5Tzl) and analogues, in a convenient modular way. Together with Dr. Beke-Somfai's previous experience of foldamers constructed from β-amino acids,[279-282] as well as based on the properties of the 5Tzl monomer, and on preliminary conformational analysis, it was anticipated that oligomers built out of these 5Tzl units may have all the above key properties. Therefore, it was natural that we took the first steps towards exploring this field by synthesizing oligomers of the 5Tzl δ-amino acid mimic and investigating their structural properties and solubility.

6.2 Synthesis of oligomers of 5Tzl

The 5Tzl **42** was produced *via* a microwave assisted RuAAC reaction between methyl 2-azidoacetate and *N*-Boc-propargylamine in THF (Figure 38). The reaction works well when the commonly employed [RuClCp*(PPh_3)$_2$] catalyst is used. Nevertheless, when using flash chromatography on silica for the purification of the crude material, we were unable to

separate the catalyst remaining from this particular triazole product **42**, when using a gradient of 0-30% MeOH in CH_2Cl_2. Based on our previous work with the RuAAC reaction (chapter 5), we found that a Ru(III) catalyst $[RuCl_2Cp^*]_x$,[147,268] could be applied with excellent results in this reaction.

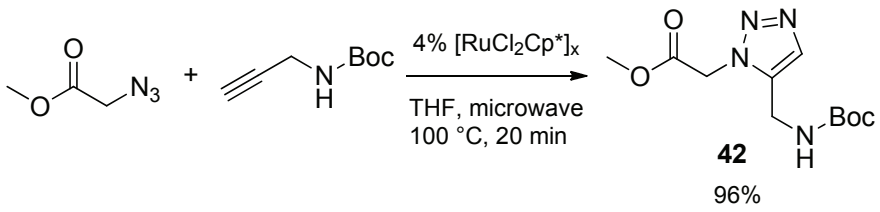

Figure 38. Synthesis of the 5Tzl monomer **42**, using 4 mol% $[RuCl_2Cp^*]_x$ as catalyst in THF for the microwave assisted RuAAC reaction.

With only 4 mol% of the $[RuCl_2Cp^*]_x$ catalyst in THF, the triazole **42** was obtained in 96% yield, in this case without the separation problems encountered with $[RuClCp^*(PPh_3)_2]$ for this particular triazole product. This is a great improvement compared to previous routes to similar compounds.[262,265] The regiochemistry of the 1,5-disubstituted triazole **42** was confirmed by 2D NOESY, see Figure 39.

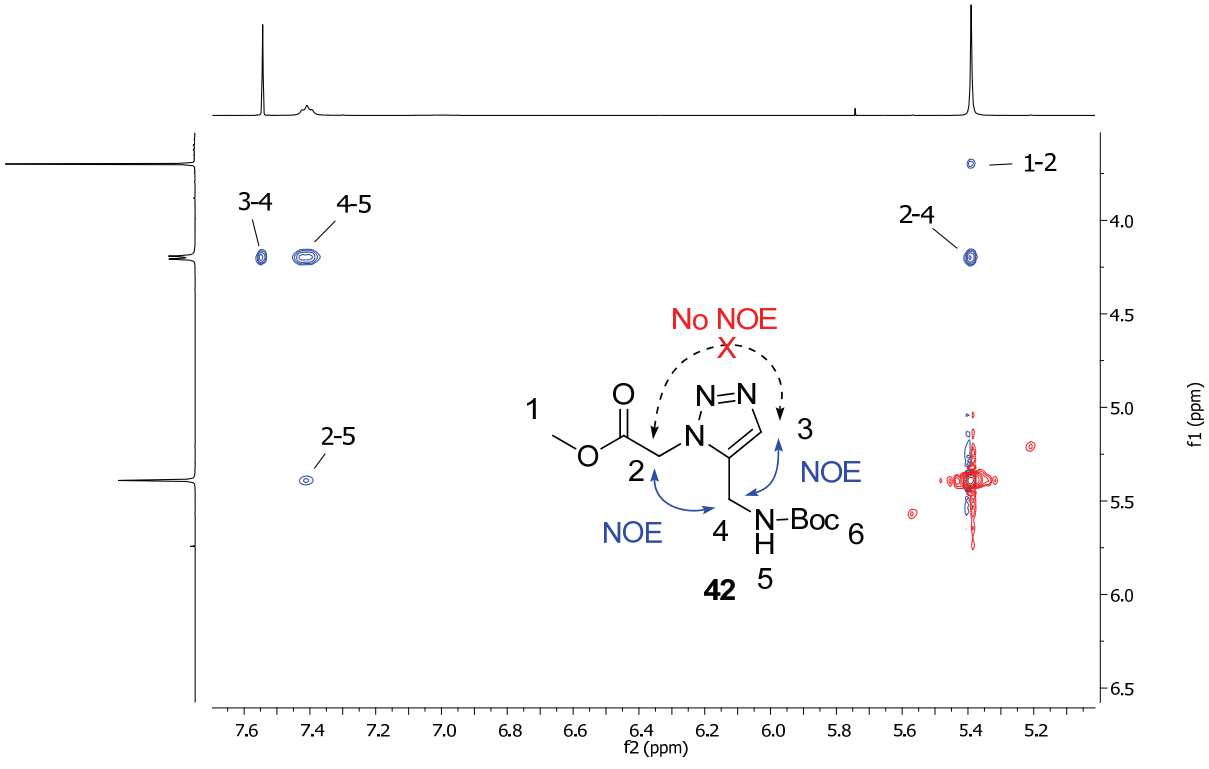

Figure 39. Selected part of the 2D NOESY spectra of **42**, recorded in DMSO-d_6 at 25 °C using a mixing time of 600ms.

From the triazole monomer **42**, dimer **45**, trimer **48** and tetramer **49** were synthesized using standard deprotection and coupling methods. The Boc-group of **42** was quantitatively

removed by treatment with TFA in CH_2Cl_2. The ester hydrolysis to form acid **44** was then optimized, and the best results were achieved with 1M LiOH (aq) (1.5 equiv.) in MeOH at ambient temperature. Amide coupling of building blocks **43** and **44** using T3P®[283-285] as the coupling agent gave dimer **45** in a moderate yield, as outlined in Figure 40.

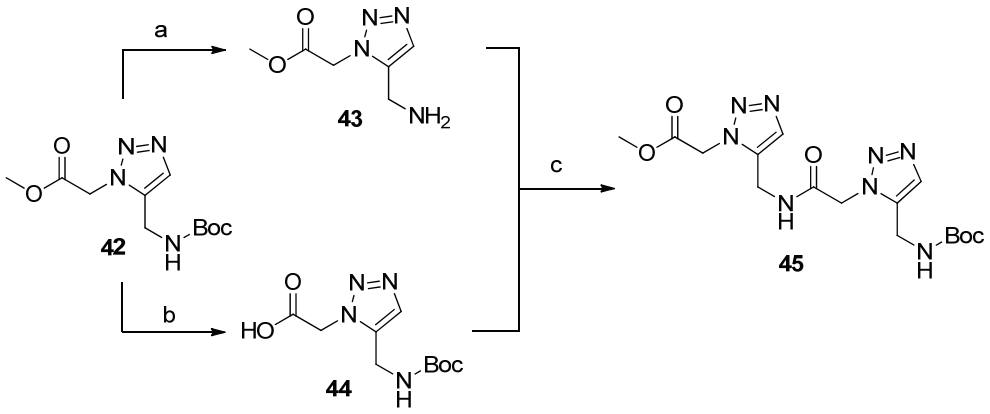

Figure 40. Synthesis of the 5Tzl-dimer **45** from 5Tzl-monomer **42**, using standard deprotection conditions and T3P as the amide coupling reagent.

The deprotection of **45** to amine **46** proceeded without any problems using either TFA in CH_2Cl_2 or HCl in dioxane/MeOH. The selective hydrolysis of the methyl ester of **45** to **47** was performed at room temperature with 1M LiOH (1.5 equiv.) in MeOH and afforded carboxylic acid **47** in 93% yield. Trimer **48** could then be formed via coupling of dimer **46** with monomer **44** using T3P® as the coupling reagent, though in a low yield (unoptimized) as outlined in Figure 41. The solubility in water of compound **48** has been measured to ~2 mg/mL.

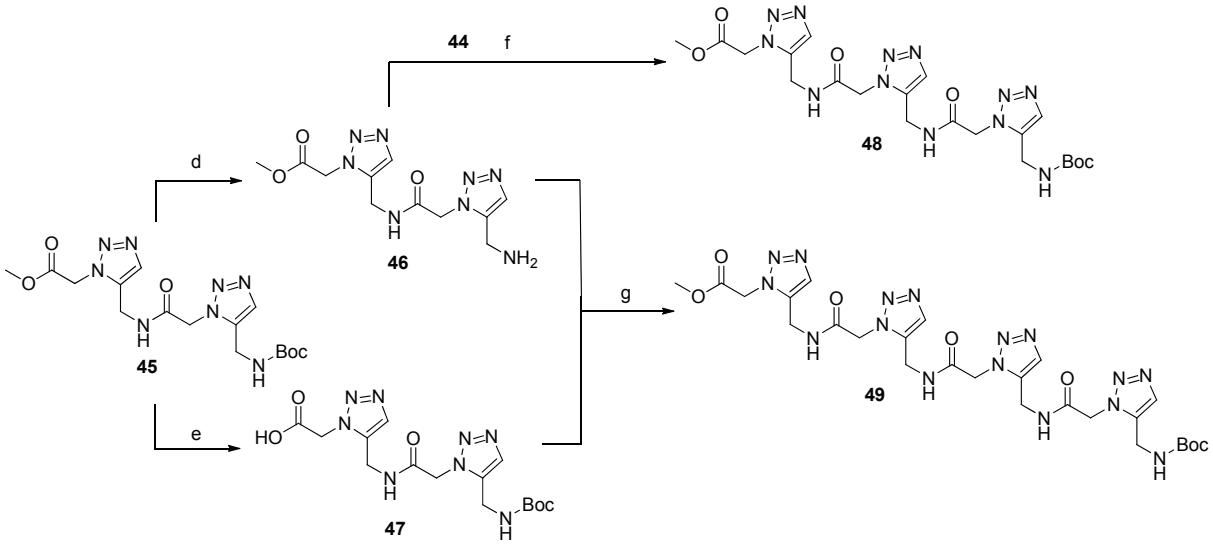

Figure 41. Synthesis of 5Tzl-trimer and 5Tzl-tetramer from 5Tzl-dimer, using standard deprotection conditions and T3P as the amide coupling reagent.

When amide-coupling of dimers **46** and **47** was performed to produce the tetrameric structure **49**, using the same reaction conditions as earlier, surprisingly no product could be found in the ethyl acetate extracts from the aqueous workup, only unreacted dimer acid **47** was isolated.

Instead, the tetramer **49** was found in the aqueous phase after the extraction and was isolated by preparative HPLC. The synthesis of trimer **48** and tetramer **49** is outlined in Figure 41.

6.3 Conformational analysis by quantum chemical calculations and NMR spectroscopy

Computational studies of a heptamer structure of the 5Tzl were performed and resulted in a number of different possible secondary structures which are shown in Figure 42.

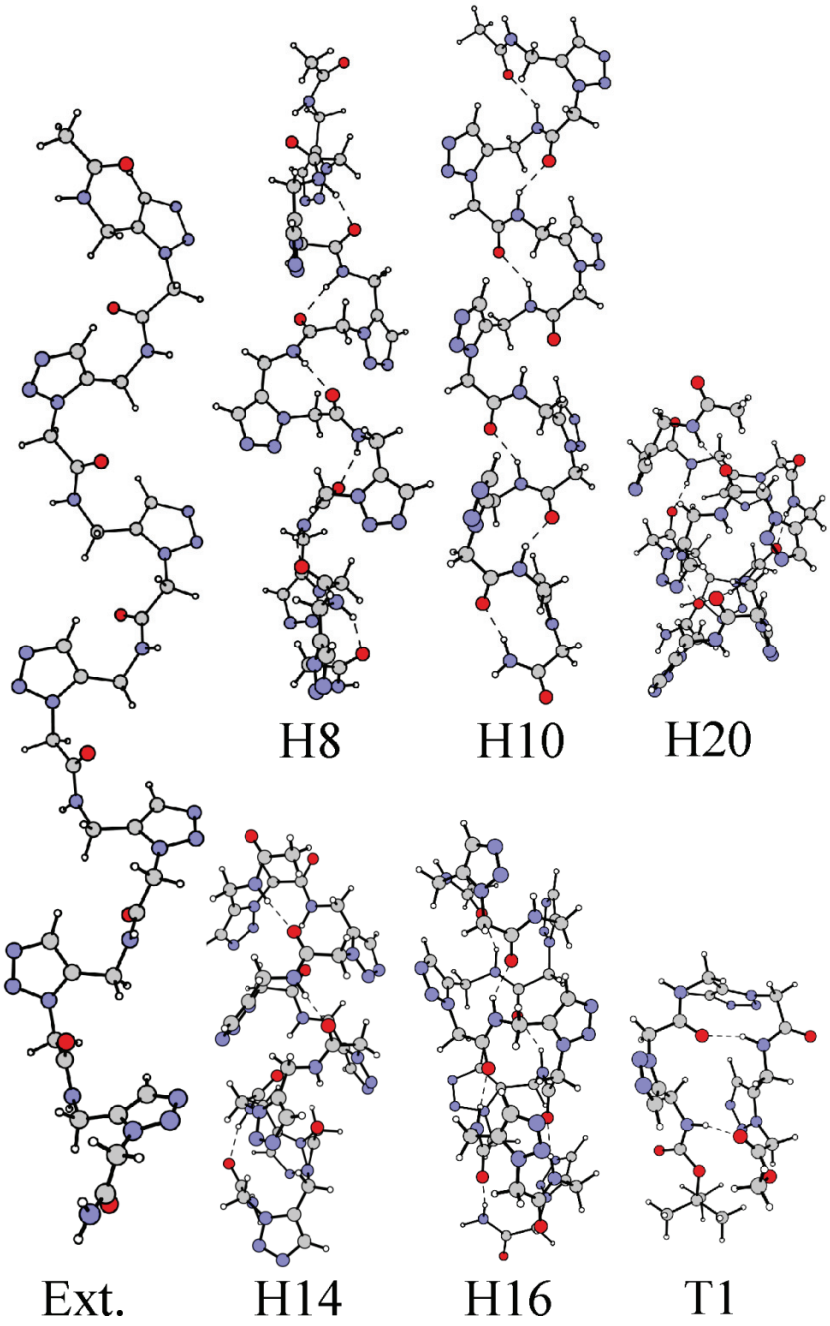

Figure 42. Investigated secondary structures of the heptamer model and the lowest energy turn conformer, **T1**, for model Tri(Boc-Est). Formed H-bonds are marked by dashed lines.

Among these conformers the helical structures with a higher number of atoms in the pseudo ring formed via hydrogen bonding, i.e. **H14**, **H16** and **H20,** were found to be more favoured than the lower number helical structures **H8** and **H10**. The extended zigzag structure without any internal H-bonds was predicted to be the least favoured.

To investigate any possible secondary structure of the synthesized trimer **48** and tetramer **49**, we performed 2D NOESY experiments. The experiments were carried out in 13 and 23 mM DMSO-d_6 solution respectively, at 25 °C, using a NOESY mixing time of 600 ms. The hydrogens in trimer **48** and tetramer **49** are numbered starting from the methyl ester terminal and going to the N-Boc terminal, and will be referred to as H_1, H_2... etc. This numbering system will be used from here and onwards in this thesis.

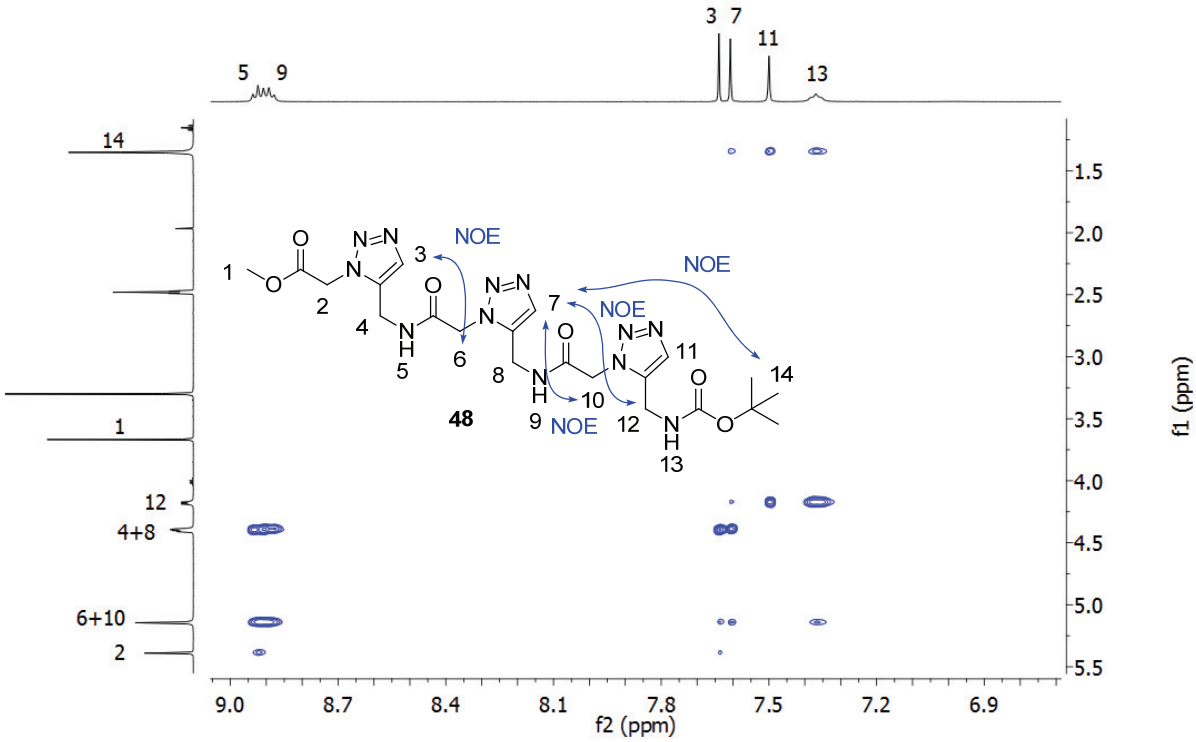

Figure 43. Selected part of the 2D NOESY spectra of trimer **48**. The experiments were carried out in 13 mM DMSO-d_6 solution at 25 °C, using a NOESY mixing time of 600 ms and were acquired with 1024 points in the $f2$ domain and 256 points in the $f1$ domain. The data were processed using MestReNova software and baseline correction was applied to both dimensions using Bernstein polynomial fit (3 orders). A 90° sine bell window function was applied in $f2$ and the data was zero-filled in $f2$ domain to give a final matrix of 1024 by 1024 real points.

Protons in the 2D NOESY spectra of trimer **48** were assigned by starting from the C-terminal and following the strong NOE cross-peaks. By combining these results with assignments starting from the N-terminal, almost all peaks could be assigned, except for the pairs of H_6, H_{10} and H_4, H_8, which were overlapping. Several interresidual cross-peaks were identified, as seen in Figure 43 and 44, such as H_3-H_6, H_7-H_{10}, H_7-H_{12}, H_7-H_{14} and H_1-H_{14}, where the latter two are maybe being the most interesting ones since they cannot originate from the same

conformer according to the calculations. Moreover, a cross-peak was found that could possibly originate from a NOE between H_1-H_6 and/or H_1-H_{10}; either of these are possible due to the signal overlap between H_6 and H_{10}. In similarity, a cross-peak was seen between H_8-H_{14} and/or H_4-H_{14}. While it is not expected that short achiral oligomers would adopt a well-defined conformation, it is apparent from the NMR spectra that several conformers might coexist.

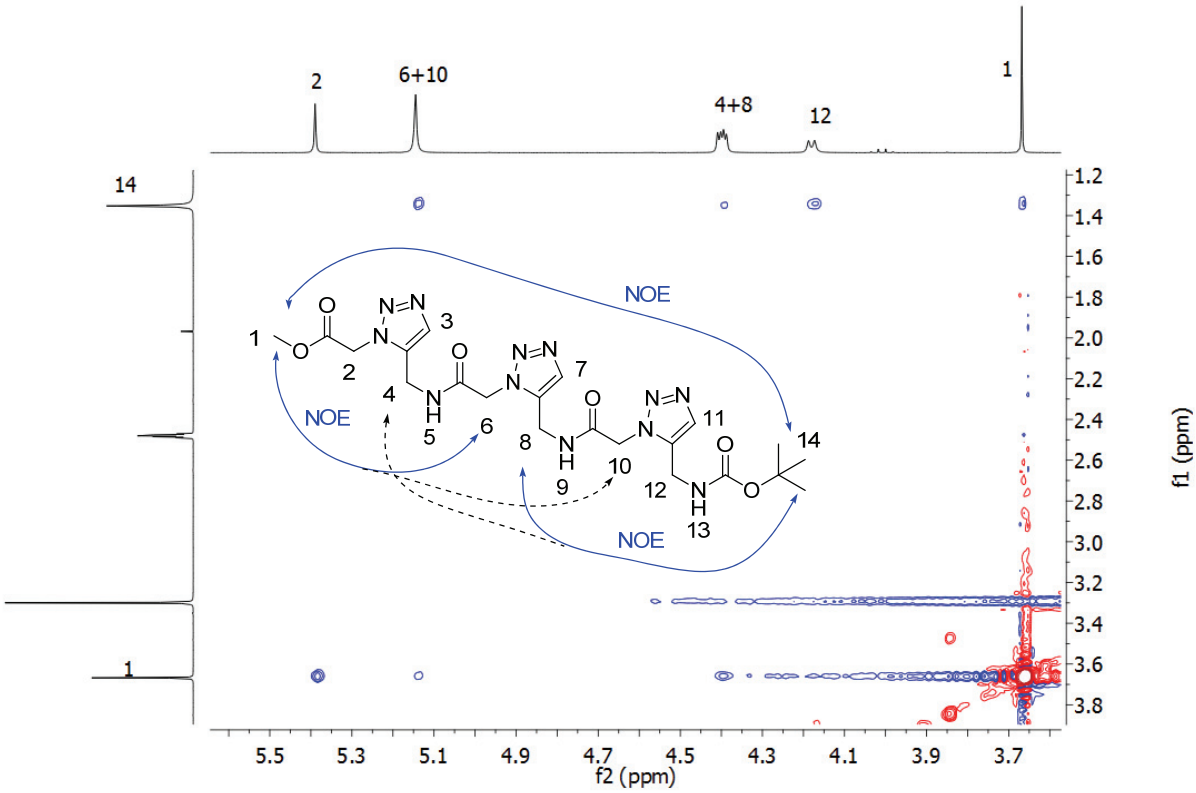

Figure 44. Selected part of the 2D NOESY spectra of trimer **48** showing the end-to-end NOE.

By using the secondary structures obtained from the theoretical calculations, the most likely conformers may be identified. Considering the two possibilities for the cross-peak between H_1-H_6 and/or H_1-H_{10}, out of the possible structures, the **H14** helix is the only one that may fit the cross-peak between H_1-H_{10}, with the closest distance of 4.5Å. However, this structure should also generate a strong cross-peak between the methyl ester H_1 and the central triazole proton H_7, as for **H14** these have a 3.0 Å distance, but this peak is missing from the spectra. Therefore, the cross-peak in question is more likely to originate from the H_1-H_6, which could arise mainly from other helix-forming conformers, such as **H8**, **H10**, **H16** or the turn **T3**, which in the Tri(Boc-Est) model have the closest H_1-H_6 distances of 3.2 Å, 5.0 Å, 3.8 Å, and 5.0 Å, respectively.

Looking at the two possibilities for the cross-peak found between H_4-H_{14} and/or H_8-H_{14}, the presence of the H_7-H_{14} cross-peak together with the calculations dictates the only matching conformer for the H_4-H_{14} NOE to be the **H16**-helix. At the same time, the H_8-H_{14} may possibly fit for **H10** and also for **H20** (when looking at the heptamer model).

The interesting end-to-end NOE, H_1-H_{14}, could not originate from a helical-structure and is a strong indication for a turn-like conformer, **T1-3** (**T1** is shown in Figure 45). However, the cross-peaks H_1-H_6, H_7-H_{14} and H_8-H_{14} cannot originate from such a turn conformer. These assignments lead to the conclusion that trimer **X** exhibits neither a random conformation nor a single, well-defined conformer, in DMSO-solution at 25 °C. Most likely it exists in a fast equilibrium between at least two conformers, making **H10**, **H16** and **T1-3** the most probable conformers.

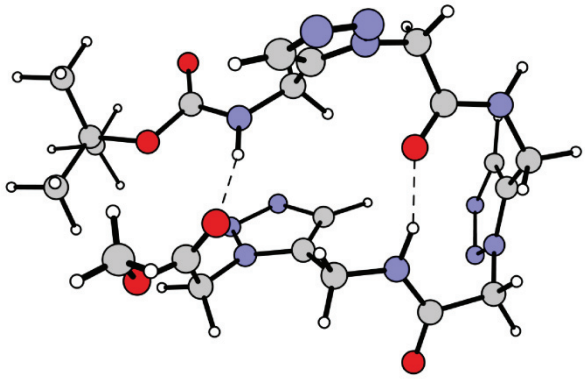

Figure 45. The turn-like **T1** conformer, exhibiting one H10-bond and one H20-bond.

The 2D NOESY data from the NMR study of tetramer **X** was unfortunately not assignable due to extensive signal overlap between the amine methylene protons H_4, H_8 and H_{12}, as well as the carbonyl methylene protons H_6, H_{10} and H_{14}, the triazole protons H_7 and H_{11}, and the amide protons H_5, H_9 and H_{13}. These extensive overlaps render the assignment of any plausible secondary structures unjustified.

6.4 Summary

We have synthesized a new set of peptidomimetic compounds constructed from 1,5-disubstituted 1,2,3-triazole (5Tzl) units. These monomer δ-amino acid derivatives were prepared via the RuAAC reaction, using $[RuCl_2Cp^*]_x$ as the catalyst, which facilitated purification, affording yields up to 96%. The building blocks were subsequently assembled to form dimeric, trimeric and tetrameric oligomers.

The conformational analysis of trimer **48** using 2-dimensional NMR spectroscopy and quantum mechanical calculations, lead to the conclusion that coexisting conformers are present, with **H10**, **H16** and **T1-3** being the most probable conformers in DMSO solution.

With our initial work within this foldamer-project, we can conclude that oligomers can be built from modular 5Tzl monomer units, synthesized via the RuAAC reaction, and serve as a good adaptable foldamer backbone that can adopt various secondary structures and offer improved properties such as water solubility. The modification of such a backbone with appropriate side-chains can potentially drive these foldamers into desired secondary structures.

6.5 Future plans

Based on our initial 'proof-of-principle' constructs, we currently aim to expand our knowledge of this new set of 5Tzl oligomers, by introduction of chirality and versatile side chains. Moreover the amide-coupling step needs to be optimized to facilitate the production of more material and also of longer oligomers such as octamers. Further NMR-studies focusing on the effects of concentration, temperature etc, are essential to provide an improved understanding of the secondary structures. Finally, studies of toxicity and other potential bioactivity are highly desired extensions of this project.

7 Synthesis of Binuclear Ruthenium complexes for DNA binding studies.

7.1 Introduction

Mononuclear ruthenium complexes, such as the ones discussed in Chapter 2.4, have been thoroughly studied as DNA binders and have also been shown to bind to the minor groove in mixed DNA sequences[286] and by intercalation in AT-DNA.[287-288] By making the "dimer" of the ruthenium complexes, not only is the binding constant increased but the binding mode is also changed into a threading intercalation state, where the bridging ligand is stacked between the base-pairs and the bulky phenanthroline ligands protruding from each side of the DNA helix, as shown in Figur 46.[289-290] This binding mode requires that one of the two ruthenium atoms must pass through the DNA-helix between the two strands. This obviously affects the kinetics of binding, and DNA threading intercalators show extremely slow association and dissociation kinetics compared to other DNA binding drugs. The first molecule to be discovered as a threading intercalator for DNA was the cytotoxic compound nogalamycin.[291-296] As there appears to be a correlation between slow dissociation kinetics and biological activity, threading intercalating agents are interesting as model compounds in the search for new DNA-targeting therapeutics. For example, the threading of [μ-(11,11'-bidppz)(phen)$_4$Ru$_2$]$^{4+}$ **50** and its bipyridine analogue [μ-(11,11'-bidppz)(bpy)$_4$Ru$_2$]$^{4+}$ have demonstrated a selectivity for [poly(dAdT)]$_2$ in comparison with mixed DNA sequences, a property that potentially can be utilized to target parasites with high AT content in their genomes, such as the malaria parasite *P. falsiparum*.[297-299]

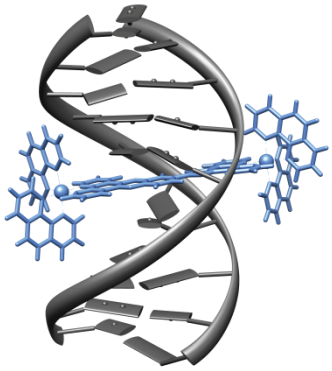

Figure 46. Illustration of how a threading binuclear Ru-complex binds to a DNA-helix.

With several binuclear ruthenium complexes synthesized and studied as DNA threading intercalators in the Lincoln group,[289-290, 297-298, 300-301] we wanted to further increase the knowledge of the effect of the bridging ligand structure. Our aim was to synthesize and study binuclear ruthenium complexes with different lengths of the bridging ligand, to complement previous complexes made in our group, see Figure 47. Recently Andersson et al. have prepared an entirely AT-specific binuclear ruthenium complex, [μ-dppzip(phen)$_4$Ru$_2$]$^{4+}$ (complex **51** in Figure 47. dppzip = 2-(dipyrido[3,2-*a*:2′,3′-*c*]phenazin-11-yl)imidazo[4,5-*f*]-1,10-phenanthroline), which does not thread mixed sequence DNA at all.[300-301] It was proposed that this increased AT-specificity arises from enhanced stress on the DNA in the

threaded state as the shorter bridging ligand brings the phenanthrolines closer to the DNA helix, resulting in steric repulsions between the complex and the DNA. The flexible AT-DNA can adapt its conformation in order to accommodate the threaded complex better, whereas such adjustments probably are associated with a large energy cost in the more rigid mixed sequence DNA making threading highly unfavourable.

We were interested to investigate whether a longer complex would show the opposite properties as the previously studied shorter $[\mu\text{-dppzip(phen)}_4\text{Ru}_2]^{4+}$ complex **51**, i.e. decreased AT-selectivity and slower dissociation kinetics for the DNA-binding. The introduction of an acetylene group between the two dppz units in $[\mu\text{-(11,11'-bidppz)(phen)}_4\text{Ru}_2]^{4+}$ **50**, would most likely retain the geometries and the photophysical properties of the complex, while increasing the distance between the two charged ruthenium atoms. In addition, the incorporation of an ethynyl linker could also lower the energy barrier for a 0 ° torsional angle between the two dppz units, potentially achieving even better π-π stacking with the DNA-bases, leading to an increased binding constant.

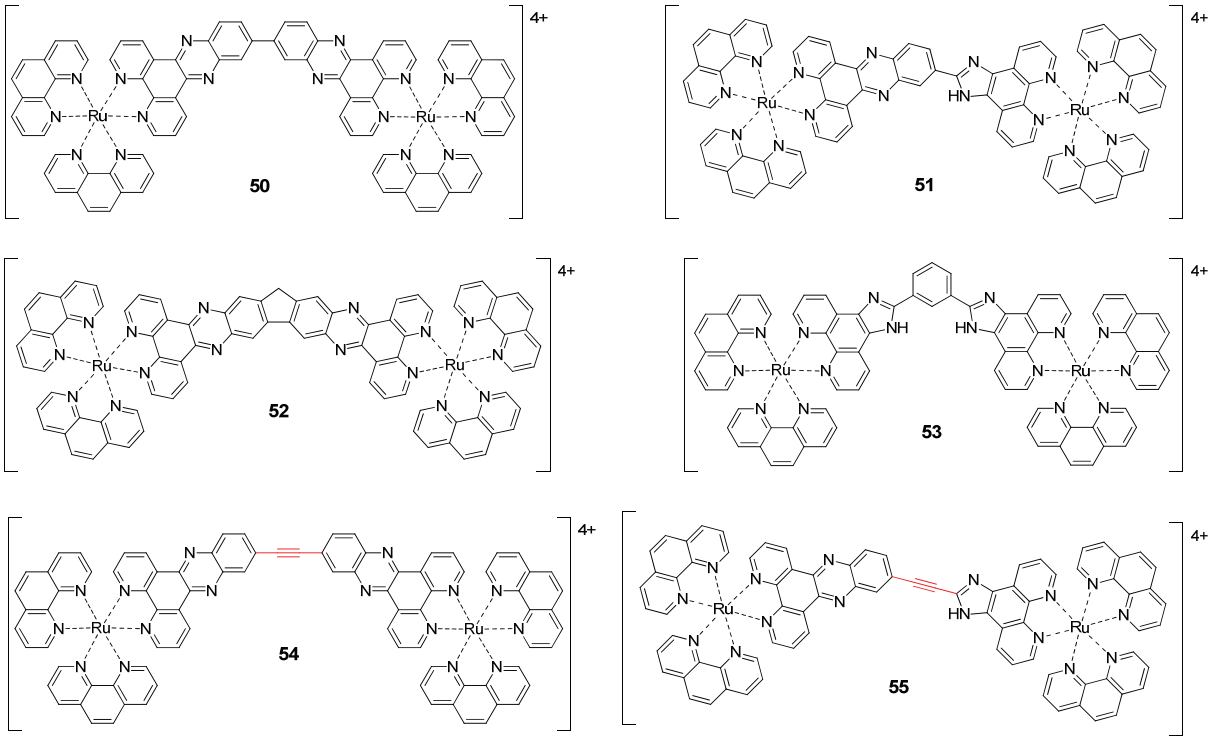

Figure 47. Structure of previously studied ruthenium complexes in the Lincoln group and our two new targets at the bottom. The ethynyl insertion is highlighted in red.

Similarly, we were also interested in making the ethynyl-analogue of $[\mu\text{-dppzip(phen)}_4\text{Ru}_2]^{4+}$ to investigate if the elongated ethynyl-analog could combine the extremely high AT-selectivity demonstrated by the $[\mu\text{-dppzip(phen)}_4\text{Ru}_2]^{4+}$ complex **51** while attaining the slower kinetics and other properties of the $[\mu\text{-bidppz(phen)}_4\text{Ru}_2]^{4+}$ complex **50**. The two new targets **54** and **55** are shown in Figure 47, and the ethynyl linker is highlighted in red.

7.2 Synthesis of binuclear ruthenium complexes

Our strategy to synthesize ruthenium complex **54**, was to prepare the tetraaniline **60** via two Sonogashira coupling reactions,[302-304] in order to create the ethynyl linker, which subsequently could be condensated reaction with enantiomerically pure Δ- or Λ-$[Ru(phen)_2pq]^{2+}$ **61** to obtain the ΔΔ- and ΛΛ- enantiomers of the target $[\mu\text{-bidppze(phen)}_4Ru_2]^{4+}$ **54** in similarity with previously used routes.[300] Our first attempts to couple trimethylsilylacetylene with 4-bromobenzene-1,2-diamine were unsuccessful. We modified our strategy, as outlined in Figure 48, by starting from 4-iodo-2-nitroaniline **56** instead, and also employing an efficient microwave assisted Sonogashira method,[305] which afforded the TMS-protected nitroaniline **57** in excellent yield. This is a slight improvement from a previously reported method by the Tour group, employed for the synthesis of molecular electronics.[306-307] A simple deprotection of the TMS-group followed by a second Sonogashira coupling yielded the symmetric bis-nitroaniline **59** as a red solid. Interestingly, the bis-nitroaniline **59** changes colour from red to yellow when dissolved in THF, or to orange when dissolved in DMSO, whereas it is practically insoluble in $CHCl_3$ which enables easy purification.

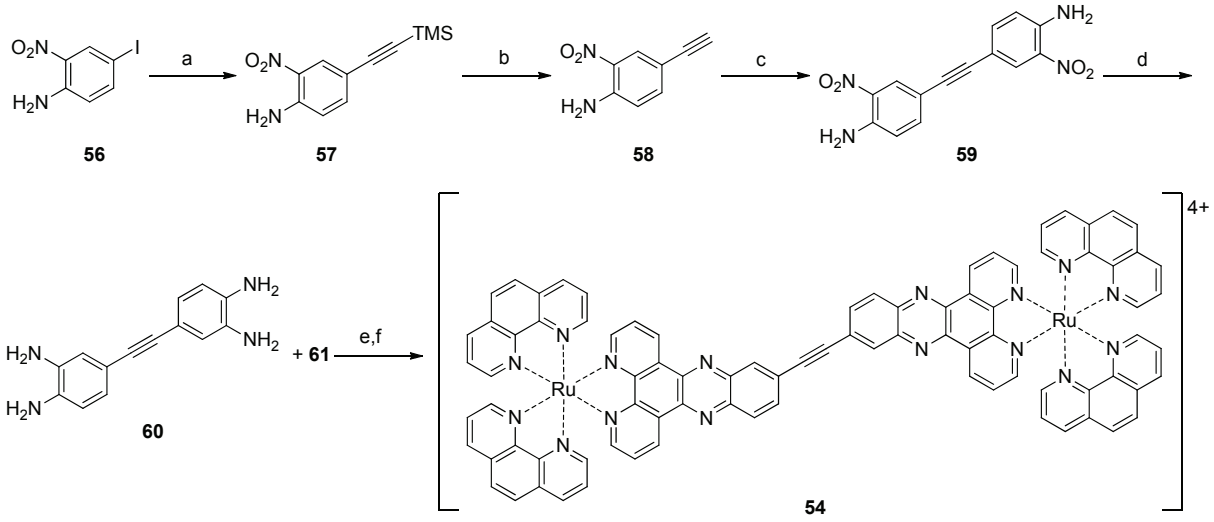

Figure 48. Synthesis of $[\mu\text{-bidppze(phen)}_4Ru_2]^{4+}$ (**54**). Reagents and conditions: (a) Ethynyltrimethyl-silane, $Pd(PPh_3)_2Cl_2$, CuI, DIPA, DMA, microwave heating 120 °C, 10 min (99%). (b) K_2CO_3, $MeOH/CH_2Cl_2$, rt 80 min (95%). (c) 4-iodo-2-nitroaniline (**56**), $Pd(PPh_3)_2Cl_2$, CuI, DIPA, DMA, microwave heating 120 °C, 10 min (60%). (d) Zn, NH_4Cl(aq), THF/MeOH, reflux 6 h. (e) $[Ru(phen)_2pq](PF_6)_2$ (**61**), AcOH, CH_3CN/MeOH, 22 °C. (f) 0.1 M SeO_2(aq), CH_3CN, 22 °C, 40 min (48% from **61**).

The reduction of the two nitro-groups to anilines is not as easy as it first may look. Reagents and reaction conditions need to be carefully selected in order to obtain selectivity for the nitro-group over the triple bond, meaning that catalytic hydrogenation is not an option. Another issue might be coordination of metals to the *ortho*-dianiline unit. Our best results were accomplished with Zn powder/NH_4Cl(aq) in a refluxing mixture of THF/MeOH. Due to the sensitivity of tetraaminotolane **60** towards oxidation and/or polymerization, the crude isolated product was used directly in the condensation reaction without further purification or characterization. As reported previously by Westerlund et al.[308] the condensation of $[Ru(phen)_2pq]^{2+}$ **61** with planar tetraaminoaryl compounds is complicated by redox side-reactions. Compared to non-planar biphenyls, the more conjugated planar π-system of 1,2-

diphenylethyne makes the corresponding tetraaminotolane **60** reactive enough to reduce the bidppze ligand as it is formed. Thus only a small amount of the expected [μ-bidppze(phen)$_4$Ru$_2$]$^{4+}$ **54** can be isolated directly from the reaction mixture, and instead a reduced complex is obtained. However, oxidation of the isolated hexafluorophosphate salt with selenium dioxide in aqueous acetonitrile proceeds smoothly to give the desired product **54**. After oxidation, the ΔΔ- and ΛΛ-enantiomers of [μ-bidppze(phen)$_4$Ru$_2$]$^{4+}$ **(54)** were first isolated as the hexafluorophosphate salts and then converted into the chloride salts by precipitation with tetra-*n*-butylammonium chloride in acetone.

Our strategy to synthesize all four enantiomers of the Ru-complex **55** was simply to couple the two halves together by a Sonogashira coupling reaction using the 2-ethynylimidazole complex **62** and dppzI complex **63**. This strategy would control the formation of the desired enantiomer of the product in a simple way. However, the synthesis was not as straightforward as it first looked, for several reasons. The first step (shown in Figure 49), i.e. the imidazole-forming condensation of [Ru(phen)$_2$pq]$^{2+}$ **61** and TMS-protected propargyl aldehyde with ammonium acetate as nitrogen source, was troublesome and only 5-10% of the TMS-deprotected product **62** could be isolated (~5 mg). The reaction suffered heavily from side-reactions, where formation of about 15-20 different species were detected, although most of these we were unable to identify.

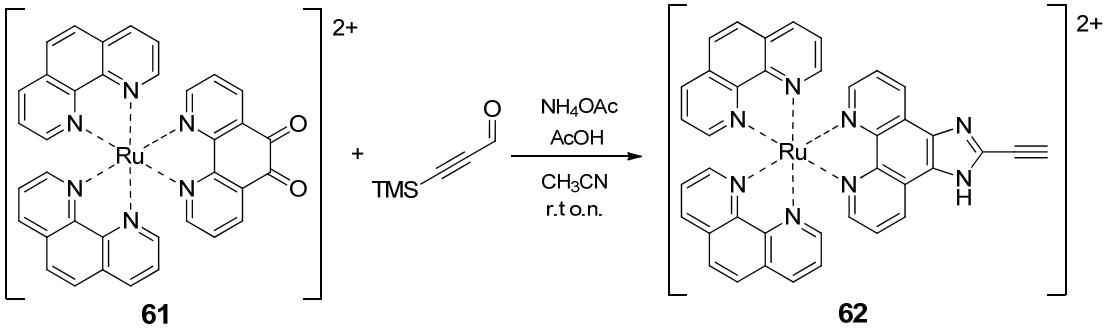

Figure 49. Acetic acid catalyzed condensation forming imidazole **62** using NH_4OAc as nitrogen source.

The synthesis of the other half was relatively straightforward, although, more care should have been taken when choosing the reaction conditions for the reduction of the nitro-group to avoid dehalogenation as a side-reaction. The condensation of the dianiline mixture proceeded smoothly to form [Ru(phen)$_2$dppzI]$^{2+}$ **63**, as outlined in Figure 50.

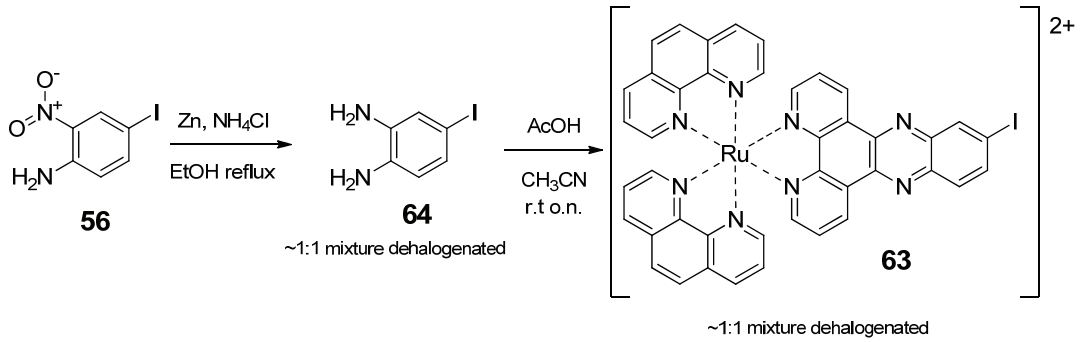

Figure 50. Synthesis of [Ru(phen)$_2$dppzI]$^{2+}$ **63**.

The final step, i.e. the Sonogashira coupling of the two halves (Figure 51), was tested and the alkyne complex **62** was consumed, but no coupling product could be identified. The route was abandoned and a new strategy was engaged, proceeding via the propargylaldehyde complex **65** and ending with the imidazole formation to couple the two halves together.

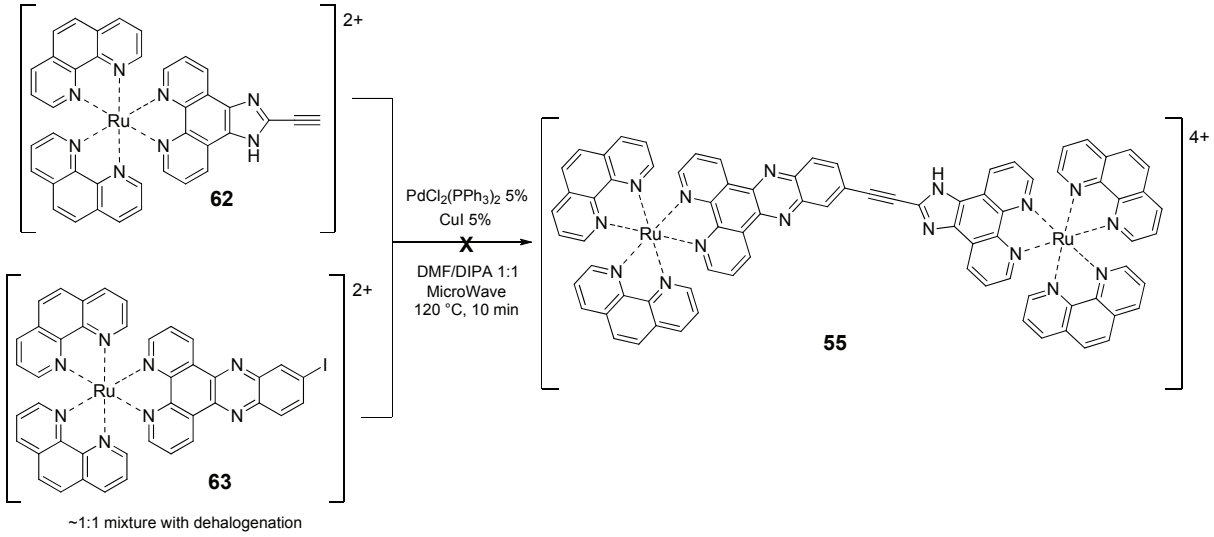

Figure 51. Attempted Sonogashira cross-coupling to form the target Ru-complex **55**.

This time we started with the Sonogashira coupling reaction of 4-iodo-2-nitroaniline **56** with propargylalcohol, which proceeded efficiently to form nitroaniline **65** in 87 % yield (see Figure 52). Reduction of the nitro group was performed with Zn powder/NH_4Cl(s) in refluxing EtOH (95%) for 1.5 hours. The crude dianiline **66** was directly used (in excess) in the acetic acid catalyzed condensation reaction (shown in Figure 53) with $[Ru(phen)_2pq]^{2+}$ **61** at 50 °C in acetonitrile to obtain the $[Ru(phen)_2dppzp]^{2+}$ **67** in 74 % yield after purification on Al_2O_3.

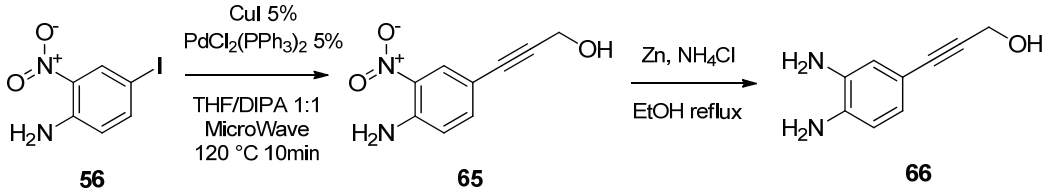

Figure 52. Synthesis of 3-(3,4-diaminophenyl)prop-2-yn-1-ol **66**.

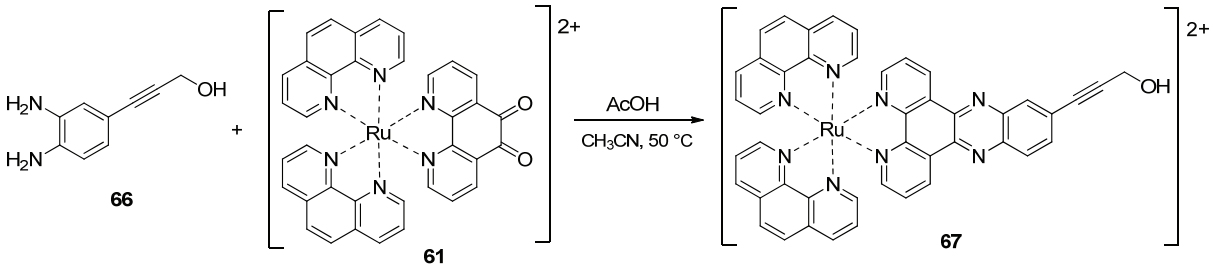

Figure 53. Acid catalyzed condensation forming Ru-complex **67**.

Interestingly, oxidation of the propargyl alcohol **67** proceeded pleasingly well with Dess-Martin periodinane (DMP)[309] in CH_2Cl_2/acetonitrile (3:1) at 0 °C to r.t. overnight, and the propargyl aldehyde **68** was produced in ~65% yield, outlined in Figure 54.

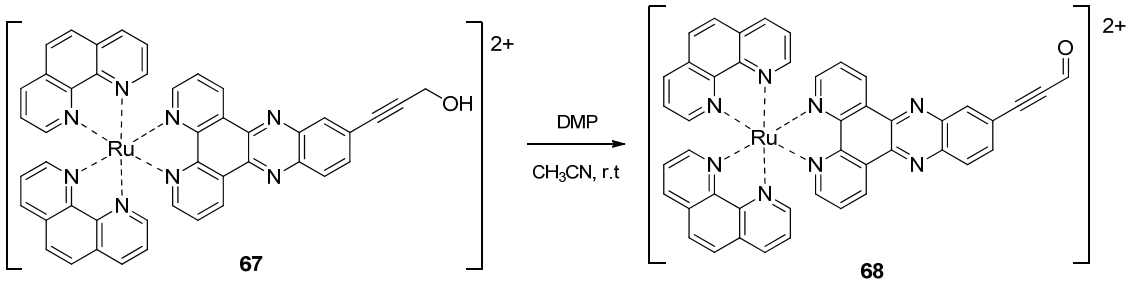

Figure 54. Propargyl alcohol oxidation with Dess-Martin periodinane. Experimental procedure and ^{1}H- and ^{13}C-NMR spectra of propargyl aldehyde **68** can be found in the Appendix.

With only one final step left (Figure 55), we were optimistic in finally obtaining the target [μ-dppzipe(phen)$_4$Ru$_2$]$^{4+}$ **55**, however, despite several careful attempts to perform the crucial condensation to form the imidazole, no desired product could be identified.

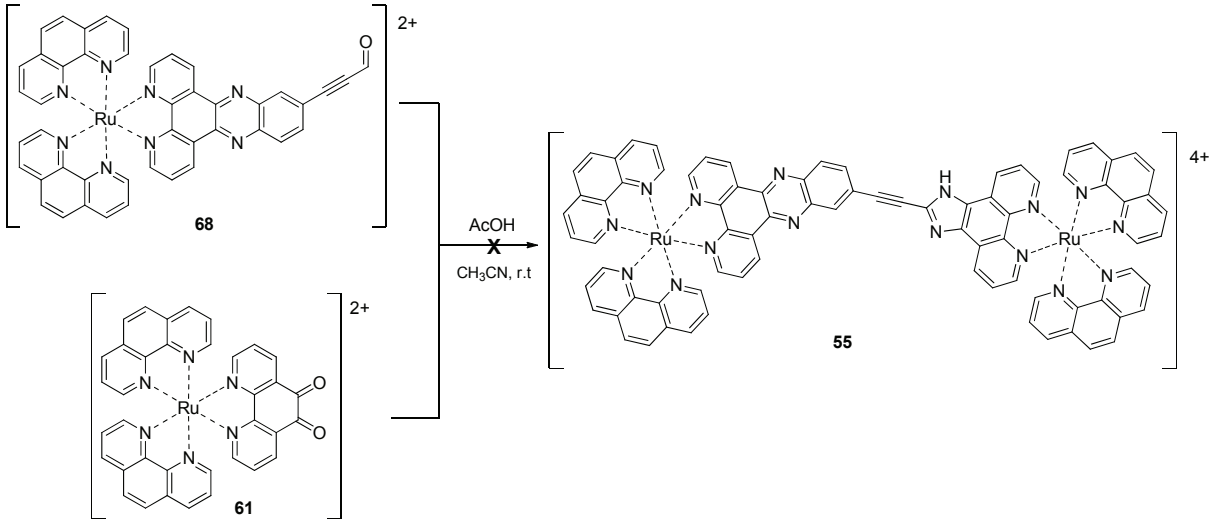

Figure 55. Attempted condensation to form [μ-dppzipe(phen)$_4$Ru$_2$]$^{4+}$ **55**, using NH_4OAc as nitrogen source.

7.3 Results of the DNA-binding study

The DNA binding of ΔΔ- and ΛΛ-[μ-bidppze(phen)$_4$Ru$_2$]$^{4+}$ **54** was studied by various spectroscopic techniques described in detail in paper III and we can conclude that ΔΔ-[μ-bidppze(phen)$_4$Ru$_2$]$^{4+}$ **54** efficiently intercalates both AT- and ct-DNA, with a dissociation rate from ct-DNA that is slower than for any other ruthenium complex we have studied with any type of DNA. We also noted that the selectivity for AT-DNA over ct-DNA was decreased, even if the AT-DNA still is favoured. It was also found that it associates faster than the parent compound **50**, as summarised in Figure 56.

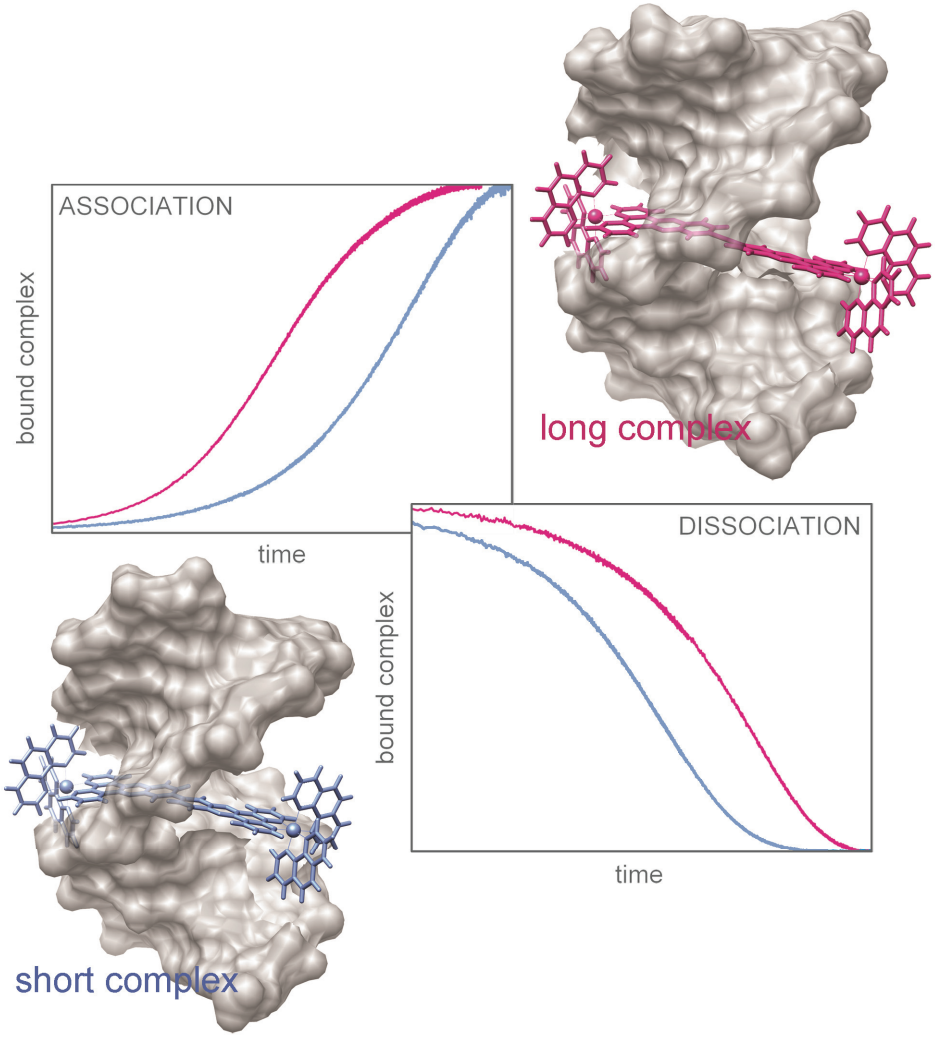

Figure 56. Summary of the DNA-binding study. ΔΔ-[μ-bidppze(phen)$_4$Ru$_2$]$^{4+}$ **54** demonstrated both faster association and slower dissociation to DNA, compared to ΔΔ-[μ-bidppz(phen)$_4$Ru$_2$]$^{4+}$ **50**.

Moreover, we saw that although the overall selectivity for the ΛΛ-[μ-bidppze(phen)$_4$Ru$_2$]$^{4+}$ **54** is groove binding to AT-DNA, threading intercalation preferentially occurs in the more rigid ct-DNA. This shows that threading intercalation is not always selective for more flexible DNA structures, and that the increased DNA flexibility may instead result in better accommodation of rigid complexes in the groove.

7.4 Summary

DNA threading intercalators show extremely slow association and dissociation kinetics compared to other DNA binding drugs. As there appears to be a correlation between slow dissociation kinetics and biological activity, threading intercalating agents are interesting as model compounds in the search for new DNA targeting therapeutics. In this work we have synthesized the new ΔΔ- and ΛΛ-[μ-bidppze(phen)$_4$Ru$_2$]$^{4+}$ **54** and investigated how the bridging ligand length affects their DNA binding properties. We have found that increasing

the length of the bridging ligand by introduction of the ethynyl linker improves threading by increasing the association rate and decreasing the dissociation rate. However, at the same time the selectivity for AT-rich DNA is impaired and the enantioselectivity is reversed. These findings are important for future design of novel DNA binding drugs with slow kinetics. Moreover, we have synthesized Δ- and Λ-$[Ru(phen)_2dppzpa]^{2+}$ **68**, which can be useful intermediates for the synthesis of new interesting Ru-complexes in the future.

8 Covalent Functionalization of Carbon Nanotube Forests Grown *In Situ* on a Metal-Silicon Chip

8.1 Aim of the project

In this carbon nanotube (CNT) based nanotechnology project, our goal was to develop a method to chemically functionalize CNTs on chip, to serve as a robust platform for several applications, such as biosensors, microelectronics, solar cells and microtweezers. We wanted to introduce a functional group on the CNTs on chip, which by a simple and mild reaction, such as the CuAAC reaction, could be used to attach the molecule of interest for the specific application.

8.2 Results

The 1,3-dipolar cycloaddition reaction of azomethine ylides to activated double bonds has previously been applied to both C_{60} and single-walled carbon nanotubes (SWCNTs) in solution.[161,310] Our strategy to functionalize the CNTs on chip is based on this reaction. Figure 57 shows the CNTs on chip we used and a schematic drawing of the chip structure.

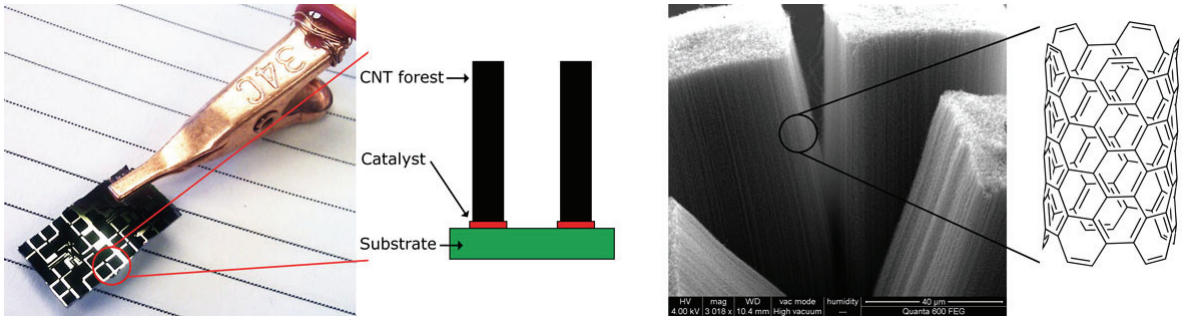

Figure 57. Black squares in the picture (left) are CNT forests and the schematic drawing (center) shows how the CNT forests are bound to the surface on chip. A SEM micrograph of CNT forest consists of a bundle of many vertically aligned CNTs (right).

The azomethine ylide can be formed *in situ* when an amino acid is heated in the presence of an aldehyde. Glycine and benzaldehyde were heated to 120 °C in dichlorobenzene to generate the azomethine ylide and the formed ylide was then allowed to react with double bonds in the CNT structures on the chip. The reaction setup is shown in Figure 58 and the reaction scheme is outlined in Figure 59. The procedure afforded the amine-modified CNT forest on chip, *f*-CNT **1**, and after a cleaning process *f*-CNT **1** was further derivatized by employing a simple amide coupling using PyBOP®[311] and O-(2-azidoethyl)-O-[2-(diglycolyl-amino)-ethyl]heptaethylene glycol to introduce azide functionalities on the CNTs. The functionalized

CNT forests on chip were then analyzed using scanning electron microscope (SEM) equipped with an energy dispersive X-ray spectroscopy (EDS or EDX) detector.

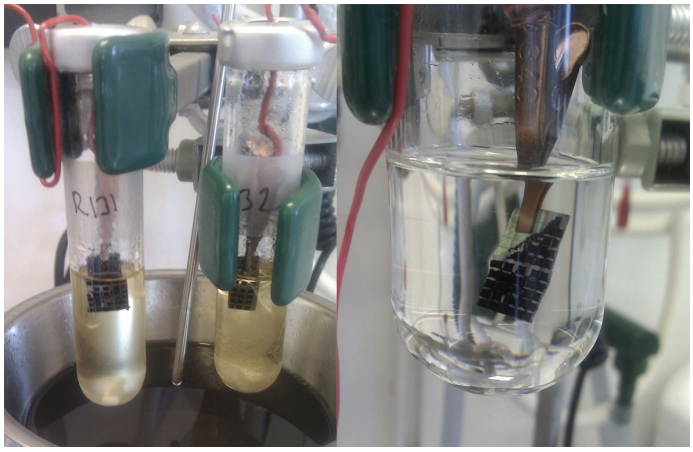

Figure 58. Left picture shows the reaction setup (after reaction) and right picture shows the cleaning setup, performed three times for a minimum of 1 h after every reaction step.

The EDS spectra of *f*-CNT **1** and *f*-CNT **2** both showed a small nitrogen peak, but did not display any significant differences that could confirm the presence of the desired azide functionality. In order to verify that the CNTs were indeed successfully functionalized with active azide groups, we employed a CuAAC reaction to introduce a new element that could be detected with EDS. We chose to introduce fluorine in the form of a trifluoromethyl group on the alkyne, and as a control experiment the CuAAC reaction was also performed on *f*-CNT **1** to verify that the expected fluorine peak in the EDS spectra of the modified chip did not originate from unspecific binding. A reaction scheme of the functionalization process is shown in Figure 59.

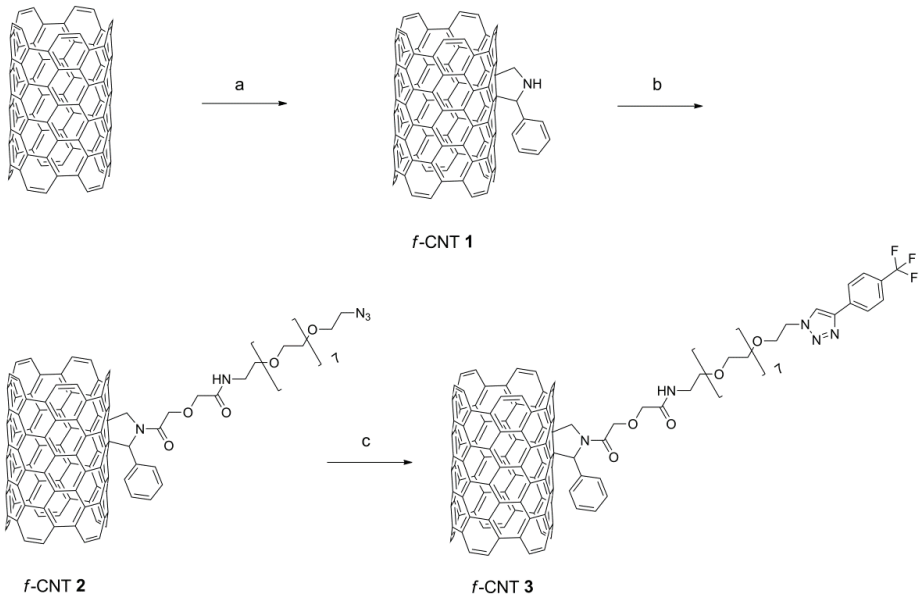

Figure 59. Reaction scheme showing the introduction of active azide groups on CNTs on chip. (a) Glycine, benzaldehyde, dichlorobenzene, 120 °C for 6 to 48 h. (b) PyBOP, O-(2-azidoethyl)-O-[2-(diglycolyl-amino)ethyl]heptaethylene glycol, DIPEA, CH_2Cl_2, 24 h at r.t. (c) 1-Ethynyl-4-(trifluoromethyl)benzene, $CuSO_4$, sodium ascorbate, DMA/H_2O 3:1, 40 h at r.t.

The SEM micrograph and EDS spectrum of *f*-CNT **3** are outlined in Figure 60, and show a clear fluorine peak at 0.68 keV, which indicates that the CNT forests are covalently functionalized with fluorine. The EDS spectrum of the control experiment showed no clear fluorine peak, only the iron peak nearby. These results together indicate that the fluorine atoms in *f*-CNT **3** are covalently attached. This also confirms that *f*-CNT **2** was successfully functionalized with active azide groups.

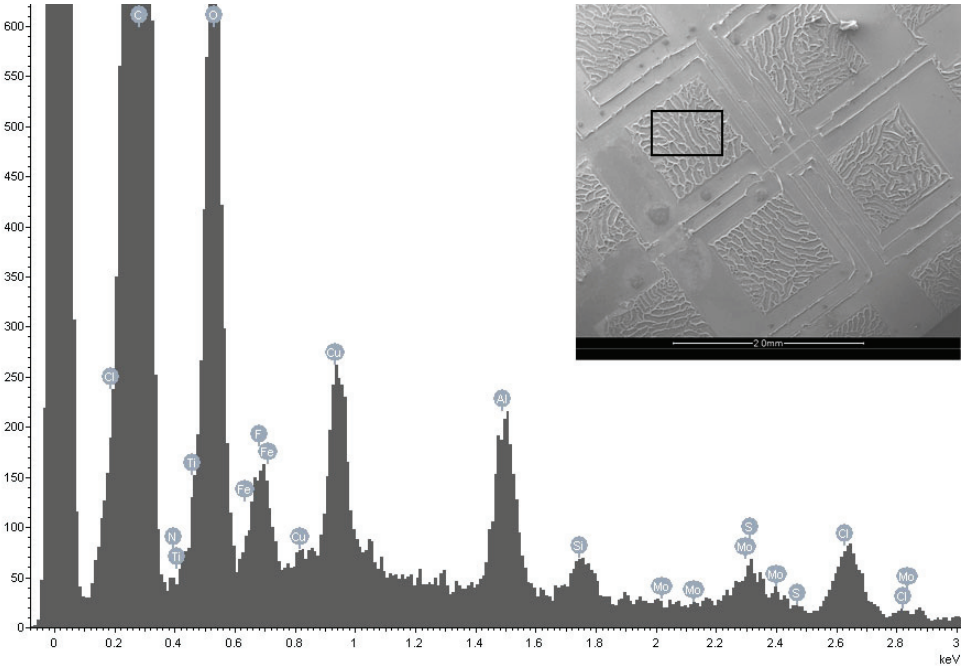

Figure 60. SEM micrograph of the section of CNT forest where EDS was performed on *f*-CNT **3**.

8.3 Summary

The presence of nitrogen in the EDS data on *f*-CNT **2** indicates successful attachment of the azide group. By performing a CuAAC reaction on *f*-CNT **2** with a fluorine source, *f*-CNT **3** was successfully synthesized. The fluorine peak in the EDS spectra (Figure 60) of *f*-CNT **3** together with the absence of fluorine in the control experiment, confirms the successful chemical reaction on the CNTs. This result also demonstrates that the azide functional group can be used to attach other interesting molecules to the CNTs grown on chip.

8.4 Future plans

Efforts to determine the degree of functionalization on the CNTs are currently ongoing. We have modified the CNTs with Fmoc protected amine groups, *f*-CNT **4** and *f*-CNT **5,** as shown in Figure 61. By removal of the Fmoc in piperidine/DMF solution followed by determination of the concentration of cleaved product in the solution with absorbance measurement,

hopefully an estimation of the degree of functionalization can be made. After Fmoc-deprotection of *f*-CNT **5**, *f*-CNT **6** will be obtained, containing two orthogonal functional groups (alkyne and amine). This structure can be used to attach two different molecules of interest.

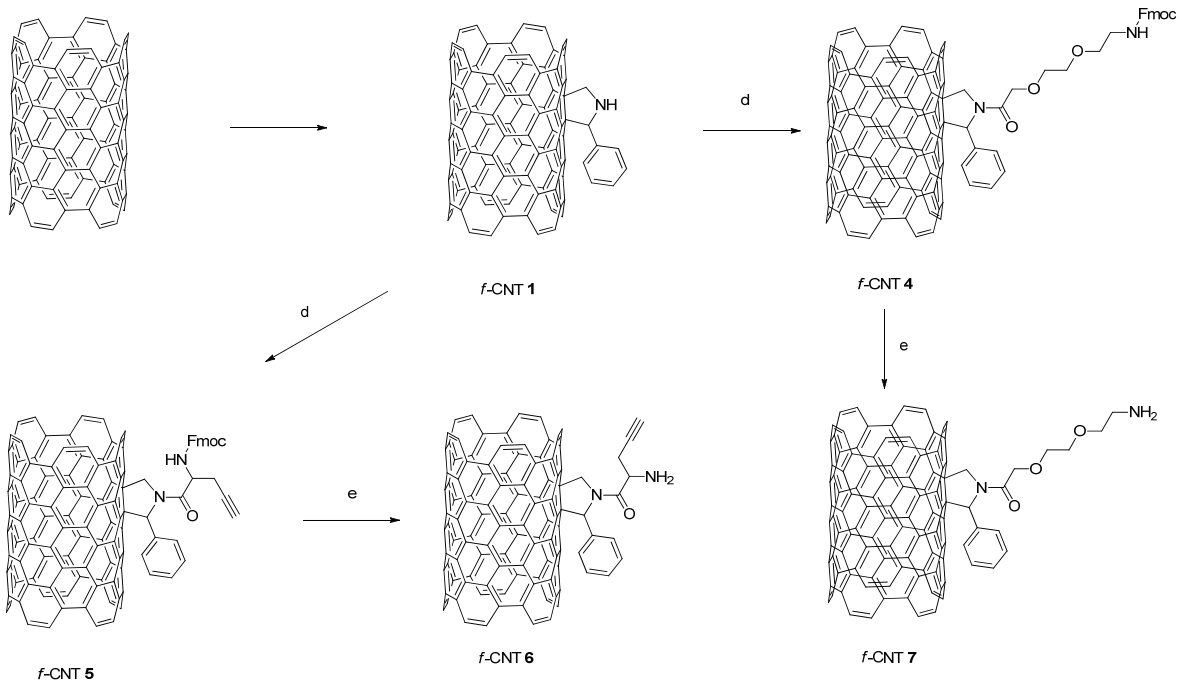

Figure 61. Reaction scheme showing the introduction of Fmoc-protected amine groups on *f*-CNT **1**.

In the future, we will investigate the possibility to use this functionalized CNT-platform to attach biomolecules such as proteins and DNA for biosensor application and microtweezer experiments.

9 Concluding Remarks

The popularity of nitrogen heterocycles in for example the pharmaceutical industry originates from the fact that nitrogen heterocycles display an exceptionally broad spectre of properties. Due to this diversity, they are one of the most commonly used structural elements in drug discovery. However, this variation in properties is also the reason why the chemistry and synthetic pathway to each heterocycle is unique. This means that research to find new methods, as well as to improve existing methods for the synthesis of nitrogen heterocycles and their chemistry, is still important for organic chemists. Many ruthenium complexes exhibit versatile properties which make them useful tools as catalysts, and many of them can also be applied in the creation of interesting nitrogen heterocycles. This makes the exploration of new Ru-complexes as both catalysts and as probes attractive.

Our research on the RuAAC reaction has lead to a new practical and simple sequential one-pot procedure, using either the $[RuClCp^*(PPh_3)_2]$ or the $[RuCl_2Cp^*]_x$ catalyst. It was also found that the reaction is sensitive to an excess of sodium azide and hence, the yield of the initial substitution reaction is crucial for a good result in the later cycloaddition. The tolerance of functional groups present in the substrate was investigated, and functionalities such as alcohols, amines, esters, fluorides, chlorides, pyridines, carbamates, amides and nitro-groups were found to be compatible with the reaction conditions. The effect of different solvents as the reaction medium was also studied.

The RuAAC reaction was also applied in the synthesis of the 5Tzl monomer **42** in excellent yield, where the monomer was used in the construction towards peptidomimetic foldamers. In our initial study, the 5Tzl-trimer **48** was investigated by 2D NOESY, and it was found that several conformers are present in DMSO solution at room temperatrue, where the helical H10 and H16 together with the turn-like structures T1-3 are the most probable ones. Future work in this field is planned, including improvement of the amide coupling step. Introduction of side-chains and chirality, together with toxicity tests also have high priority.

We have also studied the effect of the length of the bridging ligands for DNA-threading intercalation of binuclear Ru-complexes. A synthesis of the ΔΔ- and ΛΛ- enantiomers of the new DNA-binding Ru-complex $[\mu\text{-bidppze}(phen)_4Ru_2]^{4+}$ **54** was established, and binding studies showed that with increased length of the bridging ligand the DNA-threading intercalation was improved by increasing the association rate and decreasing the dissociation rate. However, at the same time the selectivity for AT-rich DNA was decreased, and the enantioselectivity was reversed. These findings are important for future design of novel DNA binding drugs with slow kinetics.

Moreover, functionalization of CNTs on a metal-silicon chip was demonstrated by covalent attachment of functional azide goups via diazomethine ylide cycloadditions to form pyrrolidines with the CNT-walls. This initial study shows the potential of this methodology for applications such as biosensors in the future.

10 References

1. Njardarson, http://cbc.arizona.edu/njardarson/group/top-pharmaceuticals-poster, downloaded March 2012.

2. S. Husted, J. J. J. van Giezen," Ticagrelor: The First Reversibly Binding Oral P2Y12 Receptor Antagonist", Cardiovascular Therapeutics 2009, 27, 259–274.

3. J. A. Joule and K. Mills, "Heterocyclic Chemistry", 5th Ed., Wiley 2010.

4. W. H. Pearson, B. W. Lian, and S. C. Bergmeier; in "Comprehensive Heterocyclic Chemistry II", A. R. Katritzky, C. W. Rees and E. F. V. Scriven, Eds.; Elsevier, Oxford, 1996, vol. 1A, p. 1.

5. T. Eicher and S. Hauptmann, "The chemistry of heterocycles: structure, reactions, syntheses, and applications", 2nd Completely Revised and Enlarged Edition, Wiley 2003.

6. H. K. Hall, "Correlation of the Base Strengths of Amines", J. Am. Chem. Soc. 1957, 79, 5441-5444.

7. G. R. Proctor and J. Redpath, "Monocyclic azepines: the syntheses and chemical properties of the monocyclic azepines", Wiley 1996. Reference 156.

8. R. Linnell, "Dissociation Constants of 2-Substituted Pyridines", J. Org. Chem. 1960, 25, 290.

9. Christian A.G.N. Montalbetti, Virginie Falque, "Amide bond formation and peptide coupling", Tetrahedron 2005, Volume 61, Issue 46, 10827–10852.

10. W. A. Herrmann, "N-Heterocyclic Carbenes: A New Concept in Organometallic Catalysis", Angew. Chem. Int. Ed. 2002, 41, 1290-1309.

11. V. P. W. Böhm, C. W. K. Gstöttmayr, T. Weskamp, W. A. Herrmann, "Catalytic C−C Bond Formation through Selective Activation of C−F Bonds", Angew. Chem. Int. Ed. 2001, 40, 3387-3389.

12. M. G. Organ, M. Abdel-Hadi, S. Avola, I. Dubovyk, N. Hadei, E. Assen, B. Kantchev, C. J. O'Brien, M. Sayah, and C. Valente, "Pd-Catalyzed Aryl Amination Mediated by Well Defined, N-Heterocyclic Carbene (NHC)–Pd Precatalysts, PEPPSI", Chem. Eur. J. 2008, 14, 2443–2452.

13. B. Springthorpe, A. Bailey, P. Barton, T. N. Birkinshaw, R. V. Bonnert, R. C. Brown, D. Chapman, J. Dixon, S. D. Guile, R. G. Humphries, S. F. Hunt, F. Ince, A. H. Ingall, I. P. Kirk, P. D. Leeson, P. Leff, R. J. Lewis, B. P. Martin, D. F. McGinnity, M. P. Mortimore, S. W. Paine, G. Pairaudeau, A. Patel, A. J. Rigby, R. J. Riley, B. J. Teobald, W. Tomlinson, P. J. H. Webborn and P. A. Willis, "From ATP to AZD6140: The discovery of an orally active reversible $P2Y_{12}$ receptor antagonist for the prevention of thrombosis", Bioorg. Med. Chem. Lett. 2007, 17, 6013–6018.

14. S. Bräse and K. Banert, "Organic Azides: Syntheses and Applications", Wiley 2010, 37-39.

15. J.P. Horwitz, B. E. Fischer, A. J. Tomasewski, "The Synthesis of 1-Substituted 5(4*H*)Tetrazolinones", J. Am. Chem. Soc. 1959, 81, 3076-3078.

16. T. Goto, S. Ito, Y. Watanabe, S. Narabu, A. Yanagi (Nihon Bayer Agrochem), EP 612735 1994, Chem. Abstr. 122, 81375.

17. T. Goto, H. Hayakawa, Y. Watanabe, S. Narabu, A. Yanagi (Nihon Bayer Agrochem), EP 578090 1994, Chem. Abstr. 121, 57514.

18. R. N. Butler, A. Fox, S. Collier and L. A. Burke, "Pentazole chemistry: the mechanism of the reaction of aryldiazonium chlorides with azide ion at –80 °C: concerted *versus* stepwise formation of arylpentazoles, detection of a pentazene intermediate, a combined ^{1}H and ^{15}N NMR experimental and *ab initio* theoretical study", J. Chem. Soc., Perkin Trans. 2 1998, 2243-2248.

19. V. N. Pitchkov, Platinum Metals, Rev. 1996, 40, 181-188.

20. M. E. Weeks, "The discovery of the elements. VIII. The platinum metals", J. Chem. Educ. 1932, 9, 1017.

21. N. N. Greenwood, A. Earnshaw, Chemistry of the Elements, 2nd edn. 1997, Elsevier Science Ltd. ISBN 0 7506 3365 4.

22. Ullmann's Encyclopedia of Industrial Chemistry, 5th edn. 1992, Vol. A21, 86-105, VCH, Weinheim.

23. T. Bell, http://metals.about.com/od/properties/a/Metal-Profile-Ruthenium.htm, downloaded August 2013.

24. Y. Gong, M. Zhou, M. Kaupp, and S. Riedel, "Formation and Characterization of the Iridium Tetroxide Molecule with Iridium in the Oxidation State +VIII", Angew. Chem. Int. Ed. 2009, 48, 7879 –7883.

25. W. P. Griffith, "The Chemistry of the Rare Platinum Metals: Os, Ru, Ir and Rh", Wiley-Interscience, New York, 1967.

26. F. A. Cotton, G. Wilkinson, C. A. Murillo, M. Bochman, "Advanced Inorganic Chemistry, 6th ed., John Wiley & Sons, New York, 1999.

27. S. Komiya, M. Hirano, "Synthesis of Organimetallic Compounds", S. Komiya (Ed.), John Wiley & Sons, New York, 1997.

28. J. Hartwig, Organotransition Metal Chemistry, From Bonding to Catalysis, 2010, University Science Books, ISBN 978-1-891389-53-5.

29. S.-I. Murahashi, "Ruthenium in Organic Synthesis", 2004, Wiley-VCH Verlag GmbH & Co. KGaA, Weinheim, ISBN: 3-527-30692-7.

30. T. Naota, H. Takaya, S.-I. Murahashi, "Ruthenium-Catalyzed Reactions for Organic Synthesis", Chem. Rev. 1998, 98, 2599-2660.

31. B. M. Trost, F. D. Toste, A. B. Pinkerton, "Non-metathesis ruthenium-catalyzed C-C bond formation", Chem. Rev. 2001, 101, 2067-2096.

32. G. Maas, "Ruthenium-catalysed carbenoid cyclopropanation reactions with diazo compounds", Chem. Soc. Rev., 2004, 33, 183-190.

33. B. Heller and M. Hapke, "The fascinating construction of pyridine ring systems by transition metal-catalysed [2 + 2 + 2] cycloaddition reactions", Chem. Soc. Rev. 2007, 36, 1085-1094.

34. J. S. M. Samec, J.-E. Bäckvall, P. G. Andersson, and P. Brandt, "Mechanistic aspects of transition metal-catalyzed hydrogen transfer reactions", Chem. Soc. Rev. 2006, 35, 237-248.

35. A. H. Hoveyda, and A. R. Zhugralin, "The remarkable metal-catalysed olefin metathesis reaction", Nature 2007, 450, 243-251.

36. B. M. Trost, M. U. Frederiksen, M. T. Rudd, "Ruthenium-Catalyzed Reactions—A Treasure Trove of Atom-Economic Transformations", Angew. Chem. Int. Ed. 2005, 44, 6630-6666.

37. S.-I. Murahashi, and D. Zhanga, “Ruthenium catalyzed biomimetic oxidation in organic synthesis inspired by cytochrome P-450”, Chem. Soc. Rev. 2008, 37, 1490-1501.

38. C.-J. Li, and L. Chen, “Organic chemistry in water”, Chem. Soc. Rev. 2006, 35, 68-82.

39. J. M. Murphy, J. D. Lawrence, K. Kawamura, C. Incarvito, and J. F. Hartwig, “Ruthenium-Catalyzed Regiospecific Borylation of Methyl C−H Bonds”, J. Am. Chem. Soc. 2006, 128, 13684–13685.

40. S. Gladiali, and E. Alberico, “Asymmetric transfer hydrogenation: chiral ligands and applications”, Chem. Soc. Rev. 2006, 35, 226-236.

41. L. Ackermann, “Carboxylate-Assisted Transition-Metal-Catalyzed C−H Bond Functionalizations: Mechanism and Scope”, Chem. Rev. 2011, 111, 1315–1345.

42. B. Martín-Matute, K. Bogár, M. Edin, F. B. Kaynak, J.-E. Bäckvall, “Highly Efficient Redox Isomerization of Allylic Alcohols at Ambient Temperature Catalyzed by Novel Ruthenium–Cyclopentadienyl Complexes—New Insight into the Mechanism”, Chem. Eur. J. 2005, 11, 5832–5842.

43. N. Ahlsten, A. Bartoszewicz, and B. Martín-Matute, “Allylic alcohols as synthetic enolate equivalents: Isomerisation and tandem reactions catalysed by transition metal complexes”, Dalton Trans. 2012, 41, 1660-1670.

44. S. Agrawal , M. Lenormand , and B. Martín-Matute , “Selective Alkylation of (Hetero)Aromatic Amines with Alcohols Catalyzed by a Ruthenium Pincer Complex”, Org. Lett. 2012, 14, 1456–1459.

45. F. Carson, S. Agrawal, M. Gustafsson, A. Bartoszewicz, F. Moraga, X. Zou, B. Martín-Matute, “Ruthenium Complexation in an Aluminium Metal–Organic Framework and Its Application in Alcohol Oxidation Catalysis”, Chem. Eur. J. 2012, 18, 15337–15344.

46. Z. Sahli , B. Sundararaju , M. Achard, and C. Bruneau, ” Ruthenium-Catalyzed Reductive Amination of Allylic Alcohols”, Org. Lett., 2011, 13, 3964–3967.

47. R. H. Crabtree, “An Organometallic Future in Green and Energy Chemistry”, Organometallics 2011, 30, 17–19.

48. B. L. Conley , M. K. Pennington-Boggio , E. Boz, and T. J. Williams, “Discovery, Applications, and Catalytic Mechanisms of Shvo’s Catalyst”, Chem. Rev. 2010, 110 , 2294–2312.

49. A. M. Appel, J. E. Bercaw, A. B. Bocarsly, H. Dobbek, D. L. DuBois, M. Dupuis, J. G. Ferry , E. Fujita, R. Hille , P. J. A. Kenis, C. A. Kerfeld, R. H. Morris , C. H. F. Peden, A. R. Portis , S. W. Ragsdale, T. B. Rauchfuss, J. N. H. Reek , L. C. Seefeldt , R. K. Thauer , and G. L. Waldrop, “Frontiers, Opportunities, and Challenges in Biochemical and Chemical Catalysis of CO2 Fixation”, Chem. Rev. 2013, 113, 6621–6658.

50. M. C. Warner and J.-E. Bäckvall, “Mechanistic Aspects on Cyclopentadienylruthenium Complexes in Catalytic Racemization of Alcohols”, Acc. Chem. Res., Article ASAP, DOI: 10.1021/ar400038g.

51. H. Yamazaki, A. Shouji, M. Kajita, M. Yagi, “Electrocatalytic and photocatalytic water oxidation to dioxygen based on metal complexes”, Coord. Chem. Rev. 2010, 254, 2483–2491.

52. J. H. Simpson, J. Godfrey, R. Fox, A. Kotnis, D. Kacsur, J. Hamm, M. Totelben, V. Rosso, R. Mueller, E. Delaney, and R. P. Deshpande, “A pilot-scale synthesis of (1R)-trans-2-(2,3-dihydro-4-benzofuranyl)cyclopropanecarboxylic acid: a practical application of asymmetric cyclopropanation using a styrene as a limiting reagent”, Tetrahedron: Asymmetry 2003, 14, 3569–3574.

53. S. Hashiguchi, A. Fujii, J. Takehara, T. Ikariya, and R. Noyori, “Asymmetric transfer hydrogenation of aromatic ketones catalyzed by chiral ruthenium(II) complexes”, J. Am. Chem. Soc. 1995, 117, 7562-7563.

54. A. J. Bailey and B. R. James, “Catalysed aerobic dehydrogenation of amines and an X-ray crystal structure of a bis(benzylamine) ruthenium(II) porphyrin species”, Chem. Commun. 1996, 2343-2344.

55. T. Nagata, M. Nakagawa, and A. Nishida, “The First Total Synthesis of Nakadomarin A”, J. Am. Chem. Soc. 2003, 125, 7484-7485.

56. Y. Fukumoto, T. Dohi, H. Masaoka, N. Chatani, and S. Murai, “Reaction of terminal alkynes with hydrazines to give nitriles, catalyzed by $TpRuCl(PPh_3)_2$: Novel catalytic transformation involving a vinylidene ruthenium intermediate”, Organometallics 2002, 21, 3445-3447.

57. B. Martín-Matute, M. Edin, K. Bogár, and J.-E. Bäckvall, “Highly Compatible Metal and Enzyme Catalysts for Efficient Dynamic Kinetic Resolution of Alcohols at Ambient Temperature”, Angew. Chem. Int. Ed. 2004, 43, 6535-6539.

58. B. Martín-Matute, M. Edin, K. Bogár, F. B. Kaynak, and J.-E. Bäckvall, “Combined Ruthenium(II) and Lipase Catalysis for Efficient Dynamic Kinetic Resolution of Secondary Alcohols. Insight into the Racemization Mechanism”, J. Am. Chem. Soc. 2005, 127, 8817-8825.

59. S. Agrawal, M. Lenormand, and B. Martín-Matute, “Selective alkylation of (hetero)aromatic amines with alcohols catalyzed by a ruthenium pincer complex”, Org. Lett. 2012, 14, 1456-1459.

60. B. M. Trost and R. C. Livingston, “Two-metal catalyst system for redox isomerisation of propargyl alcohols to enals and enones”, J. Am. Chem. Soc. 1995, 117, 9586-9587.

61. T. Fukuyama, N. Chatani, J. Tatsumi, F. Kakiuchi, and S. Murai, “$Ru_3(CO)_{12}$-Catalyzed Site-Selective Carbonylation Reactions at a C−H Bond in Aza-Heterocycles”, J. Am. Chem. Soc. 1998, 120, 11522-11523.

62. N. Chatani, T. Fukuyama, F. Kakiuchi, S. Murai, “$Ru_3(CO)_{12}$-Catalyzed Coupling of Heteroaromatic C−H/CO/Olefins. Regioselective Acylation of the Imidazole Ring”, J. Am. Chem. Soc. 1996, 118, 493-494.

63. Y. Nishibayashi, I. Wakiji, and M. Hidai, J. Am. Chem. Soc. 2000, 122, 11019.

64. Y. Nishibayashi, M. D. Milton, Y. Inada, M. Yoshikawa, I. Wakiji, M. Hidai, and S. Uemura, Chem. Eur. J. 2005, 11, 1433.

65. Y. Nishibayashi, I. Wakiji, Y. Ishii, S. Uemura, and M. Hidai, J. Am. Chem. Soc. 2001, 123, 1433.

66. Y. Nishibayashi, M. Yoshikawa, Y. Inada, M. Hidai, and S. Uemura, J. Am. Chem. Soc. 2002, 124, 11846.

67. Y. Nishibayashi, M. Yoshikawa, Y. Inada, M. Hidai, and S. Uemura, J. Org. Chem. 2004, 69, 3408.

68. Y. Nishibayashi, Y. Inada, M. Hidai, and S. Uemura, J. Am. Chem. Soc. 2002, 124, 7900.

69. Y. Nishibayashi, Y. Inada, M. Hidai, and S. Uemura, J. Am. Chem. Soc. 2003, 125, 6060.

70. Y. Nishibayashi, Y. Inada, M. Hidai, and S. Uemura, J. Am. Chem. Soc. 2002, 124, 15172.

71. Y. Nishibayashi, Y. Inada, M. Yoshikawa, M. Hidai, and S. Uemura, Angew. Chem. Int. Ed. 2003, 42, 1495.

72. L. U. Nordstrøm, H. Vogt, and R. Madsen, “Amide Synthesis from Alcohols and Amines by the Extrusion of Dihydrogen”, J. Am. Chem. Soc. 2008, 130, 17672–17673.

73. C. K. Prier, D. A. Rankic, and D. W. C. MacMillan, “Visible Light Photoredox Catalysis with Transition Metal Complexes: Applications in Organic Synthesis”, Chem. Rev. 2013, 113, 5322−5363.

74. A. Juris, V. Balzani, F. Barigelletti, S. Campagna, P. Belser, and A. von Zelewsky, Coord. Chem. Rev. 1988, 84, 85.

75. A. Juris, V. Balzani, P. Belser, and A. von Zelewsky, Helv. Chim. Acta 1981, 64, 2175.

76. D. A. Nicewicz and D. W. C. MacMillan, “Merging Photoredox Catalysis with Organocatalysis: The Direct Asymmetric Alkylation of Aldehydes”, Science 2008, 322, 77-80.

77. P. Lincoln, A. Broo, B. Nordén, “Diastereomeric DNA-Binding Geometries of Intercalated Ruthenium(II) Trischelates Probed by Linear Dichroism: $[Ru(phen)_2DPPZ]^{2+}$ and $[Ru(phen)_2BDPPZ]^{2+}$”, J. Am. Chem. Soc. 1996, 118, 2644-2653.

78. K. E. Erkkila, D. T. Odom, and J. K. Barton, “Recognition and Reaction of Metallo-interactions with DNA”, Chem. Rev. 1999, 99, 2777-2795.

79. C. Metcalfe and J. A. Thomas, “Kinetically Inert Transition Metal Complexes That Reversibly Bind to DNA”, Chem. Soc. Rev. 2003, 32, 215-224.

80. J. G. Vos and J. M. Kelly, “Ruthenium Polypyridyl Chemistry, from Basic Research to Applications and Back Again”, Dalton Trans. 2006, 41, 4869-4883.

81. A. E. Friedman, J. C. Chambron, J. P. Sauvage et al., “Molecular Light Switch for DNA – $Ru(bpy)_2(dppz)^{2+}$”, J. Am. Chem. Soc. 1990, 112, 4960-4962.

82. C. Hiort, P. Lincoln, and B. Nordén, “DNA-Binding of Δ-$[Ru(phen)_2dppz]^{2+}$ and Λ-$[Ru(phen)_2dppz]^{2+}$”, J. Am. Chem. Soc. 1993, 115, 3448-3454.

83. J. Olofsson, L. M. Wilhelmsson, and P. Lincoln, “Effects of Methyl Substitution on Radiative and Solvent Quenching Rate Constants of $[Ru(phen)_2dppz]^{2+}$ in Polyol Solvents and Bound to DNA”, J. Am. Chem. Soc. 2004, 126, 15458-15465.

84. J. R. Lakowicz, Principles of Fluorescence Spectroscopy, 3rd Ed, Springer 2006, New York. 683-695.

85. J. K. Barton, A. T. Danishefsky, and J. M. Goldberg, “Tris(phenanthroline)Ruthenium(II) – Stereoselectivity in Binding to DNA”, J. Am. Chem. Soc. 1984, 106, 2172-2176.

86. F. R. Keene, J. A. Smith, and J. G. Collins, “Metal Complexes as Structure-Selective Binding Agents for Nucleic Acids”, Coord. Chem. Rev. 2009, 253, 2021-2035.

87. S. S. Bhat, et al. , ”Ruthenium(II) Polypyridyl Complexes as Carriers for DNA Delivery”, Chem. Commun. 2011, 47, 11068-11070.

88. E. Musatkina, et al. , “Mono- and dicarboxylic Polypyridyl-Ru Complexes as Potential Cell DNA Dyes and Transfection Agents”, J. Inorg. Biochem. 2007, 101, 1086-1089.

89. E. S. Antonarakis and A. Emadi, “Ruthenium-Based Chemotherapeutics: Are They Ready for Prime Time?”, Cancer Chemother. Pharmacol. 2010, 66, 1-9.

90. L. Salassa, “Polypyridyl Metal Complexes with Biological Activity”, Eur. J. Inorg. Chem. 2011, 32, 4931-4947.

91. V. Fernandez-Moreira, F. L. Thorp-Greenwood, and M. P. Coogan, "Application of d^6 Transition Metal Complexes in Fluorescence Cell Imaging", Chem. Commun. 2010, 46, 186-202.

92. M. R. Gill, J. Garcia-Lara, S. Foster, et al., "A Ruthenium(II) Polypyridyl Complex for Direct Imaging of DNA Structure in Living Cells", Nat. Chem. 2009, 1, 662-667.

93. Q. Zhao, C. H. Huang, and F. Y. Li, "Phosphorescent Heavy-Metal Complexes for Bioimaging", Chem. Soc. Rev. 2011, 40, 2508-2524.

94. T. Curtius, Ber. Dtsch. Chem. Ges. 1883, 16, 2230-2231.

95. E. Buchner, Ber. Dtsch. Chem. Ges. 1888, 21, 2637-2647.

96. R. Huisgen, Angew. Chem. Int. Ed. 1963, 2, 565-632.

97. L. I. Smith, Chem. Rev. 1938, 23, 193-285.

98. R: Huisgen, G. Szeimies, L. Möbius, Chem. Ber. 1967, 100, 2494-2507.

99. K. V. Gothelf, K. A. Jørgensen, "Asymmetric 1,3-Dipolar Cycloaddition Reactions", Chem. Rev. 1998, 98, 863-909.

100. F. Avemaria, V. Zimmermann, S. Bräse, "Synthesis of Aryl Azides via Post-Cleavage Modification of Polymer-Bound Triazenes", Synlett. 2004, 1163-1165.

101. K. N. Houk, J. Gonzáles, Y. Li, "Pericyclic Reaction Transition States: Passions and Punctilios, 1935-1995", Acc. Chem. Res. 1995, 28, 81-90.

102. C. Di Valentin, M. Freccero, R. Gandolfi, A. Rastelli, "Concerted vs Stepwise Mechanism in 1,3-Dipolar Cycloaddition of Nitrone to Ethene, Cyclobutadiene, and Benzocyclobutadiene. A Computational Study", J. Org. Chem. 2000, 65, 6112-6120.

103. K. N. Houk and T. Strassner, "Establishing the (3 + 2) Mechanism for the Permanganate Oxidation of Alkenes by Theory and Kinetic Isotope Effects", J. Org. Chem. 1999, 64, 800-802.

104. S. Bräse, A. Friedrich, M. Gartner, T. Grab, T. Schröder, Topics in Heterocycl. Springer, Berlin 2008.

105. M. J. S. Dewar, R. C. Dougherty, "The P.M.O. Theory of Organic Chemistry", Plenum Press, New York, 1975.

106. M. J. S. Dewar, "Molecular Orbital Theory for Organic Chemist", McGraw Hill, New York, 1969.

107. C. A. Coulson, H. C. Longuet-Higgins, Proc. Roy. Soc. A 1947, 192, 16.

108. I. Fleming, "Frontier Molecular Orbitals and Organic Chemical Reactions, Wiley, London, 1976, p. 23.

109. G. S. Hammond, "A Correlation of Reaction Rates", J. Am. Chem. Soc. 1955, 77, 334.

110. M. B. Smith, "Organic Synthesis", 2nd ed., McGraw Hill, New York, 2002.

111. S. Bräse, C. Gil, K. Knepper, V. Zimmermann, "Organic Azides: An Exploding Diversity of a Unique Class of Compounds", Angew. Chem., Int. Ed. 2005, 44, 5188-5240.

112. C. I. Schilling, S. Bräse, "Stable organic azides based on rigid tetrahedral methane and adamantane structures as high energetic materials", Org. Biomol. Chem. 2007, 5, 3586-3588.

113. C. W. Tornøe, C. Christensen, M. Meldal, “Peptidotriazoles on Solid Phase: [1,2,3]-Triazoles by Regiospecific Copper(I)-Catalyzed 1,3-Dipolar Cycloadditions of Terminal Alkynes to Azides”, J. Org. Chem. 2002, 67, 3057-3064.

114. V. V. Rostovtsev, L. G. Green, V. V. Fokin, K. B. Sharpless, “A Stepwise Huisgen Cycloaddition Process: Copper(I)-Catalyzed Regioselective Ligation of Azides and Terminal Alkynes”, Angew. Chem., Int. Ed. 2002, 41, 2596-2599.

115. H. C. Kolb, M. G. Finn and K. B. Sharpless, “Click Chemistry: Diverse Chemical Function from a Few Good Reactions”, Angew Chem. Int. Ed. 2001, 40, 2004-2021.

116. M. Meldal, C. W. Tornøe, “Cu-catalyzed azide-alkyne cycloaddition”, Chem. Rev. 2008, 108, 2952-3015.

117. G. Chouhan and K. James, “CuAAC Macrocyclization: High Intramolecular Selectivity through the Use of Copper Tris(triazole) Ligand Complexes”, Org. Lett. 2011, 13, 2754–2757.

118. V. O. Rodionov, V. V. Fokin, M. G. Finn, “Mechanism of the Ligand-Free CuI-Catalyzed Azide–Alkyne Cycloaddition Reaction”, Angew. Chem. Int. Ed. 2005, 44, 2210-2215.

119. B. H. M. Kuijpers, S. Groothuys, A. R. Keereweer, P. J. L. M. Quaedflieg, R. H. Blaauw, F. L. van Delft, F. P. J. T. Rutjes, “Expedient Synthesis of Triazole-Linked Glycosyl Amino Acids and Peptides”, Org. Lett. 2004, 6, 3123-3126.

120. D. A. Ossipov, J. Hilborn, “Poly(vinyl alcohol)-Based Hydrogels Formed by “Click Chemistry””, Macromol. 2006, 39, 1709-1718.

121. T. R. Chan, R. Hilgraf, K. B. Sharpless, V. V. Fokin, “Polytriazoles as Copper(I)-Stabilizing Ligands in Catalysis”, Org. Lett. 2004, 6, 2853-2855.

122. M. Malkoch, K. Schleicher, E. Drockenmuller, C. J. Hawker, T. P. Russell, P. Wu, and V. V. Fokin “Structurally Diverse Dendritic Libraries: A Highly Efficient Functionalization Approach Using Click Chemistry”, Macromol. 2005, 38, 3663-3678.

123. P. Wu, A. K. Feldman, A. K. Nugent, C. J. Hawker, A. Scheel, B. Voit, J. Pyun, J. M. Fréchet, K. B. Sharpless, V. V. Fokin, “Efficiency and fidelity in a click-chemistry route to triazole dendrimers by the copper(I)-catalyzed ligation of azides and alkynes.”, Angew. Chem., Int. Ed. 2004, 43, 3928-3932.

124. H. N. Gopi, K. C. Tirupula, S. Baxter, S. Ajith, I. M. Chaiken, “Click Chemistry on Azidoproline: High-Affinity Dual Antagonist for HIV-1 Envelope Glycoprotein gp120”, ChemMedChem 2006, 1, 54-57.

125. J. H. van Maarseveen, W. S. Horne, M. R. Ghadiri, “Efficient route to C2 symmetric heterocyclic backbone modified cyclic peptides.”, Org. Lett. 2005, 7, 4503-4506.

126. W. M. Xu, X. Huang, E. J. Tang, “Solid-phase synthesis of 1,2-diheterocyclic-substituted (E)-olefins from a supported selenium resin.”, Comb. Chem. 2005, 7, 726-733.

127. A. K. Feldman, B. Colasson, V. V. Fokin, “One-pot synthesis of 1,4-disubstituted 1,2,3-triazoles from in situ generated azides.”, Org. Lett. 2004, 6, 3897-3899.

128. X. Zhang, R. P. Hsung, L. You, “Tandem azidination- and hydroazidination-Huisgen [3 + 2] cycloadditions of ynamides. Synthesis of chiral amide-substituted triazoles”, Org. Biomol. Chem. 2006, 4, 2679-2682.

129. V. O. Rodionov, S. I. Presolski, D. D. Diaz, V. V. Fokin, M. G. Finn, “Ligand-accelerated Cu-catalyzed azide-alkyne cycloaddition: a mechanistic report”, J. Am. Chem. Soc. 2007, 129, 12705-12712.

130. K. Tanaka, C. Kageyama, K. Fukase, “Acceleration of Cu(I)-mediated Huisgen 1,3-dipolar Click cycloaddition by histidine deriv”, Tetrahedron Lett. 2007, 48, 6475-6479.

131. Q. Wang, T. R. Chan, R. Hilgraf, V. V. Fokin, K. B. Sharpless, M. G. Finn, “Bioconjugation by copper(I)-catalyzed azide-alkyne [3 + 2] cycloaddition.”, J. Am. Chem. Soc. 2003, 125, 3192-3193.

132. S. I. Van Kasteren, H. B. Kramer, H. H. Jensen, S. J. Campbell, J. Kirkpatrick, N. J. Oldham, D. C. Anthony, B. G. Davis, ”Expanding the diversity of chemical protein modification allows post-translational mimicry.”, Nature, 2007, 446, 1105-1109.

133. V. O. Rodionov, S. I. Presolski, S. Gardinier, Y. H. Lim, M. G. Finn, “Benzimidazole and Related Ligands for Cu-Catalyzed Azide−Alkyne Cycloaddition”, J. Am. Chem. Soc. 2007, 129, 12696-12704.

134. W. G. Lewis, F. G. Magallon, V. V. Fokin, M. G. Finn, “Discovery and Characterization of Catalysts for Azide−Alkyne Cycloaddition by Fluorescence Quenching”, J. Am. Chem. Soc. 2004, 126, 9152-9153.

135. X. L. Sun, C. L. Stabler, C. S. Cazalis, E. L. Chaikof, “Carbohydrate and protein immobilization onto solid surfaces by sequential Diels-Alder and azide-alkyne cycloadditions.”, Bioconjugate Chem. 2006, 17, 52-57.

136. W. H. Zhan, H. N. Barnhill, K. Sivakumar, H. Tian, Q. Wang, “Synthesis of hemicyanine dyes for ‘click’ bioconjugation”, Tetrahedron Lett. 2005, 46, 1691-1695.

137. F. Tian, M. L. Tsao, P. G. Schultz, “A Phage Display System with Unnatural Amino Acids”, J. Am. Chem. Soc. 2004, 126, 15962-15963.

138. C. Girard, E. Onen, M. Aufort, S. Beauvière, E. Samson, J. Herscovici, “Reusable Polymer-Supported Catalyst for the [3+2] Huisgen Cycloaddition in Automation Protocols”, Org. Lett. 2006, 8, 1689-1692.

139. R. Guezguez, K. Bougrin, K. El Akri, R. Benhida, “A highly efficient microwave-assisted solvent-free synthesis of α- and β-2′-deoxy-1,2,3-triazolyl-nucleosides”, Tetrahedron Lett. 2006, 47, 4807-4811.

140. S. Chassaing, A. S. S. Sido, A. Alix, M. Kumarraja, P. Pale, J. Sommer, “"Click chemistry" in zeolites: copper(I) zeolites as new heterogeneous and ligand-free catalysts for the Huisgen [3+2] cycloaddition.”, Chem. Eur. J. 2008, 14, 6713-6721.

141. S.Chassaing, M. Kumarraja, A. S. S. Sido, P. Pale, J. Sommer, “Click chemistry in CuI-zeolites: the Huisgen [3 + 2]-cycloaddition.”,Org. Lett. 2007, 9, 883-886.

142. M. L. Kantam, V. S. Jaya, B. Sreedhar, M. M. Rao, B. M. J. Choudary, “Preparation of alumina supported copper nanoparticles and their application in the synthesis of 1,2,3-triazoles”, Mol. Catal. 2006, 256, 273-277.

143. V. D. Bock, H. Hiemstra, J. H. Van Maarseveen, “CuI-Catalyzed Alkyne-Azide “Click” Cycloadditions from a Mechanistic and Synthetic Perspective”, Eur. J. Org. Chem. 2006, 51-68.

144. B. F. Straub, “mu-Acetylide and mu-alkenylidene ligands in "click" triazole syntheses”, Chem. Commun. 2007, 37, 3868-3870.

145. M. Ahlquist, V. V. Fokin, “Enhanced Reactivity of Dinuclear Copper(I) Acetylides in Dipolar Cycloadditions”, Organometallics 2007, 26, 4389-4391.

146. F. Himo, T. Lovell, R. Hilgraf, V. V. Rostovtsev, L. Noodleman, K. B. Sharpless, V. V. Fokin, “Copper(I)-Catalyzed Synthesis of Azoles. DFT Study Predicts Unprecedented Reactivity and Intermediates”, J. Am. Chem. Soc. 2005, 127, 210-216.

147. L. Zhang, X. Chen, P. Xue, H. H. Y. Sun, I. D. Williams, K. B. Sharpless, V. V. Fokin, and G. Jia, “Ruthenium-Catalyzed Cycloaddition of Alkynes and Organic Azides”, J. Am. Chem. Soc. 2005, 127, 15998-15999.

148. M. M Majireck and S. M. Weinreb, “A Study of the Scope and Regioselectivity of the Ruthenium-Catalyzed [3 + 2]-Cycloaddition of Azides with Internal Alkynes”, J. Org. Chem. 2006, 71, 8680-8683.

149. L. K. Rasmussen, B. C. Boren and V. V. Fokin, “Ruthenium-Catalyzed Cycloaddition of Aryl Azides and Alkynes”, Org. Lett. 2007, 9, 5337-5339.

150. B. C. Boren, S. Narayan, L. K. Rasmussen, L. Zhang, H. Zhao, Z. Lin, G. Jia and V. V. Fokin, “Ruthenium-Catalyzed Azide−Alkyne Cycloaddition: Scope and Mechanism”, J. Am. Chem. Soc. 2008, 130, 8923-8930.

151. M. Lamberti, G. C. Fortman, A. Poater, J. Broggi, A. M. Z. Slawin, L. Cavallo, and S. P. Nolan, “Coordinatively Unsaturated Ruthenium Complexes As Efficient Alkyne–Azide Cycloaddition Catalysts”, Organometallics, 2012, 31, 756–767.

152. U. Pradere, V. Roy, T. R. McBrayer, R. F. Schinazi, L. A. Agrofoglio, “Preparation of ribavirin analogues by copper- and ruthenium-catalyzed azide-alkyne 1,3-dipolar cycloaddition”, Tetrahedron 2008, 64, 9044-9051.

153. A. R. Kelly, J. Wei, S. Kesavan, J-C. Marie, N. Windmon, D. W. Young, L. A. Marcaurelle, “Accessing Skeletal Diversity Using Catalyst Control: Formation of n and n + 1 Macrocyclic Triazole Rings”, Org. Lett. 2009, 11, 2257-2260.

154. H. Nulwala, K. Takizawa, A. Odukale, A. Khan, R. J. Thibault, B. R. Taft, B. H. Lipshutz and C. J. Hawker, “Synthesis and Characterization of Isomeric Vinyl-1,2,3-triazole Materials by Azide-Alkyne Click Chemistry”, Macromolecules 2009, 42, 6068-6074.

155. J. Zhang, J. Kemmink, D. T. S. Rijkers, and R. M. J. Liskamp, “Cu(I)- and Ru(II)-Mediated “Click” Cyclization of Tripeptides Toward Vancomycin-Inspired Mimics”, Org. Lett. 2011, 13, 3438–3441.

156. D.-R. Hou, T.-C. Kuan, Y.-K. Li, R. Lee and K.-W. Huang, “Electronic effects of ruthenium-catalyzed [3+2]-cycloaddition of alkynes”, Tetrahedron 2010, 66, 9415-9420.

157. X. Creary, A. Andersson, C. Brophy, F. Crowell, and Zachary Funk, “Method for assigning structure of 1,2,3-triazoles”, J. Org. Chem. 2012, 77, 8756-8761.

158. A. Arrieta, D. Otaegui, A. Zubia, F. P. Cossío, A. Díaz-Ortiz, A. de la Hoz, M. A. Herrero, P. Prieto, C. Foces-Foces, J. L. Pizarro, and M. I. Arriortua, “Solvent-Free Thermal and Microwave-Assisted [3 + 2] Cycloadditions between Stabilized Azomethine Ylides and Nitrostyrenes. An Experimental and Theoretical Study” J. Org. Chem. 2007, 72, 4313-4322.

159. S. Sanchez, J. H. Bateson, P. J. O'Hanlon, and T. Gallagher, “S-Alkyl Dithioformates as 1,3-Dipolarophiles. Generation of C(2)-Unsubstituted Penems”, Org. Lett. 2004, 6, 2781–2783.

160. T. Gallagher, S. Sanchez, J. H. Bateson, and P. J. O’Hanlon, “Thiocarbonyl-based 1,3-dipolarophiles for the synthesis of C(2)-unsubstituted penems”, Pure Appl. Chem. 2005, 77, 2033-2040.

161. M. Maggini, G. Scorrano and M. Prato, “Addition of azomethine ylides to C60: synthesis, characterization, and functionalization of fullerene pyrrolidines”, J. Am. Chem. Soc. 1993, 115, 9798-9799.

162. P. de la Cruz, A. de la Hoz and F. Langa, “Cycloadditions to [60]fullerene using microwave irradiation: A convenient and expeditious procedure”, Tetrahedron 1997, 53, 2599-2608.

163. S. Wang, J. Zhang, L. Song, H. Jiang and S. Zhu, “One-pot three-component reaction of C_{60}, amino acid and fluorinated benzaldehyde to C_{60}-pyrrolidine derivatives”, J. Fluorine Chem. 2005, 126, 349-353.

164. J. J. Oviedo, P. de la Cruz, J. Garín, J. Orduna and F. Langa, “Ruthenocene as a new donor fragment in [60]fullerene–donor dyads”, Tetrahedron Lett. 2005, 46, 4781–4784.

165. H. P. Zeng, T. Wang, A. S. D. Sandanayaka, Y. Araki, and O. Ito, “Photoinduced Charge Separation and Charge Recombination in [60]Fullerene−Ethylcarbazole and [60]Fullerene−Triphenylamines in Polar Solvents”, J. Phys. Chem. A 2005, 109, 4713–4720.

166. F. Langa, P. de la Cruz, A. de la Hoz, E. Espíldora, F. P. Cossío and B. Lecea “Modification of Regioselectivity in Cycloadditions to C_{70} under Microwave Irradiation”, J. Org, Chem. 2000, 65, 2499-2507.

167. F. G. Brunetti, M. A. Herrero, J. M. Muñoz, S. Giordani, A. Díaz-Ortiz, S. Filippone, G. Ruaro, M. Meneghetti, M. Prato, and E. Vázquez, “Reversible Microwave-Assisted Cycloaddition of Aziridines to Carbon Nanotubes”, J. Am. Chem. Soc. 2007, 129, 14580–14581.

168. F. G. Brunetti, M. A. Herrero, J. M. Muñoz, A. Díaz-Ortiz, J. Alfonsi, M. Meneghetti, M. Prato and E. Vázquez, “Microwave-Induced Multiple Functionalization of Carbon Nanotubes”, ”, J. Am. Chem. Soc. 2008, 130, 8094-8100.

169. S. Marchesan, T. Da Ros, M. Prato, “Isolation and characterization of nine tris-adducts of N-methylfulleropyrrolidine derivatives”, J. Org. Chem. 2005, 70, 4706-4713.

170. G. Pastorin , W. Wu , S. Wieckowski , J.-P. Briand , K. Kostarelos , M. Prato and A. Bianco, “Double functionalisation of carbon nanotubes for multimodal drug delivery”, Chem. Commun., 2006, 1182-1184.

171. D. Tasis, N. Tagmatarchis, A. Bianco and M. Prato, “Chemistry of carbon nanotubes”, Chem Rev 2006, 106, 1105-1136.

172. P. A. Denis and F. Iribarne, “The 1,3 Dipolar Cycloaddition of Azomethine Ylides to Graphene, Single Wall Carbon Nanotubes, and C60”, International Journal of Quantum Chemistry, 2010, 110, 1764-1771.

173. V. Lovat, D. Pantarotto, L. Lagostena, B. Cacciari, M. Grandolfo, M. Righi, G. Spalluto, M. Prato and L. Ballerini, “Carbon Nanotube Substrates Boost Neuronal Electrical Signaling”, Nano Lett. 2005, 5, 1107-1110.

174. M. Quintana, M. Grzlczak and M. Prato, “Organic functionalization of carbon nanostructures via 1,3-dipolar cycloadditions”, Phys. Status Solidi B 2010, 247, 2645-2648.

175. A. Martinek, F. Fülöp, “Peptidic foldamers: ramping up diversity”, Chem. Soc. Rev. 2012, 41, 687-702.

176. D. Seebach, A. K. Beck, and D. J. Bierbaum, “The World of β- and γ-Peptides Comprised of Homologated Proteinogenic Amino Acids and Other Components”, Chem. Biodivers., 2004, 1, 1111-1239.

177. C. Baldauf and H-J. Hofmann, “Ab initio MO Theory – An Important Tool in Foldamer Research: Prediction of Helices in Oligomers of ω-Amino Acids”, Helv. Chim. Acta, 2012, 95, 2348-2383.

178. C. M Goodman, S. Choi, S. Shandler and W. F DeGrado, “Foldamers as versatile frameworks for the design and evolution of function”, Nat Chem Biol 2007, 3, 252 – 262.

179. M. Rueping, Y. Mahajan, M. Sauer, and D. Seebach “Cellular Uptake Studies with β-Peptides”, ChemBioChem, 2002, 3, 257-259.

180. T. B. Potocky, A. K. Menon, and S. H. Gellman, “Cytoplasmic and nuclear delivery of a TAT-derived peptide and a beta-peptide after endocytic uptake into HeLa cells”, J. Biol. Chem. 2003, 278, 50188-50194.

181. J. Frackenpohl, P. I. Arvidsson, J. V. Schreiber, and D. Seebach, “The Outstanding Biological Stability of β- and γ-Peptides toward Proteolytic Enzymes: An In Vitro Investigation with Fifteen Peptidases”, ChemBioChem, 2001, 2, 445-455.

182. F. Yang, N. G. Nickols, B. C. Li, G. K. Marinov, J. W. Said, and P. B. Dervan, “Antitumor activity of a pyrrole-imidazole polyamide”, Proc. Natl. Acad. Sci. USA 2013, 110, 1863-1868.

183. P. I. Arvidsson, J. Frackenpohl, N. S. Ryder, B. Liechty, F. Petersen, H. Zimmermann, G. P. Camenisch, R. Woessner, and Dieter Seebach, “On the Antimicrobial and Hemolytic Activities of Amphiphilic b-Peptides”, ChemBioChem, 2001, 2, 771-773.

184. D. Seebach, M. Overhand, F. N. M. Kühnle, B. Martinoni, L. Oberer, U. Hommel, and H. Widmer, “β-Peptides: Synthesis by Arndt-Eistert Homologation with Concomitant Peptide Coupling. Structure Determination by NMR and CD Spectroscopy and by X-Ray Crystallography. Helical Secondary Structure of a P-Hexapeptide in Solution and Its Stability towards Pepsin”, Helv. Chim. Acta 1996, 79, 913-941.

185. D. H. Appella, L. A. Christianson, I. L. Karle, D. R. Powell, and S. H. Gellman, “β-Peptide Foldamers: Robust Helix Formation in a New Family of β-Amino Acid Oligomers”, J. Am. Chem. Soc. 1996, 118, 13071-13072.

186. J. Wang, C. L. Ma, G. Fiorin, V. Carnevale, T. Wang, F.H. Hu, R. A. Lamb, L. H. Pinto, M. Hong, M. L. Klein, and W. F. DeGrado, “Molecular Dynamics Simulation Directed Rational Design of Inhibitors Targeting Drug-Resistant Mutants of Influenza A Virus M2”, J. Am. Chem. Soc. 2011, 133, 12834-12841.

187. E. Takashiro, I. Hayakawa, T. Nitta, A. Kasuya, S. Miyamoto, Y. Ozawa, R. Yagi, I. Yamamoto, T. Shibayama, A. Nakagawa, Y. Yabe, “Structure-activity relationship of HIV-1 protease inhibitors containing alpha-hydroxy-beta-amino acids. Detailed study of P1 site”, Bioorg Med Chem 1999, 7, 2063-2072.

188. A. J. Karlsson, W. C. Pomerantz, K. J. Neilsen, S. H. Gellman, S. P. Palecek, “Effect of Sequence and Structural Properties on 14-Helical β-Peptide Activity against Candida albicans Planktonic Cells and Biofilms”, Acs Chem Biol 2009, 4, 567-579.

189. K. Ziegelbauer, P. Babczinski, W. Schönfeld, “Molecular Mode of Action of the Antifungal β-Amino Acid BAY 10-8888”, Antimicrob Agents Chemother 1998, 42, 2197-2205.

190. G. N. Tew, R. W. Scott, M. L. Klein, W. F. Degrado, ” De Novo Design of Antimicrobial Polymers, Foldamers, and Small Molecules: From Discovery to Practical Applications”, Accounts Chem Res 2010, 43, 30-39.

191. R. W. Scott, W. F. DeGrado, G. N. Tew, “De novo designed synthetic mimics of antimicrobial peptides”, Curr Opin Biotech 2008, 19, 620-627.

192. G. J. Gabriel, A. E. Madkour, J. M. Dabkowski, C. F. Nelson, K. Nusslein, G. N. Tew, “Synthetic Mimic of Antimicrobial Peptide with Nonmembrane-Disrupting Antibacterial Properties”, Biomacromolecules 2008, 9, 2980-2983.

193. E. A. Porter, B. Weisblum, S. H. Gellman, “Mimicry of Host-Defense Peptides by Unnatural Oligomers: Antimicrobial â-Peptides”, J. Am. Chem. Soc. 2002, 124, 7324-7330.

194. K. Gademann, M. Ernst, D. Hoyer, D. Seebach, “Synthesis and Biological Evaluation of a Cyclo-β-tetrapeptide as a Somatostatin Analogue”, Angew. Chem. Int. Ed. 1999, 38, 1223-1226.

195. J. D. Sadowsky, M. A. Schmitt, H. S. Lee, N. Umezawa, S. M. Wang, Y. Tomita, and S. H. Gellman, “Chimeric (α/β + α)-Peptide Ligands for the BH3-Recognition Cleft of Bcl-x_L: Critical Role of the Molecular Scaffold in Protein Surface Recognition”, J. Am. Chem. Soc. 2005, 127, 11966-11968.

196. E. P. English, R. S. Chumanov, S. H. Gellman, and T. Compton, “Rational Development of β-Peptide Inhibitors of Human Cytomegalovirus Entry”, J. Biol. Chem. 2006, 281, 2661-2667.

197. J. A. Kritzer, J. D. Lear, M. E. Hodsdon, and A. Schepartz, “Helical β-Peptide Inhibitors of the p53-hDM2 Interaction”, J. Am. Chem. Soc. 2004, 126, 9468-9469.

198. J. A. Kritzer, O. M. Stephens, D. A. Guarracino, S. K. Reznik, A. Schepartz, “β-Peptides as inhibitors of protein–protein interactions”, Bioorg. Med. Chem. 2005, 13, 11-16.

199. J. A. Kritzer, M. E. Hodsdon, and A. Schepartz, “Solution Structure of a β-Peptide Ligand for hDM2”, J. Am. Chem. Soc. 2005, 127, 4118-4119.

200. O. M. Stephens, S. Kim, B. D. Welch, M. E. Hodsdon, M. S. Kay, and A. Schepartz, “Inhibiting HIV Fusion with a β-Peptide Foldamer”, J. Am. Chem. Soc. 2005, 127, 13126-13127.

201. C. Nunn , M. Rueping, D. Langenegger, E. Schuepbach, T. Kimmerlin, P. Micuch, K. Hurth, D. Seebach, and D. Hoyer,“ Beta(2)/beta(3)-di- and alpha/beta(3)-tetrapeptide derivatives as potent agonists at somatostatin sst(4) receptors”, Naunyn Schmiedebergs Arch. Pharmacol. 2003, 367, 95-103.

202. M. A. Gelman, S. Richter, H. Cao, N. Umezawa, S. H. Gellman, and T. M. Rana, “Selective Binding of TAR RNA by a Tat-Derived β-Peptide”, Org. Lett. 2003, 5, 3563-3565.

203. D. M. Chenoweth, J. L. Meier, and P. B. Dervan, “Pyrrole-Imidazole Polyamides Distinguish Between Double-Helical DNA and RNA”, Angew. Chem. Int. Ed. 2012, 51, 1 – 5.

204. N. G. Nickols and P. B. Dervan, “Suppression of androgen receptor-mediated gene expression by a sequence-specific DNA-binding polyamide”, Proc. Natl. Acad. Sci. USA 2007, 104, 10418-10423.

205. M. Werder, H. Hauser, S. Abele, D. Seebach, “β-Peptides as Inhibitors of Small-Intestinal Cholesterol and Fat Absorption”, Helv. Chim. Acta 1999, 82, 1774-1783.

206. Y. Hamuro, J. P. Schneider, and W. F. DeGrado, “De Novo Design of Antibacterial β-Peptides”, J. Am. Chem. Soc. 1999, 121, 12200-12201.

207. E. A. Porter, X. Wang, H. S. Lee, B. Weisblum and S. H. Gellman, “Antibiotics: Non-haemolytic β-amino-acid oligomers”, Nature 2000, 404, 565.

208. D. Liu and W. F. DeGrado, “De Novo Design, Synthesis, and Characterization of Antimicrobial β-Peptides”, J. Am. Chem. Soc. 2001, 123, 7553-7559.

209. R. F. Epand, T. L. Raguse, S. H. Gellman, and R. M. Epand, "Antimicrobial 14-Helical β-Peptides: Potent Bilayer Disrupting Agents", Biochemistry 2004, 43, 9527-9535.

210. R. F. Epand, M. Schmitt, S. H. Gellman, A. Sen, M. Auger, D. Hughes, R. M. Epand, "Bacterial species selective toxicity of two isomeric α/β-peptides: Role of membrane lipids", Mol. Membr. Biol. 2005, 43, 457-469.

211. R. F. Epand, M. Schmitt, S. H. Gellman, R. M. Epand, "Role. Of membrane lipids in the mechanism of bacterial species selective toxicity by two alpha/beta-antimicrobial peptides.", Biochim. Biophys. Acta 2006, 1758, 1343–1350.

212. S. L. Seurynck, J. A. Patch, A. E. Barron, "Simple, helical peptoid analogs of lung surfactant protein B.", Chem. Biol. 2005, 12, 77-88.

213. James A. Patch and Annelise E. Barron, "Helical Peptoid Mimics of Magainin-2 Amide", J. Am. Chem. Soc. 2003, 125, 12092-12093.

214. P. I. Arvidsson, N. S. Ryder, H. M. Weiss, G. Gross, O. Kretz, R. Woessner, and D. Seebach, "Antibiotic and Hemolytic Activity of a β^2/β^3 Peptide Capable of Folding into a 12/10-Helical Secondary Structure", ChemBioChem 2003, 4, 1345-1347.

215. S. Choi, D. J. Clements, V. Pophristic, I. Ivanov, S. Vemparala, J. S. Bennett, M. L. Klein, J. D. Winkler, and W. F. DeGrado, "The Design and Evaluation of Heparin-Binding Foldamers", Angew. Chem. Int. Ed. 2005, 44, 6685 –6689.

216. J. Solà, M. Helliwell, and J. Clayden, "N- versus C-Terminal Control over the Screw-Sense Preference of the Configurationally Achiral, Conformationally Helical Peptide Motif Aib8GlyAib8", J. Am. Chem. Soc. 2010, 132, 4548–4549.

217. I. M. Mándity, L. Fülöp, E. Vass, G. K. Tóth, T. A. Martinek, and F. Fülöp, "Building β-Peptide H10/12 Foldamer Helices with Six-Membered Cyclic Side-Chains: Fine-Tuning of Folding and Self-Assembly", Org. Lett. 2010, 12, 5584–5587.

218. R. P. Cheng, S. H. Gellman, W. F. DeGrado, "β-Peptides: From Structure to Function", Chem Rev 2001, 101, 3219-3232.

219. D. Seebach, D. F. Hook, A. Glättli, "Helices and other secondary structures of β- and γ-peptides", Biopolymers 2006, 84, 23-37.

220. G. V. M. Sharma, P. Jayaprakash, K. Narsimulu, A. R. Sankar, K. R. Reddy, P. R. Krishna, and A. C. Kunwar, "A Left-Handed 9-Helix in γ-Peptides: Synthesis and Conformational Studies of Oligomers with Dipeptide Repeats of C-Linked Carbo-γ^4-amino Acids and γ-Aminobutyric Acid", Angew. Chem. Int. Ed. 2006, 45, 2944 –2947.

221. J. Farrera-Sinfreu, L. Zaccaro, D. Vidal, X. Salvatella, E. Giralt, M. Pons, F. Albericio, and M. Royo, "A New Class of Foldamers Based on cis-γ-Amino-L-proline", J. Am. Chem. Soc., 2004, 126, 6048–6057.

222. P. G. Vasudev, N. Shamala, K. Ananda, and P. Balaram, "C9 Helices and Ribbons in γ-Peptides: Crystal Structures of Gabapentin Oligomers", Angew. Chem. Int. Ed. 2005, 44, 4972 –4975.

223. H.-D. Arndt, B. Ziemer, and U. Koert, "Folding Propensity of Cyclohexylether-δ-peptides", Org. Lett. 2004, 6, 3269-3272.

224. A. Trabocchi, F. Guarna, A. Guarna, "γ- and δ-Amino Acids: Synthetic Strategies and Relevant Applications", Curr. Org. Chem. 2005, 9, 1127-1153.

225. A. Violette, M. C. Averlant-Petit, V. Semetey, C. Hemmerlin, R. Casimir, R. Graff, M. Marraud, J-P. Briand, D. Rognan, and G. Guichard, "N,N'-Linked Oligoureas as Foldamers: Chain Length Requirements for Helix Formation in Protic Solvent Investigated by Circular Dichroism, NMR Spectroscopy, and Molecular Dynamics", J. Am. Chem. Soc. 2005, 127, 2156-2164.

226. A. Salaün, M. Potel, T. Roisnel, P. Gall, and P. Le Grel, "Crystal Structures of Aza-β^3-peptides, A New Class of Foldamers Relying on a Framework of Hydrazinoturns", J. Org. Chem. 2005, 70, 6499-6502.

227. A. Zega, "Azapeptides as pharmacological agents", Curr. Med. Chem. 2005, 12, 589-597.

228. A. B. Smith, III, S. D. Knight, P. A. Sprengeler and R. Hirschmann, "The Design and Synthesis of 2,5-Linked Pyrrolinones. A Potential Non-Peptide Peptidomimetic Scaffold", Bioorg. Med. Chem. 1996, 4, 1021-1034.

229. C. Baldauf, R. Gunther and H. J. Hofmann, "Helices in peptoids of α- and β-peptides", Phys. Biol. 2006, 3, S1-S9.

230. F. Fülöp, T. A. Martinek and G. K. Toth, "Application of alicyclic β-amino acids in peptide chemistry", Chem. Soc. Rev. 2006, 35, 323-334.

231. S. De Pol, C. Zorn, C. D. Klein, O. Zerbe, and O. Reiser, "Surprisingly Stable Helical Conformations in α/β-Peptides by Incorporation of *cis*-β-Aminocyclopropane Carboxylic Acids", Angew. Chem. Int. Ed. 2004, 43, 511 –514.

232. S. Izquierdo, M. J. Kogan, T. Parella, A. G. Moglioni, V. Branchadell, E. Giralt and R. M. Ortuño, "14-helical folding in a cyclobutane-containing β-tetrapeptide", J. Org. Chem. 2004, 69, 5093-5099.

233. E. Torres, J. Puigmartí-Luis, Á. Pérez del Pino, R. M. Ortuño and D. B. Amabilino, "Use of unnatural β-peptides as a self-assembling component in functional organic fibres", Org. Biomol. Chem. 2010, 8, 1661-1665.

234. F. Rúa, S. Boussert, T. Parella, I. Díez-Pérez, V. Branchadell, E. Giralt, and R. M. Ortuno, "Self-Assembly of a Cyclobutane β-Tetrapeptide To Form Nanosized Structures", Org. Lett. 2007, 9, 3643-3645.

235. E. Torres, E. Gorrea, K. K. Burusco, E. Da Silva, P. Nolis, F. Rúa, S. Boussert, I. Díez-Pérez, S. Dannenberg, S. Izquierdo, E. Giralt, C. Jaime, V. Branchadell, R. M. Ortuño, "Folding and self-assembling with beta-oligomers based on (1R,2S)-2-aminocyclobutane-1-carboxylic acid.", Org. Biomol. Chem. 2010, 8, 564-575.

236. C. Fernandes, S. Faure, E. Pereira, V. Théry, V.Declerck, R.Guillot, and D. J. Aitken, "12-Helix Folding of Cyclobutane-Amino Acid Oligomers", Org. Lett. 2010, 12, 3606-3609.

237. M. De Poli, M. De Zotti, J. Raftery, J. A. Aguilar, G. A. Morris, and J. Clayden, "Left-Handed Helical Preference in an Achiral Peptide Chain Is Induced by an L-Amino Acid in an N-Terminal Type II β-Turn", J. Org. Chem. 2013, 78, 2248−2255.

238. S. J. Pike, M. De Poli, W. Zawodny, J. Raftery, S. J. Webba, and J. Clayden, "Diastereotopic fluorine substituents as 19F NMR probes of screw-sense preference in helical foldamers", Org. Biomol. Chem. 2013, 11, 3168–3176.

239. R. A. Brown, T. Marcelli, M. De Poli, J. Solà, and J. Clayden, "Induction of Unexpected Left-Handed Helicity by an N-Terminal L-Amino Acid in an Otherwise Achiral Peptide Chain", Angew. Chem. Int. Ed. 2012, 51, 1395 –1399.

240. J. Solà, G. A. Morris, and J. Clayden, "Measuring Screw-Sense Preference in a Helical Oligomer by Comparison of ^{13}C NMR Signal Separation at Slow and Fast Exchange", J. Am. Chem. Soc. 2011, 133, 3712–3715.

241. J. Clayden, A. Castellanos, J. Solà, and G. A. Morris, "Quantifying End-to-End Conformational Communication of Chirality through an Achiral Peptide Chain", Angew. Chem. Int. Ed. 2009, 48, 5962 –5965.

242. J. Solà, S. P. Fletcher, A. Castellanos, and J. Clayden, Nanometer-Range Communication of Stereochemical Information by Reversible Switching of Molecular Helicity", Angew. Chem. Int. Ed. 2010, 49, 6836 –6839.

243. O. Mitsunobu, and M. Yamada, "Preparation of esters of carboxylic and phosphoric acid via quarternary phosphonium salts", Bull. Chem. Soc. Jpn. 1967, 40, 2380-2382.

244. O. Mitsunobu, M. Yamada, and T. Mukaiyama, "Preparation of esters of phosphoric acid by the reaction of trivalent phosphorus compounds with diethyl azodicarboxylate in the presence of alcohols", Bull. Chem. Soc. Jpn. 1967, 40, 935-939.

245. J. A. Dodge, and S. A. Jones, "Advances in the Mitsunobu reaction for the stereochemical inversion of hindered secondary alcohols", Rec. Res. Dev. Org. Chem. 1997, 1, 273-283.

246. D. S. Pedersen and A. Abell, "1,2,3-Triazoles in Peptidomimetic Chemistry", Eur. J. Org. Chem. 2011, 2399–2411.

247. M. Meldal, and C. W. Tornøe, "Cu-Catalyzed Azide-Alkyne Cycloaddition", Chem. Rev. 2008, 108, 2952–3015.

248. C. W. Tornøe, and M. Meldal, "Peptidotriazoles: Copper(I)-catalyzed 1,3-dipolar cycloadditions on solid phase", Peptides 2001, Proc. Am. Pept. Symp. 2001, 263-264, San Diego, American Peptide Society and Kluwer Academic Publishers.

249. J.R. Johansson, P. Lincoln, B. Nordén and N. Kann, "Sequential One-Pot Ruthenium-Catalyzed Azide-Alkyne Cycloaddition from Primary Alkyl Halides and Sodium Azide", J. Org. Chem. 2011, 76, 2355-2359.

250. A. Deiters, P. G. Schultz, Bioorg. Med. Chem. Lett. 2005, 15, 1521-1524.

251. S. K. Mamidyala, M. G. Finn, " In situ click chemistry: probing the binding landscapes of biological molecules", Chem. Soc. Rev. 2010, 39, 1252-1261.

252. J. C. Jewett, C. R. Bertozzi, Chem. Soc. Rev. 2010, 39, 1272-1279.

253. J. C. Jewett, E. M. Sletten, C. R. Bertozzi, J. Am. Chem. Soc. 2010, 132, 3688-3690.

254 P. V. Chang, J. A. Prescher, E. M. Sletten, J. M. Baskin, I. A. Miller, N. J. Agard, A. Lo, C. R. Bertozzi, Proc. Natl. Acad. Sci. USA 2010, 107, 1821-1826.

255. Y. L. Angell and K. Burgess, "Peptidomimetics via copper-catalyzed azide-alkyne cycloadditions", Chem. Soc. Rev. 2007, 36, 1674-1689.

256. O. D. Montagnat, G. Lessene, A. B. Hughes, J. Org. Chem 2010, 75, 390-398.

257. N. G. Angelo, P. S. Arora, J. Am. Chem. Soc. 2005, 127, 17134-17135.

258. N. G. Angelo, P. S. Arora, J. Org. Chem. Soc. 2007, 72, 7963-7967.

259. A. L. Jochim, S. E. Miller, N. G. Angelo, P. S. Arora, Bioorg. Med. Chem. Lett 2009, 19, 6023-6026.

260. Z. Ke, H-F. Chow, M-C. Chan, Z. Liu, and K-H. Sze, "Head-to Tail Dimerization and Organogelating Properties of Click Peptidomimetics", Org. Lett. 2012, 14, 394-397.

261. G. Chouhan and K. James, "CuAAC Macrocyclization: High Intramolecular Selectivity through the Use of Copper – Tris(triazole) Ligand Complexes", Org. Lett. 2011, 13, 2754-2757.

262. K. Buysse, J. Farard, A. Nikolaou, P. Vanderheyden, G. Vauquelin, D. S. Pedersen, D. Tourwé, and S. Ballet, "Amino Triazolo Diazepines (Ata) as Constrained Histidine Mimics", Org. Lett. 2011, 13, 6468-6471.

263. J. Zhang, J. Kemmink, D. T. S. Rijkers, and R. M. J. Liskamp, "Cu(I)- and Ru(II)-mediated "Click" Cyclization of Tripeptides Toward Vancomycin-Inspired Mimics", Org. Lett. 2011, 13, 3438-3441.

264. A. Tam, U. Arnold, M. B. Soellner, and R. T. Raines, "Protein Prosthesis: 1,5-Disubstituted[1,2,3]triazoles as *cis*-Peptide Bond Surrogates", J. Am. Chem. Soc. 2007, 129, 12670-12671.

265. J. K. Pokorski, L. M. Miller Jenkins, H. Feng, S. R. Durell, Y. Bai, and D. H. Appella, "Introduction of a Triazole Amino Acid into a Peptoid Oligomer Induces Turn Formation in Aqueous Solution", Org. Lett. 2007, 9, 2381-2383.

266. M. Daniels and R. U. Kirss, "Dimerization of terminal alkynes catalyzed by chloro(η^5-pentadienyl) bis(triphenylphosphine)ruthenium(II) and kinetics of phosphine substitution", Journal of Organometallic Chemistry 2007, 692, 1716–1725.

267. M. M. T. Khan, M. M. Bhadbhade, M. R. H. Siddiqui, K. Venkatasubramanian, J. A. Tikhonova, "Azido(η^5-cyclopentadienyl)bis(triphenylphosphine)ruthenium(II)", Acta Crystallogr. Sect. C-Cryst. Struct. Commun. 1994, 50, 502.

268. C.-T. Zhang, X.Zhang, and F.-L. Qing, "Ruthenium-catalyzed 1,3-dipolar cycloaddition of trifluoromethylated propargylic alcohols with azides", Tetrahedron Lett. 2008, 49, 3927-3930.

269. D. Wang, L. Salmon, J. Ruiz, and D. Astruc, "A recyclable ruthenium(II) complex supported on magnetic nanoparticles: a regioselective catalyst for alkyne-azide cycloaddition", Chem. Commun. 2013, 49, 6956-6958.

270. T. Beke, A. Czajlik, B. Balint, and A. Perczel, "A Theoretical Comparison of Self-Assembling α- and β-Peptide Nanostructures: Toward Design of β-Barrel Frameworks", Acs Nano 2008, 2, 545-553.

271. P. G. Vasudev, S. Chatterjee, N. Shamala, and P. Balaram, "Structural Chemistry of Peptides Containing Backbone Expanded Amino Acid Residues: Conformational Features of β, γ, and Hybrid Peptides", Chem Rev 2011, 111, 657-687.

272. H. W. Sunnemann, A. Hofmeister, J. Magull, and A. de Meijere, "An Efficient Access to Novel Enantiomerically Pure Steroidal δ-Amino Acids", Chem. Eur. J. 2006, 12, 8336-8344.

273. E. A. Porter, X. F. Wang, M. A. Schmitt, and S. H. Gellman, "Synthesis and 12-Helical Secondary Structure of β-Peptides Containing (2R,3R)-Aminoproline", Org Lett 2002, 4, 3317-3319.

274. P. R. LePlae, N. Umezawa, H. S. Lee, and S. H. Gellman, J. Org. Chem. 2001, 66, 5629-5632.

275. H. S. Lee, F. A. Syud, X. F. Wang, and S. H. Gellman, J. Am. Chem.Soc. 2001, 123, 7721-7722.

276. C. Baldauf, R. Gunther, and H. J. Hofmann, J. Org. Chem. 2004, 69, 6214-6220.

277. X. Zhao, M. X. Jia, X. K. Jiang, L. Z. Wu, Z. T. Li, and G. J. Chen, J. Org. Chem. 2004, 69, 270-279.

278. G. V. M. Sharma, B. S. Babu, K. V. S. Ramakrishna, P. Nagendar, A. C. Kunwar, P. Schramm, C. Baldauf, and H. J. Hofmann, "Synthesis and Structure of α/δ-Hybrid Peptides—Access to Novel Helix Patterns in Foldamers", Chem. Eur. J. 2009, 15, 5552-5566.

279. T. Beke, I. G. Csizmadia, and A. Perczel, "On the flexibility of β-peptides", J. Computational Chemistry, 2004, 25, 285–307.

280. T. Beke, I. G. Csizmadia, and A. Perczel, "Theoretical Study on Tertiary Structural Elements of β-peptides: Nanotubes Formed from Parallel-Sheet-Derived Assemblies of β-Peptides", J. Am. Chem. Soc. 2006, 128, 5158–5167.

281. T. Beke, C. Somlai, and A. Perczel, "Toward a rational design of β-peptide structures", Journal of Computational Chemistry 2006, 27, 20–38.

282. T. Beke, C. Somlai, G. Magyarfalvi, A. Perczel and G. Tarczay, "Chiral and Achiral Fundamental Conformational Building Units of β-Peptides: A Matrix Isolation Conformational Study on Ac-β-HGly-NHMe and Ac-β-HAla-NHMe", J. Phys. Chem. B, 2009, 113, 7918–7926.

283. H. Wissmann, and H. J. Kleiner, "New Peptide Synthesis", Angew. Chem. Int. Ed. 1980, 19, 133-134.

284. A. L. L. Garcia, "T3P: A Convenient and Useful Reagent in Organic Synthesis", Synlett 2007, 1328-1329.

285. D. S. MacMillan, J. Murray, H. F. Sneddon, C. Jamieson, and A. J. B. Watson, "Evaluation of alternative solvents in common amide coupling reactions: replacement of dichloromethane and N,N-dimethylformamide", Green Chem 2013, 15, 596-600.

286. J.Andersson , L. H. Fornander , M. Abrahamsson , E. Tuite , P. Nordell , and P. Lincoln, "Lifetime Heterogeneity of DNA-Bound dppz Complexes Originates from Distinct Intercalation Geometries Determined by Complex–Complex Interactions", Inorg. Chem. 2013, 52, 1151–1159.

287. P. Lincoln A. Broo, and B. Nordén, "Diastereomeric DNA-Binding Geometries of Intercalated Ruthenium(II) Trischelates Probed by Linear Dichroism: $[Ru(phen)_2dppz]^{2+}$ and $[Ru(phen)_2bdppz]^{2+}$", J. Am. Chem. Soc. 1996, 118, 2644-2653.

288. P. Lincoln and B. Nordén, "DNA Binding Geometries of Ruthenium(II) Complexes with 1,10-Phenanthroline and 2,2'-Bipyridine Ligands Studied with Linear Dichroism Spectroscopy. Borderline Cases of Intercalation. J. Phys. Chem. B 1998, 102, 9583-9594.

289. L. M. Wilhelmsson, F. Westerlund, P. Lincoln, and B. Nordén, "DNA-binding of Semirigid Binuclear Ruthenium Complex ΔΔ-$[\mu$-(11,11'-bidppz)$(phen)_4$ $Ru_2]^{4+}$: Extremely Slow Intercalation Kinetics", J. Am. Chem. Soc. 2002, 124, 12092-12093.

290. J. Andersson, "Structural Requirements for Selective DNA Binding, Studies on Mono- and Binuclear Ruthenium Complexes", PhD Thesis, Chalmers University of Technology, Gothenburg, 2012.

291. B. K. Bhuyan and C. G. Smith, "Differential interaction of nogalamycin with DNA of varying base composition", Proc. Natl. Acad. Sci. U. S. A. 1965, 54, 566-572.

292. D. A. Collier, S. Neidle, and J. R. Brown, "Molecular models for the interaction of the anti-tumour drug nogalamycin with DNA", Biochem. Pharmacol. 1984, 33, 2877-2880.

293. K. R. Fox, C. Brassett, and M. J. Waring, Biochim. Biophys. Acta 1985, 840, 383-392.

294. K. R. Fox and M. J. Waring, Biochim. Biophys. Acta 1984, 802, 162-168.

295. W. Kersten, H. Kersten, and Szybalski.W, Biochemistry 1966, 5, 236-244.

296. C. K. Smith, G. J. Davies, E. J. Dodson, and M. H. Moore, "DNA-Nogalamycin Interactions: The Crystal Structure of d(TGATCA) Complexed with Nogalamycin", Biochemistry 1995, 34, 415-425.

297. P. Nordell, F. Westerlund, A. Reymer, A. H. El-Sagheer, T. Brown, B. Norden, and P. Lincoln, " DNA Polymorphism as an Origin of Adenine-Thymine Tract Length-Dependent Threading Intercalation Rate", J. Am. Chem. Soc. 2008, 130, 14651-14658.

298. P. Nordell, F. Westerlund, L. M. Wilhelmsson, B. Norden, and P. Lincoln, "Kinetic Recognition of AT-Rich DNA by Ruthenium Complexes", Angew. Chem., Int. Ed. 2007, 46, 2203-2206.

299. M. J. Gardner, N. Hall, E. Fung, O. White, M. Berriman, R. W. Hyman, J. M. Carlton, A. Pain, K. E. Nelson, S. Bowman, I. T. Paulsen, K. James, J. A. Eisen, K. Rutherford, S. L. Salzberg, A. Craig, S. Kyes, M. S. Chan, V. Nene, S. J. Shallom, B. Suh, J. Peterson, S. Angiuoli, M. Pertea, J. Allen, J. Selengut, D. Haft, M. W. Mather, A. B. Vaidya, D. M. A. Martin, A. H. Fairlamb, M. J. Fraunholz, D. S. Roos, S. A. Ralph, G. I. McFadden, L. M. Cummings, G. M. Subramanian, C. Mungall, J. C. Venter, D. J. Carucci, S. L. Hoffman, C. Newbold, R. W. Davis, C. M. Fraser, and B. Barrell, Nature 2002, 419, 498-511.

300. J. Andersson, M. N. Li, and P. Lincoln, "AT-Specific DNA Binding of Binuclear Ruthenium Complexes at the Border of Threading Intercalation", Chem. Eur. J. 2010, 16, 11037-11046.

301. J. Andersson and P. Lincoln, "Stereoselectivity for DNA Threading Intercalation of Short Binuclear Ruthenium Complexes", J. Phys. Chem. B 2011, 115, 14768-14775.

302. L. Cassar, J. Organomet. Chem. 1975, 93, 253 –257.

303. H. A. Dieck, F. R. Heck, J. Organomet. Chem. 1975, 93, 259 –263.

304. K. Sonogashira, Y. Tohda, N. Hagihara, Tetrahedron Lett. 1975, 16, 4467 – 4470.

305. M. Erdélyi and A. Gogoll, "Rapid Homogeneous-Phase Sonogashira Coupling Reactions Using Controlled Microwave Heating", J. Org. Chem. 2001, 66, 4165-4169.

306. D. W. Price, Jr., S. M. Dirk, F. Maya, and J. M. Tour, "Improved and new synthesis of potential molecular electronics devices", Tetrahedron 2003, 59, 2497-2518.

307. F. Maya, S. H. Chanteau, L. Cheng, M. P. Stewart, and J. M. Tour, "Synthesis of Fluorinated Oligomers towards Physical Vapor Deposition Molecular Electronics Candidates", Chem. Mater. 2005, 17, 1331-1345.

308. F. Westerlund, M. P. Eng, M. U. Winters, and P. Lincoln, J. Phys. Chem. B 2007, 111, 310-317.

309. D. B. Dess and J. C. Martin, "A useful 12-I-5 triacetoxyperiodinane (the Dess-Martin periodinane) for the selective oxidation of primary or secondary alcohols and a variety of related 12-I-5 species", J. Am. Chem. Soc. 1991, 113, 7277–7287.

310. V. Georgakilas, K. Kordatos, M. Prato, D. M. Guldi, M. Holzinger, A. Hirsch, "Organic Functionalization of Carbon Nanotubes", J. Am. Chem. Soc. 2002, 124, 760-761.

311. J. Coste, D. Le-Nguyen, B. Castro, "PyBOP®: A new peptide coupling reagent devoid of toxic by-product", Tetrahedron Lett. 1990, 31, 205-208.

Acknowledgements

I am very grateful for the opportunity to perform my PhD studies at the Department of Chemical and Biological Engineering and being part of the Nordén group. I would like to thank my team of supervisors, **Nina**, **Per** and **Bengt**,* for all your trust, support, funding, feedback and possibilities. I have developed a lot thanks to you!

Sincere gratitude to **Nina, Johanna, Tamás and Lars** for proofreading the thesis. I am fascinated and grateful for your sharp hawk eyes!

I wish to send my gratitude to my collaborators and co-authors, **Johanna**, **Tamás**, **Waqas**, **Niklas** and **Björn** for all your great contributions and stimulating discussions.

I also wish to thank the students who have been working in my lab, **Elin**, **Nirup** and **Yubo**, it has been a pleasure to teach and develop your synthesis-dexterity skills in the lab.

Further I wish to show my appreciation for their essential and hard work which keeps the department running, **Anna**, **Carina**, **Frida**, **Gunilla** and **Roger**, thanks!

Special thanks to Mr pro-photoshoper **Sandin** for help with Photoshop to put together the cover picture and the size issue for the dedication page, and of course all the photo-talks during coffee! (Even though you don´t have a Canon yet... ;-)

Thank you **Anna S-S** for all the fun and positive energy you spread in the lab and all the enjoyable cappuccinos at Ines!

Thank you **Fredrik** and **Kim**, for our fantastic office atmosphere and for being willing recruits for the floorball squad.

Many thanks to **all** the floorball players for all fun games and for letting me do a tunnel one and a while...

Another thanks goes to **Mate** for great advice concerning NMR, kindness and your enthusiastic energy.

I wish to thank **ALL** my great colleges and friends at CTH and GU, floor **5**, **8** and **9,** for your contribution to a fun and good working-environment.

Further I wish to thank all great colleges and friends on AZ, and special thanks to **Thomas A.**, **Peter Bonn** and **Micke S.** for all your discussions, support and encouragement, and to **Annika W.** for always gladly willing to provide me with HRMS data.

A big thanks and a sorry! To all the people I have forgotten to list in this acknowledgement.

A special thanks also to the “Climbing team”, **Johanna**, **Peter**, **Fabian, Louise**, **Anke** and **Basti**, for all the good times indoor and outdoor. You Rock!

Big thanks to all **family** and **friends** for support and love. And extra thanks to the Johansson and Vinblad families for all your kind hosting, good food and babysitting which provided me with many extra hours to dedicate on this thesis over the last two weeks.

Last and most important, **Johanna V. & Ellen** you are my life! Thanks for all support, understanding? :-), happiness, fun, cheering and **love**! (I owe you a lot of quality time after this...)

10 h to printing,
Gothenburg 2013

Johan

Appendix for unpublished data

3-(4-Amino-3-nitrophenyl)prop-2-yn-1-ol (65): 4-Iodo-2-nitroaniline (1.26 g, 4.6 mmol), propargyl alcohol (0.30 mL, 5.2 mmol), $Pd(PPh_3)_2Cl_2$ (140 mg, 0.20 mmol) and CuI (38 mg, 0.20 mmol) were placed in a 20 mL microwave vial and THF (5 mL) was added followed by DIPA (5 mL). The vial was sealed and flushed with N_2 for ~2 min. The reaction mixture was heated to 120 °C for 10 min in a microwave reactor. The reaction mixture was filtered through a plug of Celite and 1M HCl (aq) was added until pH ~1 was reached. The mixture was extracted with ethyl acetate/THF three times and the combined organic phases were washed with $NaHCO_3$(aq) and dried over anhydrous Na_2SO_4. The drying agent was filtered off and the solution concentrated under reduced pressure. The crude product was purified on silica using 5% MeOH in DCM, yielding the product as an orange solid. Yield 768 mg (87%) ^{1}H NMR (400 MHz, DMSO-d_6, 25 °C) δ 7.95 (d, *J* = 2.0 Hz, 1H), 7.68 (s, 2H), 7.39 (dd, *J* = 8.8, 2.0 Hz, 1H), 6.99 (d, *J* = 8.8 Hz, 1H), 5.28 (t, *J* = 5.9 Hz, 1H), 4.26 (d, *J* = 5.9 Hz, 3H).

3-(3,4-Diaminophenyl)prop-2-yn-1-ol (66): 3-(4-Amino-3-nitrophenyl)prop-2-yn-1-ol **65** (100 mg, 0.52 mmol), zinc powder (817 mg, 12.5 mmol) and NH_4Cl (s) (669 mg, 12.5 mmol) were suspentioned in absolute EtOH (20 mL) and the reaction mixture was heated to reflux for 1.5 h. The reaction mixture was filtered through a syringe filter and concentrated to approximately half the volume and used as such directly in the next step.

Δ-[Ru(phen)$_2$dppzp](PF$_6$)$_2$ (67), (dppzp = 3-(dipyrido[3,2-a:2',3'-c]phenazin-11-yl)prop-2-yn-1-ol): To the crude 3-(3,4-diaminophenyl)prop-2-yn-1-ol **66** (excess) from previous step was added Δ-[Ru(phen)$_2$pq](PF$_6$)$_2$ **61** (47 mg, 49μmol) dissolved in acetonitrile (3 mL), and sodium acetate (95 mg) and acetic acid (7 drops) were then added. The reaction mixture was heated to 50 °C for 2 h. The product was precipitated by dropwise addition of NH_4PF_6 (aq), filtered and the crude product was purified on Al_2O_3 (neutral, activity grad 1) and eluted with acetonitrile to obtain the product as a red solid. Yield: 39 mg (74%). ^{1}H NMR (400 MHz, CD_3CN) δ 9.63 (ddd, *J* = 8.2, 3.7, 1.3 Hz, 2H), 8.66 – 8.61 (m, 4H), 8.54 (d, *J* = 1.5 Hz, 1H), 8.44 (d, *J* = 8.9 Hz, 1H), 8.29 (s, 4H), 8.23 (ddd, *J* = 5.3, 2.0, 1.3 Hz, 2H), 8.13 (ddd, *J* = 5.0, 2.3, 1.2 Hz, 2H), 8.09 (dd, *J* = 8.9, 1.8 Hz, 1H), 8.04 (dd, *J* = 5.2, 1.3 Hz, 2H), 7.79 (ddd, *J* = 8.4, 5.4, 3.2 Hz, 2H), 7.70 – 7.63 (m, 4H), 4.53 (d, *J* = 6.0 Hz, 2H), 3.43 (t, *J* = 6.0 Hz, 1H).

Λ-[Ru(phen)$_2$dppzpa](PF$_6$)$_2$ (68), (dppzpa = 3-(dipyrido[3,2-a:2',3'-c]phenazin-11-yl)propiolaldehyde): Dess-Martin periodane (DMP) (44 mg, 103 μmol) was dissolved in CH_2Cl_2 (5 mL) and Λ-[Ru(phen)$_2$dppzp]$^{2+}$ **67** (102 mg, 93.6 μmol) dissolved in acetonitrile (2 mL) was added dropwise. The reaction mixture was stirred at r.t for 16 h and then quenched with 10 % $Na_2S_2O_3$ (aq) (1 mL). The mixture was stirred at r.t. for 30 min and saturated NH_4PF_6(aq) was added. The mixture was extracted with CH_2Cl_2 (three times) and filtered through a phase separator and evaporated. The crude product was purified on Al_2O_3 (neutral, activity grade 1) using a step wise gradient from 10 to 50% acetonitrile in CH_2Cl_2 to obtain the product as a red solid. Yield: 67 mg (65%). ^{1}H NMR (400 MHz, CD_3CN): δ 9.65 – 9.60 (m, 2H), 9.54 (s, 1H), 8.80 (d, *J* = 1.4 Hz, 1H), 8.67 – 8.62 (m, *J* = 8.3, 5.8, 1.2 Hz, 4H), 8.52 (dd, *J* = 8.8, 0.4 Hz, 1H), 8.29 (s, 4H), 8.26 – 8.20 (m, 3H), 8.15 (dd, *J* = 5.4, 1.3 Hz, 2H), 8.04 (dd, *J* = 5.2, 1.3 Hz, 2H), 7.82 – 7.78 (m, 2H), 7.72 – 7.63 (m, 4H). ^{13}C NMR (101 MHz, CD_3CN): δ 177.57, 154.71, 154.64, 153.26, 152.97, 151.25, 151.16, 147.86, 147.79, 143.26, 142.01, 141.29, 141.24, 137.01, 136.95, 135.37, 134.18, 133.68, 133.52, 131.08, 131.06, 130.61, 130.46, 130.45, 128.10, 128.08, 127.39, 127.36, 125.94, 125.88, 123.07, 90.92, 90.19.

3-(4-Amino-3-nitrophenyl)prop-2-yn-1-ol (65)

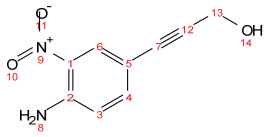

^{1}H NMR (400 MHz, DMSO-d6, 25 °C) δ 7.95 (d, *J* = 2.0 Hz, 1H), 7.68 (s, 2H), 7.39 (dd, *J* = 8.8, 2.0 Hz, 1H), 6.99 (d, *J* = 8.8 Hz, 1H), 5.28 (t, *J* = 5.9 Hz, 1H), 4.26 (d, *J* = 5.9 Hz, 3H).

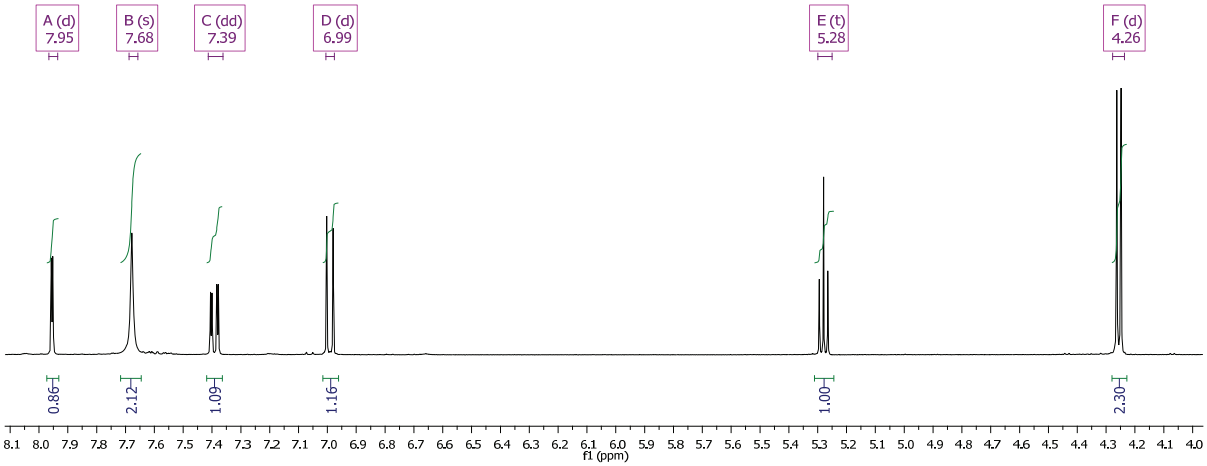

Δ-[Ru(phen)$_2$dppzp](PF$_6$)$_2$ (67)

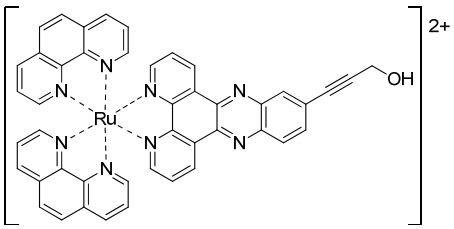

^{1}H NMR (400 MHz, CD$_3$CN) δ 9.63 (ddd, *J* = 8.2, 3.7, 1.3 Hz, 2H), 8.66 – 8.61 (m, 4H), 8.54 (d, *J* = 1.5 Hz, 1H), 8.44 (d, *J* = 8.9 Hz, 1H), 8.29 (s, 4H), 8.23 (ddd, *J* = 5.3, 2.0, 1.3 Hz, 2H), 8.13 (ddd, *J* = 5.0, 2.3, 1.2 Hz, 2H), 8.09 (dd, *J* = 8.9, 1.8 Hz, 1H), 8.04 (dd, *J* = 5.2, 1.3 Hz, 2H), 7.79 (ddd, *J* = 8.4, 5.4, 3.2 Hz, 2H), 7.70 – 7.63 (m, 4H), 4.53 (d, *J* = 6.0 Hz, 2H), 3.43 (t, *J* = 6.0 Hz, 1H).

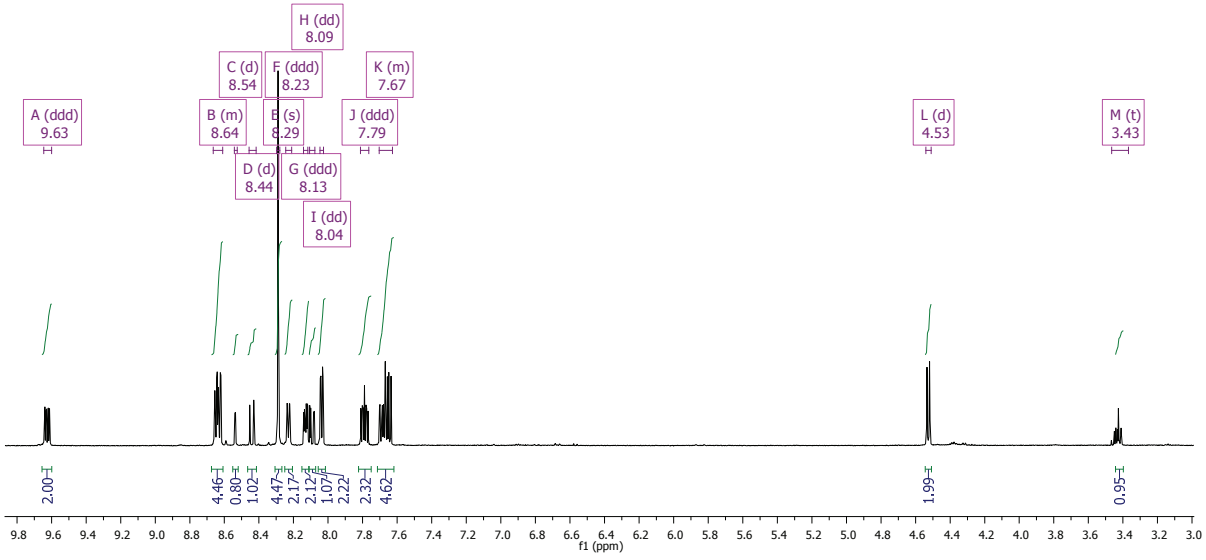

Λ-[Ru(phen)$_2$dppzpa](PF$_6$)$_2$ (68)

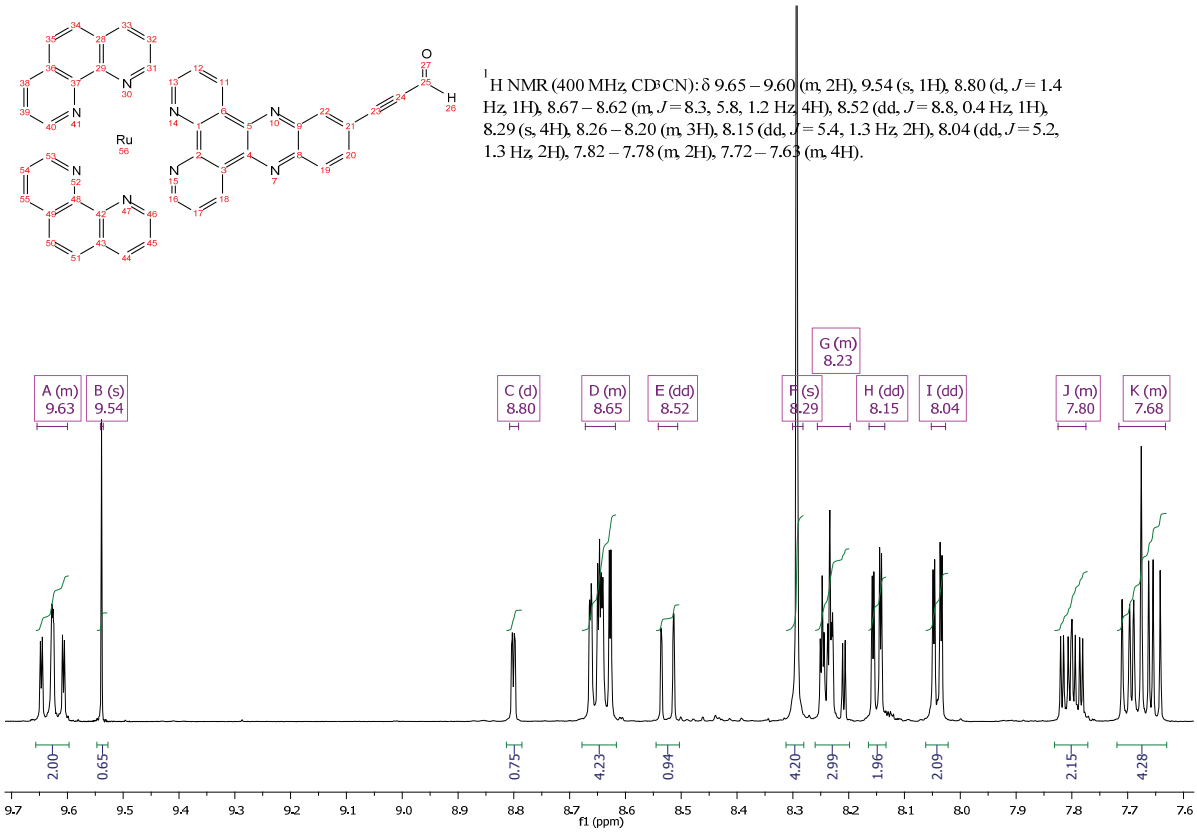

^{1}H NMR (400 MHz, CD$_3$CN): δ 9.65 – 9.60 (m, 2H), 9.54 (s, 1H), 8.80 (d, *J* = 1.4 Hz, 1H), 8.67 – 8.62 (m, *J* = 8.3, 5.8, 1.2 Hz, 4H), 8.52 (dd, *J* = 8.8, 0.4 Hz, 1H), 8.29 (s, 4H), 8.26 – 8.20 (m, 3H), 8.15 (dd, *J* = 5.4, 1.3 Hz, 2H), 8.04 (dd, *J* = 5.2, 1.3 Hz, 2H), 7.82 – 7.78 (m, 2H), 7.72 – 7.63 (m, 4H).

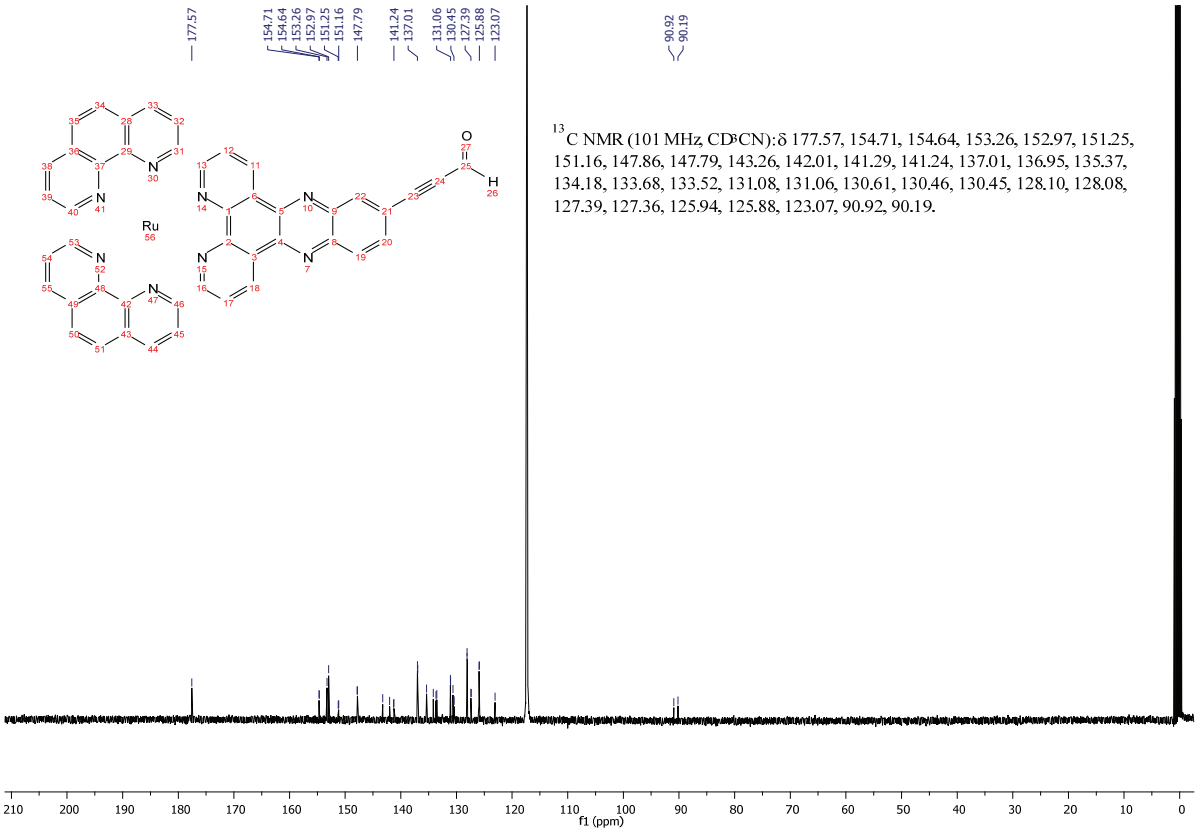

^{13}C NMR (101 MHz, CD$_3$CN): δ 177.57, 154.71, 154.64, 153.26, 152.97, 151.25, 151.16, 147.86, 147.79, 143.26, 142.01, 141.29, 141.24, 137.01, 136.95, 135.37, 134.18, 133.68, 133.52, 131.08, 131.06, 130.61, 130.46, 130.45, 128.10, 128.08, 127.39, 127.36, 125.94, 125.88, 123.07, 90.92, 90.19.